Fiber-Reinforced Concrete and Performance Engineered Concrete Mixture Design

A Thesis

SUBMITTED TO THE FACULTY OF

UNIVERSITY OF MINNESOTA

BY

Alieu Kamara, EIT

IN PARTIAL FULFILLMENT OF THE REQUIREMENTS

FOR THE DEGREE OF

MASTER OF SCIENCE

Dr. Manik Barman

May 2021

DEDICATION

This thesis is dedicated to my grandmother, Madolley Donzo, who raised me during a critical time in my life and supported me through all my experiences. To my mother, Mabongo Kamara, for her support and encouragement throughout my studies. To my late uncle, Mohammed Kamara, who supported my studies early on in my life and encouraged me to set high goals. And to all my family, friends and teachers for their continuous support, enthusiasm, and encouragement.

ACKNOWLEDGMENTS

I would like to express my sincere appreciation to my advisor, Dr. Manik Barman, for his continuous support, encouragement and general interest in my well-being. The door to Dr. Barman office was always open whenever I had questions about my research or writing. I would also like to thank my committee members Dr. Andrea Schokker and Dr. Emmanuel Enemuoh for their participation, insightful inputs and advice.

I would like to thank Minnesota Department of Transportation for funding the research project, donating coarse aggregates and providing the opportunity to study Performance Engineered Mixture (PEM) design. Special thanks to Duluth Ready Mix for fine aggregate donation, BASF Corporation for fiber and admixture donation, Forta Corporation for fiber donation and Boral Resource (coal creek station) for Fly-ash donation.

I would also like to thank all of the faculty, staff and my fellow peers for their valuable assistance in the laboratory.

ABSTRACT

A challenging objective for the concrete industry, in using structural fibers in concrete pavements and overlays while moving towards the implementation of the Performance Engineered Mixture (PEM) design, is to understand the influence of fibers on tests performed in the PEM design procedure. The goal of the PEM design procedure is to produce concretes that resist climate and material related distresses, such as durability cracks and concrete-degradation due to chloride-ion penetration. The addition of fibers in a concrete mixture also increases concrete durability by enhancing post-cracking performance. Using PEM procedure for fiber reinforced concrete (FRC) pavements will produce durable concrete pavements that resist environmental- and material- driven distresses as well as possess an improved post-crack performance. The objective of this research is to study the relationship between different fresh concrete properties and their influence on the hardened concrete behavior and durability.

The materials used in this study includes two types of coarse aggregates, fine aggregate, two types of fiber, cement, fly ash and admixtures. Two different fiber types (twisted and embossed geometries) and two fiber dosages (4 lb/ yd^3 and 7.6 lb/ yd^3) were considered in this study. Fresh and Hardened concrete test results for all the FRC mixes were compared to results of the control plain concrete mixes. Fresh concrete tests such as slump, air content, super air meter number (SAM), Box, and V-Kelly tests were conducted. Hardened concrete properties such as compressive strength, modulus of elasticity, beam flexural strength, resistance to distresses caused by multiple freeze-thaw cycles, and surface/electrical resistivity was determined. Based on the results of this study, it was found that fiber dosages and types significantly influence the V-Kelly index, while moderately influence SAM number and box test rating.

The fibers used in this study had significant influence on the post-crack behavior of concrete. The freeze-thaw durability and surface resistivity test results indicated that fibers have less influence on the concrete resistance to freeze-thaw durability issues.

TABLE OF CONTENTS

Abstract iii

CHAPTER 1: Introduction 1

1.1 Thesis Organization 2

CHAPTER 2: Literature Review 3

2.1 Performance Engineered Mixture 3

2.1.1 Aggregate Durability 3

2.1.2 Fluid Transport Property 4

2.1.3 Cold Weather Resistance 5

2.1.4 Shrinkage 8

2.1.5 Strength 11

2.1.6 Workability 13

2.2 Fibers 14

2.2.1 Steel Fiber Reinforced Concrete (SFRC) 17

2.2.2 Synthetic Fiber Reinforced Concrete (SyFRC) 21

2.3 Conclusion 29

CHAPTER 3: Research Methodology 30

3.1 Conclusion 32

CHAPTER 4: Materials and Testing 33

4.1 Fibers 33

4.2 Cement 33

4.3 Aggregate 34

4.4 Concrete Mixture 38

4.4.1 Mixture Designation 39

4.4.2 Mixing Procedure 39

4.5 Fresh Concrete Tests 41
4.5.1 Slump Test 41
4.5.2 Air Content and Super Air Meter (SAM) Test 42
4.5.3 Box Test 42
4.5.4 Vibrating Kelly Ball Test (V-Kelly Test) 44
4.6 Hardened Concrete tests 44
4.6.1 Compressive Strength Test 44
4.6.2 Electrical/Surface Resistivity Test 45
4.6.3 Flexural Strength Test 46
4.6.4 Formation Factor Bucket Test 48
4.6.5 Modulus of Elasticity Test 48
4.6.6 Rapid Freeze-Thaw Test 49
4.7 Conclusion 51
CHAPTER 5: Results and Discussions 52
5.1 Analysis and Discussion of Results 54
5.1.1 Discussion of Fresh Concrete Properties 55
5.1.2 Discussion of Hardened Concrete Properties 65
5.1.3 Correlation Between Fresh and Hardened Concrete Properties 84
CHAPTER 6: Conclusions 95
6.1 Recommendation for Future Studies 97
REFERENCES 98
APPENDIX 100
Lab Data 100
Load vs Displacement Plots 103
Box Test Images 115

Freeze-Thaw Images 119

LIST OF FIGURES

Figure 2-1. Resistivity test setup 4

Figure 2-2. Time vs. degree of saturation (Cackler, 2017) 6

Figure 2-3. Spacing factor vs SAM number (Ley, 2015) 7

Figure 2-4. SAM number vs durability factor as a result of freeze-thaw testing (Ley, 2015) 8

Figure 2-5. SAM number as a function of air content (Barman and Hansen, 2018) 8

Figure 2-6. Concrete moisture warping and temperature curling (Mack 2009) 9

Figure 2-7. Strain vs. time graph of drying shrinkage components (Mindess et al., 2008) 9

Figure 2-8. Long-term alternate wetting and drying shrinkage (Komatska and Wilson, 2016) 10

Figure 2-9. Tarantula curve showing recommended limits for aggregate gradation (Ley and Cook, 2014) 12

Figure 2-10. Influence of fly-ash in reducing calcium oxychloride content (Cackler et al., 2017) 13

Figure 2-11. Crack control and bridging effect of fibers (Gaddam, 2016) 15

Figure 2-12. Illustration of load vs deflection in plain concrete and FRC (after ACI Commitee 544, 2009) 15

Figure 2-13. Stages of FRC failure (ACI.544.4R-18) 16

Figure 2-14. Strain softening and hardening behaviors (ACI.544.4R-18) 16

Figure 2-15. Various steel fiber geometries (Komatska and Wilson 2016) 17

Figure 2-16. Steel fibers with hooked end (Barman, 2018) 18

Figure 2-17. Slump test output (Acikgenc et al., 2013) 18

Figure 2-18: Fibers used in the (Kevern et al., 2016) study: polypropylene fibrillated fiber (left), polypropylene macro fiber (left middle), carbon fiber (right middle) and steel fiber (right) 19

Figure 2-19. SFRC strength at 28-day: a) Compressive strength, and b) Flexural strength (Acikgenc et al., 2013) 20

Figure 2-20. Effect of fiber reinforcement in peak differential displacement (Arnold et al., 2005) 21

Figure 2-21. Residual load characteristics of different shaped structural synthetic fibers (Bordelon, 2005) 23

Figure 2-22. Residual load capacities of FRC vs. fiber volume fraction for synthetic fibers (Bordelon, 2005) 23

Figure 2-23. Shrinkage vs. curing time for plain and FRC mixes in Alhassan and Ashur (2012) study (LMC = latex modified concrete; ARGF = alkali resistant glass fiber; SX= microtype polyolefin fiber; GF = micro type 100% virgin; NXL = macrotype polyolefin fiber; RSC = microtype polyvinyl alcohol fiber; RF = macrotype polyvinyl alcohol fiber). 24

Figure 2-24. (a) Compressive strength, (b) Modulus of elasticity, and (c) and (d) Modulus of rupture as a function of reinforcement index and fibers' volume fraction. 27

Figure 2-25. (a) RSR vs. Vf, (b) Correlation between RSR and Vf, (c) RS vs. Vf, (d) RSR as a function of Vf and fiber geometry. 28

Figure 3-1. Flowchart of work conducted 30

Figure 4-1. ¾" and 1 ½" Granite Class A Aggregates 35

Figure 4-2. ¾" plus and ¾" minus Limestone Class B Aggregates 35

Figure 4-3. Fine aggregates (river sand) 36

Figure 4-4. Gradation curves of the aggregates used 37

Figure 4-5. Combined aggregate gradation on a tarantula curve. 37

Figure 4-6. Concrete mixer used. 40

Figure 4-7. Slump test on FRC mixture 41

Figure 4-8. Ongoing SAM test 42

Figure 4-9. Box test in progress 43

Figure 4-10. Surface air voids ranking system for box test (Cook et al. 2016) 43

Figure 4-11. Vibrating Kelly Ball Test (V-Kelly Test) 44

Figure 4-12. Compressive strength test 45

Figure 4-13. Surface resistivity test 46

Figure 4-14. Four-point flexural bending test as per ASTM C 1609 47

Figure 4-15. Fibers bridging a crack during an ongoing four-point flexural bending test. 48

Figure 4-16.Modulus of Elasticity test 49
Figure 4-17.Freeze-Thaw Chamber 50
Figure 5-1.SAM number vs Air content 55
Figure 5-2.Influence of fiber dosage on SAM Number 56
Figure 5-3.Influence of fiber type on SAM Number 57
Figure 5-4.Influence of aggregate type on SAM Number 58
Figure 5-5.Box test rating vs Air content 59
Figure 5-6.Box test rating vs Slump 59
Figure 5-7.Influence of fiber dosage on box test rating 60
Figure 5-8.V-Kelly slump values vs slump test results 61
Figure 5-9. V-Kelly index vs slump test results 61
Figure 5-10.V-Kelly Sump vs Air Content 62
Figure 5-11.Influence of fiber dosage on V-Kelly index 63
Figure 5-12.Influence of fiber dosage on V-Kelly Slump 64
Figure 5-13.Influence of fiber type on V-Kelly index 64
Figure 5-14. Influence of aggregate type on V-Kelly index 65
Figure 5-15. Compressive strength vs Air content 66
Figure 5-16. Influence of fiber on compressive strength 67
Figure 5-17.Influence of fiber type on compressive strength 67
Figure 5-18.Influence of aggregate type on compressive strength 68
Figure 5-19. Modulus of elasticity vs Air Content 69
Figure 5-20.Influence of fiber dosage on the modulus of elasticity 69
Figure 5-21. Influence of fiber type on the modulus of elasticity 70
Figure 5-22.Influence of Aggregate type on the modulus of elasticity 70
Figure 5-23. MOR vs Air content 71

Figure 5-24.Influence of fiber dosage on MOR 72
Figure 5-25.Influence of fiber type on MOR 73
Figure 5-26.Influence of aggregate type on MOR 73
Figure 5-27. Load vs displacement curve for 6A1.26 and 6A1.50 74
Figure 5-28. Toughness vs Air content 75
Figure 5-29.Influence of fiber dosage on toughness 75
Figure 5-30.Influence of fiber type on toughness 76
Figure 5-31.Influence of aggregate type on toughness 76
Figure 5-32. RSR vs air content 77
Figure 5-33. Influence of fiber dosage on RSR 78
Figure 5-34. Influence of fiber type on RSR 78
Figure 5-35. Influence of aggregate type on RSR 79
Figure 5-36. Saturation surface resistivity vs Air content 81
Figure 5-37. Surface resistivity vs Air content 82
Figure 5-38. Relative dynamic modulus (RDM) vs number of F-T cycles 83
Figure 5-39. Toughness vs V-Kelly index 85
Figure 5-40. RSR vs V-Kelly index 85
Figure 5-41. RDM vs V-Kelly index 86
Figure 5-42. MOR vs V-Kelly index 86
Figure 5-43. Compressive Strength vs V-Kelly index 87
Figure 5-44. Surface Resistivity vs V-Kelly index 87
Figure 5-45. Toughness vs SAM number 88
Figure 5-46. RSR vs SAM number 89
Figure 5-47. MOR vs SAM number 89
Figure 5-48. Compressive Strength vs SAM number 90

Figure 5-49. RDM vs SAM number 90
Figure 5-50. Surface resistivity vs SAM number 91
Figure 5-51. Toughness vs Box test rating 92
Figure 5-52. RSR vs Box test rating 92
Figure 5-53. MOR vs Box test rating 93
Figure 5-54. Compressive Strength vs Box test rating 93
Figure 5-55. RDM vs Box test rating 94
Figure 5-56. Surface resistivity vs box test rating 94
Figure 0-1. V-Kelly test results 102
Figure 0-2. Load vs Displacement for A. PC 103
Figure 0-3. Load vs Displacement for 4A1.50 103
Figure 0-4. Load vs Displacement for 4A1.26 104
Figure 0-5. Load vs Displacement for 6A1.26 104
Figure 0-6. Load vs Displacement for 6A1.50-1 105
Figure 0-7. Load vs Displacement for 6A1.50-2 105
Figure 0-8. Load vs Displacement for 8A1.26 106
Figure 0-9. Load vs Displacement for 8A1.50 106
Figure 0-10. Load vs Displacement for 4A2.26 107
Figure 0-11. Load vs Displacement for 4A2.50 107
Figure 0-12. Load vs Displacement for 6A2.26 108
Figure 0-13. Load vs Displacement for 6A2.50 108
Figure 0-14. Load vs Displacement for 8A2.26-1 109
Figure 0-15. Load vs Displacement for 8A2.26-2 109
Figure 0-16. Load vs Displacement for 8A2.50-1 110
Figure 0-17. Load vs Displacement for 8A2.50-2 110

Figure 0-18. Load vs Displacement for B.PC 111
Figure 0-19. Load vs Displacement for 4B1.26 111
Figure 0-20. Load vs Displacement for 4B1.50 112
Figure 0-21. Load vs Displacement for 6B1.26 112
Figure 0-22. Load vs Displacement for 6B1.50 113
Figure 0-23. Load vs Displacement for 8B1.26 113
Figure 0-24. Load vs Displacement for 8B1.50 114
Figure 0-25. Box test images for mix A.PC 115
Figure 0-26.Box test images for mix 4A1.26 115
Figure 0-27.Box test images for mix 4A1.50 116
Figure 0-28. Box test images for mix 6A1.26 116
Figure 0-29. Box test images for mix 6A1.50 117
Figure 0-30. Box test images for mix 8A1.26 117
Figure 0-31. Box test images for mix B.PC-1 118
Figure 0-32. Before (Left) and After (Right) image of mix 6B1.50 beams subjected to 300 freeze-thaw cycles 119
Figure 0-33. Image of mix 6A1.50 beams after 300 freeze-thaw cycles 119
Figure 0-34. Image of mix 8A1.26 beams after 300 freeze-thaw cycles 120

LIST OF TABLES

Table 2-1. Properties of fibers in Kevern et al. (2016) study 19

Table 2-2. Properties of structural synthetic fibers and FRC in Roesler et al. (2008) study 22

Table 2-3.Summary of fiber details from Barman and Hansen (2018) Study 26

Table 3-1. Tests to be considered in the study. 32

Table 4-1. Description of fibers investigated in this task. 33

Table 4-2. Aggregate's characteristics 34

Table 4-3.Sieve analysis results of the aggregates used 36

Table 4-4. Summary mixture design for concrete mixes used in this study 38

Table 4-5. Nomenclature for mixture designation 39

Table 5-1. Fresh Concrete Properties 52

Table 5-2. Hardened Concrete Properties 53

Table 5-3. Hardened Concrete Properties continued 54

Table 5-4. Performance limits from the Rapid Chloride Permeability Test (RCPT), along with equivalent resistivity values of a saturated system (ASTM C1202) 80

Table 5-5.Chloride Ion Penetration Classification (AASHTO TP 95) 82

Table 0-1. Data collected from Bucket Test. 100

Table 0-2. Composition of Class-F fly-ash 101

CHAPTER 1: INTRODUCTION

Premature pavement distress and failure have become more frequent and severe due to increasing traffic volume, aggressive winter roadway maintenance practices, and increasing use of recycled materials (Cackler et al., 2017). Also, many concrete pavement mixture specifications are prescriptive-based, outdated, and incapable of verifying many vital engineering field properties. For example, the slump cone and pressure meter, which are used to determine the workability and air content of concrete, were introduced in 1922 and 1949, respectively. These equipment are still used to measure specification compliances but don't yield sufficient correlation with the field conditions and the causes of pavement deterioration. Current specifications generally use strength as the main indicator for concrete quality despite its limited correlation with durability (Taylor et al., 2014). A recent study shows that approximately 8% of the concrete pavements reviewed experienced premature deterioration or distress despite being compliant with the specifications at the time of the mixture design (Taylor, 2017). It is not unlikely for concrete pavement structure designed to last 10-plus years to start showing signs of premature distress and failure within the first few years of service despite following specifications. Thus, there is a need to develop more durable concrete mixtures with updated mixture specifications.

Increased durability in a concrete mix can be achieved by implementing the Performance Engineered Mixture (PEM) design procedure. Different tests conducted in the PEM procedure help to design and produce durable concrete mixtures. The other strategy for achieving a durable mixture for pavement and bridge deck is the use of fiber-reinforced concrete (FRC). The addition of fibers in a concrete mixture increases concrete durability by enhancing post-cracking performance. Structural fibers are known to improve the long-term performance of concrete pavements and overlays. Structural fibers increase the residual strength and Load Transfer Efficiency (LTE) of concrete when used in pavement. Even though the PEM procedure is relatively new, several research studies were conducted on the plain concrete (with no fiber) to establish the target specifications for the fresh concrete properties; however, this is not the same for fiber reinforced concrete. In a first attempt, this study focuses on establishing the target

values for various fresh concrete test parameters for the FRC for designing the mixture using the PEM procedure.

The objective of this research is to study the relationship between different fresh concrete properties and their influence on hardened concrete behavior and durability.The University of Minnesota Duluth (UMD) research team (Barman et al., 2018) and several other researchers completed studies that suggested the target values of hardened concrete properties for FRC. However, those studies did not implement the PEM design method. Under the scope of the current study, concrete mixtures were designed and tested according to the PEM design requirements with varying fresh concrete properties, fibers, and coarse aggregates. Fresh concrete tests such as slump, air content, Super Air Meter (SAM), Box, and V-Kelly tests were conducted. These tests measure the engineering properties of concrete that are essential to pavement performance. SAM number characterizes the resistance of concrete to freeze-thaw distress, and Box test ratings assess the response of concrete to vibration and its ability to hold its shape without crumbling during slip-form paving application. V-Kelly test examines the workability of concrete mixture and its response to vibration.

1.1 THESIS ORGANIZATION

Chapter 1 presents an introduction to the work conducted in this research. Chapter 2 consists of a comprehensive literature review on current research studies on PEM, implementation status of PEM design in the US, PEM program updates, challenges in PEM design implementation, use of FRC , and fresh and hardened concrete properties of FRC. Chapter 3 discusses the research methodology, and present the details about materials used. The laboratory tests are provided in Chapter 4. Chapter 5 presents the test results along with the analysis and discussion of the findings. Chapter 6 presents the conclusions and recommendations.

CHAPTER 2: LITERATURE REVIEW

2.1 PERFORMANCE ENGINEERED MIXTURE

Advances in testing technology over the years have allowed the concrete pavement industry to recognize the strengths and weaknesses of concrete materials in a better way and helped to iron out many of the concrete's durability challenges that create obstacles to sustainability. In the concrete pavement context, sustainability focuses on developing concrete mixtures that are more efficient in their usage of materials yet do not compromise engineering performance (Taylor et al., 2014). The PEM design procedure assesses the quality of concrete based on what it encounters in the field during pouring and its service life. The goal of the PEM mixture design procedure is to produce concrete mixtures that resist climate- and material-related distresses, such as freeze-thaw damages and concrete degradation due to chloride-ion penetration. Some important factors affecting the efficiency of the PEM design method are discussed in this section.

2.1.1 Aggregate Durability

The type of aggregate used in a concrete mixture can have a significant impact on concrete pavement performance. The aggregates used in a concrete mixture encounter distress when the concrete structure is exposed to extreme heat, cold, moisture, chemical deicers, and freeze-thaw (Cackler et al., 2017). To ensure the durability of aggregates in a concrete mixture, the PEM method specifies the following:

I. Coarse aggregates pass specific freeze-thaw requirements and are not prone to fracture/dilation when subjected to harsh winter conditions (Cackler et al., 2017).
II. Coarse aggregates are not prone to alkali-silica reactivity (ASR) or alkali-carbonate reactivity (ACR); Supplementary Cementing Materials (SCM) should be used, if necessary.

2.1.2 Fluid Transport Property

Transport properties of a concrete pavement material help assess the resistance of materials against failure due to alkali-carbonate reaction (ACR), chloride penetration, and freeze-thaw. The PEM design requires that an electrical/surface resistivity test (AASHTO TP95, 2011) should be conducted to evaluate the transport properties of concrete. The test method is based on the understanding that solid concrete is a poor conductor of electricity compared to concrete with fluid-filled pores. Therefore, the resistivity of concrete is lower when the volume and connectivity of the pore system are higher (Cackler et al., 2017). Figure 2-1 shows the resistivity test in progress.

Figure 2-1. Resistivity test setup

The fluid transport property in the PEM method is controlled by:

I. Maintaining water-cementitious material ratio between 0.40 and 0.45 to reduce capillary pore volume and connectivity while avoiding undesired shrinkage.
II. Encouraging the use of advance SCMs at a specified dosage to improve the long-term transport performance.
III. Controlling concrete mixture hydration time and temperature, especially in cold climate regions, to resist freeze-thaw damage.

2.1.3 Cold Weather Resistance

The PEM design uses ASTM C666 test method to determine the resistance of concrete against rapid freezing and thawing in cold climate regions. Figure 2-2 shows the critical saturation values of concrete and indicates that freeze-thaw damage is more likely when the concrete is saturated (Cackler et al., 2017). The figure illustrates that air-entrained concrete has a lower saturation rate and a lower risk of freezing damage than the concrete mix with entrapped air voids.

To protect concrete from freeze-thaw damage, PEM method suggests the inclusion of an air-entraining admixture (AEA) in the mixture. The addition of AEA aids in stabilizing spherical air voids (0.0005” to 0.05” in dia.) and yields better workability while lowering segregation and bleeding (Ley, 2015). However, the compressive strength of concrete decreases by approximately 500 psi for every 1% increase in air content (Ley, 2015).

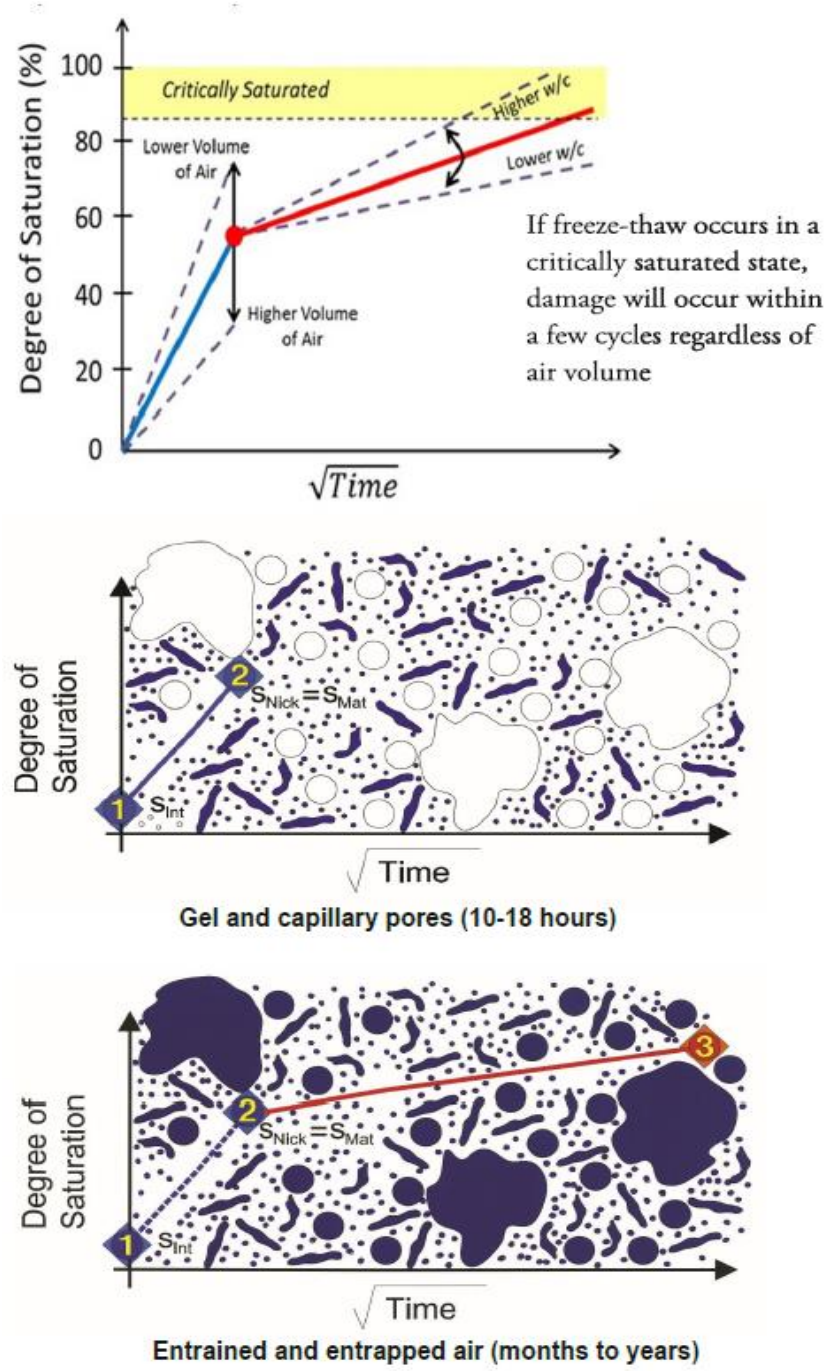

Figure 2-2. Time vs. degree of saturation (Cackler, 2017)

Super Air Meter (SAM) was developed by Oklahoma State University to measure the quality of air void system in fresh concrete. The SAM test, as described by AASHTO TP 118, provides a SAM number that defines air bubble spacing**.** Figure 2-3 and Figure 2-4 show results of 300 unique concrete mixtures (prepared in the laboratory and field)

comparing the SAM number to spacing factor (bubble spacing) and durability factor in freeze-thaw testing, respectively (Ley 2015). The spacing factor illustrates the air-void system quality, and the durability factor indicates the concrete performance in a freeze-thaw cycle. A SAM number of 0.20 (corresponding to the spacing factor = 0.008 inches and durability factor = 70%) or below is recommended for plain concrete mixtures subjected to harsh climate regions that include freezing and thawing. Barman and Hansen (2018) found that concrete mixtures with steel fibers consistently had a higher SAM number of more than 0.20 (Figure 2-5). It is observed that an increase in entrained air content decreased the SAM number, and a large set of SAM numbers were above 0.2.

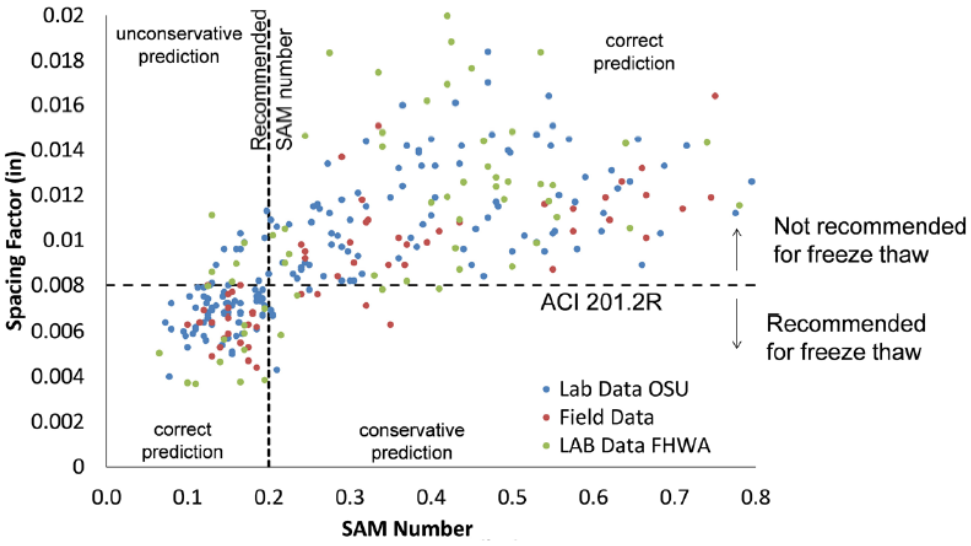

Figure 2-3. Spacing factor vs SAM number (Ley, 2015)

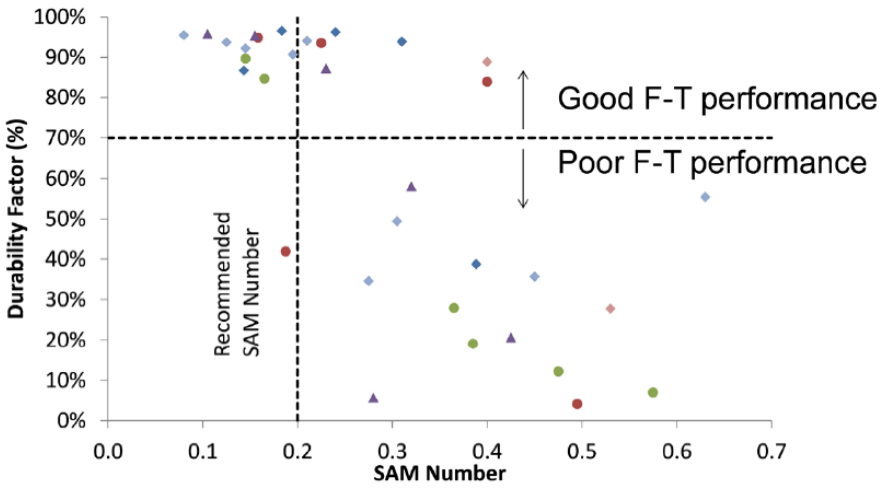

Figure 2-4. SAM number vs durability factor as a result of freeze-thaw testing (Ley, 2015)

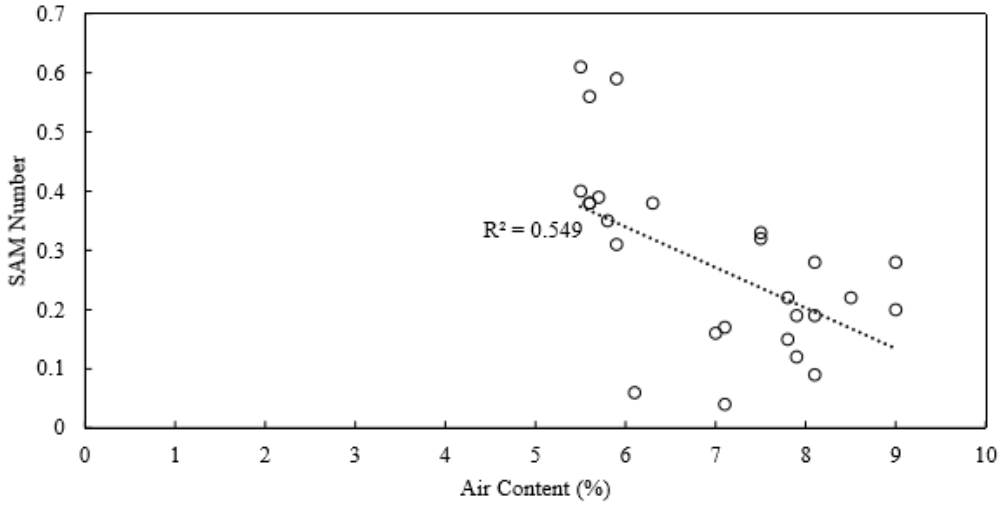

Figure 2-5. SAM number as a function of air content (Barman and Hansen, 2018)

2.1.4 Shrinkage

Concrete pavements experience plastic and drying shrinkage due to moisture evaporation, uniform temperature change, temperature gradients, and moisture gradients. Upward and downward curvatures are caused due to temperature gradients during the night-time (warmer bottom) and daytime (warmer surface) conditions, respectively (Cackler et al., 2017). Figure 2-6 depicts moisture warping and temperature curling in concrete pavements.

Figure 2-7 shows drying shrinkage phases of a concrete structure as the bottom remains saturated and the surface undergoes a drying and wetting cycle (Mindess et al., 2008). Drying and wetting cycles allow concrete pavements to recover some shrinkages, but some of the shrinkages remain irreversible. As shown in Figure 2-8, concrete swells when it is stored in water and shrinks when stored in air (Cackler et al., 2017). The swelling and shrinking continue until the concrete attains ultimate shrinkage.

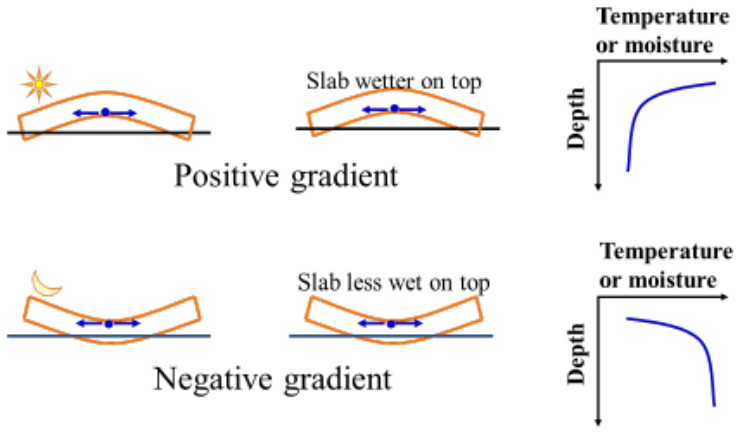

Figure 2-6. Concrete moisture warping and temperature curling (Mack 2009)

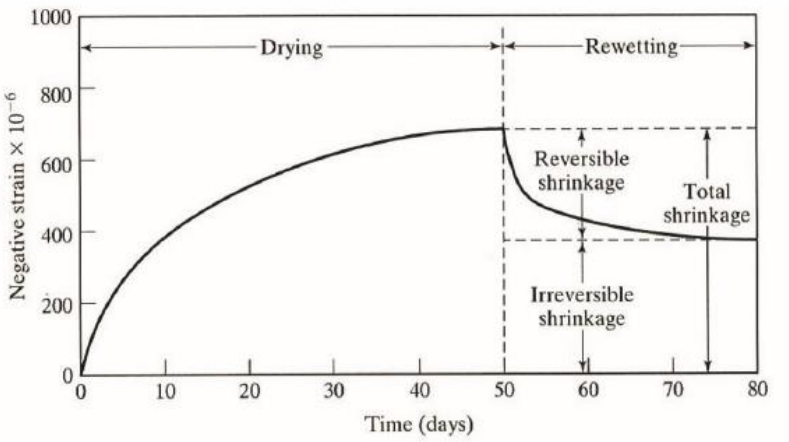

Figure 2-7. Strain vs. time graph of drying shrinkage components (Mindess et al., 2008)

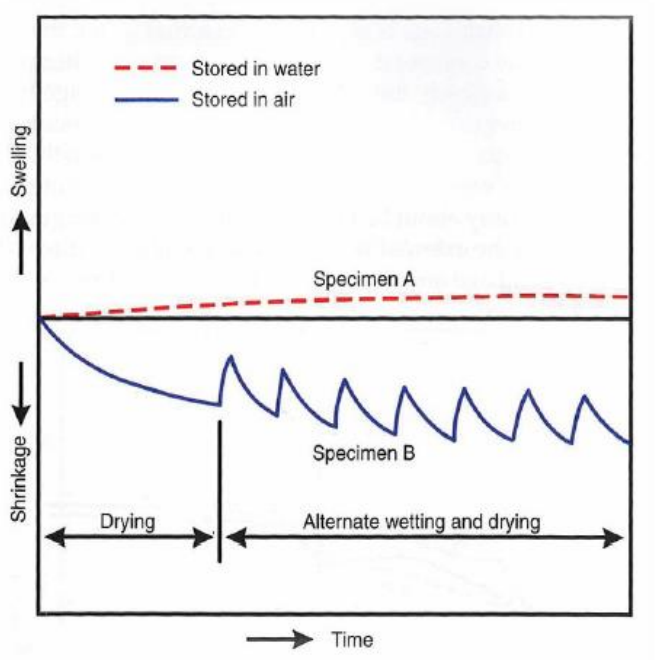

Figure 2-8. Long-term alternate wetting and drying shrinkage (Komatska and Wilson, 2016)

Destree et al. (2016) introduced a model to predict shrinkage cracking and curling of slabs subjected to restraint by ground friction and fiber bridging. The model simulates the sequential development of multiple cracks and opening responses because of shrinkage. The model showed that an increase in fiber content, interfacial bond strength, and ground friction could reduce the average crack width (ACI.544.4R-18). In comparison with field data of several slabs, the simulated model results accurately predicted crack openings (ACI.544.4R-18). To reduce the effect of moisture warping and curling due to shrinkage, the PEM design recommends the following (Cackler et al., 2017):

I. Sufficient curing.
II. Reduced permeability.
III. Low paste volume or reduced cementitious material and increased aggregate volume.
IV. Good pore system in the concrete structure.

2.1.5 Strength

Concrete pavement strength is defined as its ability to carry static and dynamic loads (Taylor, 2017). Although concrete's strength is a key element needed to assure structural performance, it does not fully measure concrete pavement's potential to sustain serviceable performance when subjected to harsh environmental conditions. PEM design provides durable and workable concrete pavements that meet the strength criteria necessary to ensure serviceable performance under local environmental conditions. In the PEM method, special attention is given to the aggregate gradation and paste system to achieve the desired strength.

2.1.5.1 Aggregate Gradation

Aggregate properties have more influence than cement content on the performance of concrete mixtures at a specific water-cement ratio (Dhir et al., 2006). Angular aggregates with rough textures are preferred (Taylor et al., 2014). Determining the aggregate percentage in a concrete pavement mixture is critical for mixture consolidation and cohesiveness. A well-graded aggregate gradation is necessary to reduce water demand, provide sufficient workability, lower paste requirement, and increase the strength and durability of the pavement (Delatte, 2007; Taylor et al., 2014). The gap-graded aggregate system consists of a blend of material with high and low quantities retained on different sieve sizes (Ley et al., 2014). In comparison, the well-graded aggregates system consists of aggregates retained on adjacent sieve sizes (Ley et al., 2014). The Tarantula Curve (Ley, 2014), shown in Figure 2-9, provides gradation limits to select the optimum aggregate gradation in the PEM design procedure. The theoretical optimum gradation is obtained by fitting the combined gradation of aggregates within the boundaries of the tarantula curve.

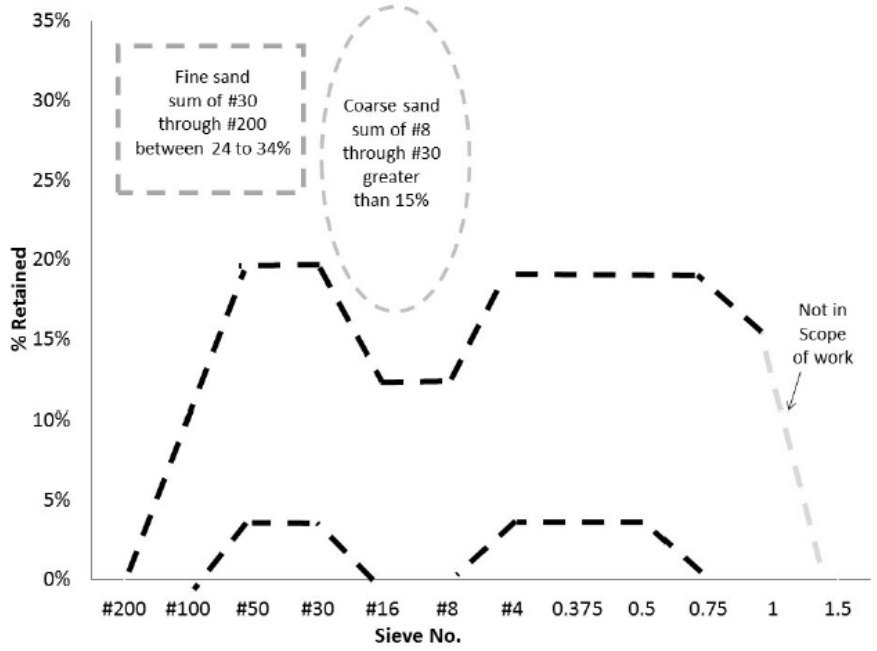

Figure 2-9. Tarantula curve showing recommended limits for aggregate gradation (Ley and Cook, 2014)

2.1.5.2 Paste System

The Hydrated Cement Paste (HCP) requirement in a concrete mixture is dependent on the amount of paste needed to hold the aggregate particles together. Too much paste can reduce design strength and design life (Cackler et al., 2017). SCMs (such as fly-ash) can be added to concrete mixtures to reduce Alkali-Silica Reaction (ASR) and mitigate calcium oxychloride formation. Figure 2-10 shows that the addition of fly-ash reduces calcium oxychloride formation. Other benefits of adding SCM to concrete mixtures are:

I. Reduced heat of hydration.
II. Increased chloride penetration resistance due to reduced permeability.
III. Less water needs to reach workability.
IV. Increased overall strength of concrete after curing.

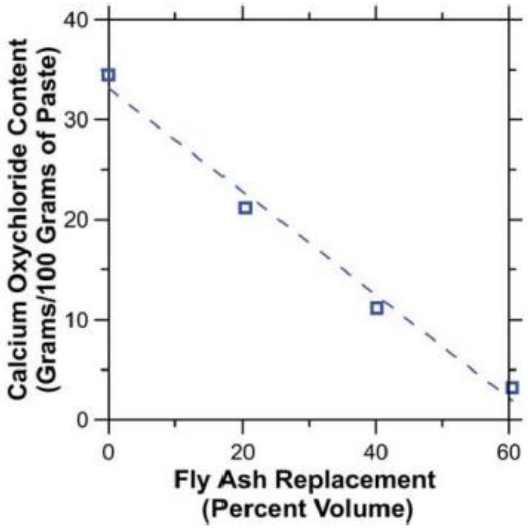

Figure 2-10. Influence of fly-ash in reducing calcium oxychloride content (Cackler et al., 2017)

2.1.6 Workability

PEM design requires workable concrete mixtures that can be easily placed without compromising strength and durability. On the other hand, the concrete mixture needs to remain stable in shape after the consolidation process is finished. This requires that the aggregate volume and gradation of a concrete mixture be carefully selected to control the creep and stiffness of the mixture. The aggregate gradation meeting the tarantula gradation criteria is likely to provide good workability. Cook et al. (2013) found that the percent retained chart is the most reliable method for determining optimum aggregate gradation.

The constructability of a concrete mixture is also critical. The addition of fibers into a concrete mixture can influence the slump of the mixture. It is recommended to add/increase water-reducing admixture or increase cementitious material (paste volume) to maintain workability and slump without compromising the water-cement ratio (ACI.544.4R, 2018). The two newly developed tests, Vibrating Kelly Ball (V-Kelly) test, and Box test, are an upgrade from the slump test.

The V-Kelly test is used to assess the workability and response to vibration of the concrete mixture (Cackler et al., 2017). The Box test is conducted to investigate the

thixotropic properties of concrete mixtures, i.e., the impact of vibration on the concrete mixture and its ability to hold an edge after vibration (Cackler et al., 2017).

2.2 FIBERS

Fiber reinforced concrete structure is developed by adding fibers to the plain concrete mixture. Unlike plain concrete, FRCs are more durable and ductile with a better post-crack performance. Structural fibers improve the post-crack performance of concrete by keeping cracks tight (Barman et al., 2018). Cracks held closer by fibers help reduce the panel fatigue crack severity and increase the load transfer between concrete slabs (Barman et al., 2018). This effect decreases joint deterioration and joint faulting. The ingredients and properties of FRC are discussed in subsequent sections.

Structural fibers improve the long-term performance of concrete pavements and overlays. The state of Minnesota has been using synthetic structural fibers in concrete pavements and overlays for many decades. Fibers are classified into two categories, micro (diameter < 0.3mm) and macro (diameter ≥ 0.3mm), and have varying lengths, geometries, and shapes. ASTM C1116 categorizes fibers into four types:

- Type I (Steel Fiber-Reinforced Concrete) – made with alloy, stainless or carbon steel fibers.
- Type II (Glass Fiber Reinforced-Concrete) – made with glass fibers that resist alkali.
- Type III (Synthetic Fiber-Reinforced Concrete) – made with synthetic fibers.
- Type IV (Natural Fiber-Reinforced Concrete) – made with natural fibers.

Unlike plain concrete, FRCs do not fail immediately after a fracture upon cracking. Figure 2-11 shows the fibers bridging a crack. As illustrated in Figure 2-12, the fibers in FRC mixtures provide post-crack support and control crack propagation while allowing the concrete to withstand residual loads. It can be seen that FRC is able to hold some amount of load after crack development.

Figure 2-11. Crack control and bridging effect of fibers (Gaddam, 2016)

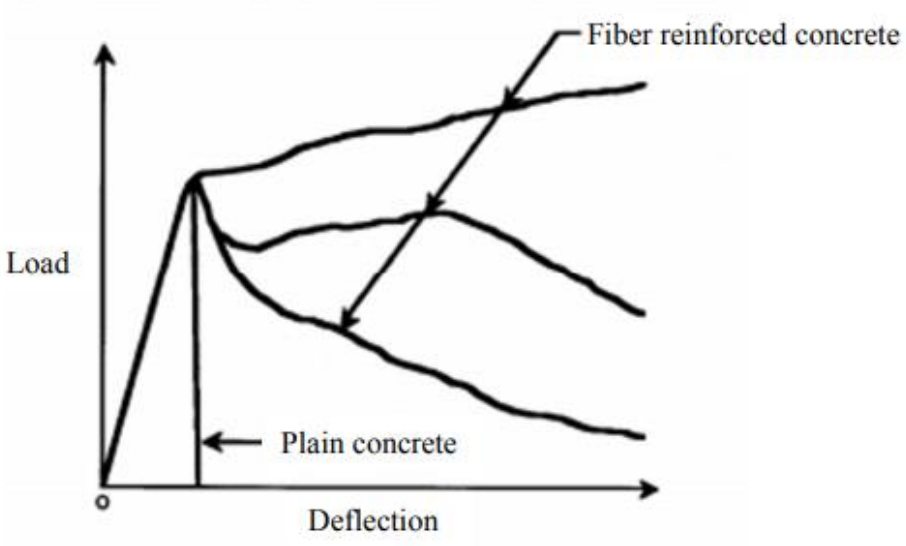

Figure 2-12. Illustration of load vs deflection in plain concrete and FRC (after ACI Commitee 544, 2009)

The area under the load-deflection curve, depicted in Figure 2-12, is the toughness of the FRC. This is a representation of the energy absorbed by the FRC due to the load it had to withstand. Fiber failure occurs when fibers can no longer sustain loads (ACI 544.4R, 2018). As shown in Figure 2-13, it occurs through various phases such as debonding and sliding between fiber and matrix, frictional sliding, fiber pullout, and fiber rupture (ACI 544.4R, 2018).

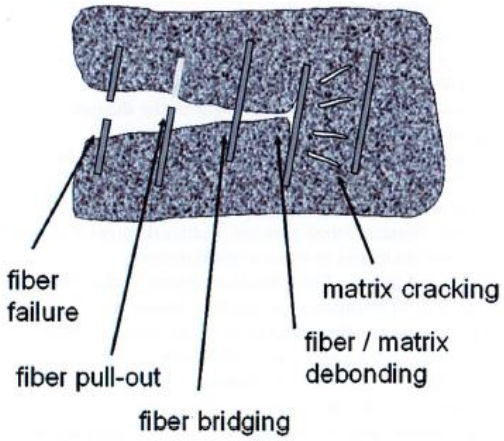

Figure 2-13. Stages of FRC failure (ACI.544.4R-18)

Strain softening occurs when the FRC residual strength decreases as crack width and deflection increase (ACI 544.4R, 2018). This occurs when a crack is held together by very few fibers and the ultimate tensile strength is greater than post cracking tensile stress. Whereas, during strain hardening, the residual strength of FRC increases as crack width and deflection increases (ACI 544.4R, 2018). Figure 2-14 shows that the number of fibers in a concrete mixture affect the strain softening and hardening behaviors of FRC.

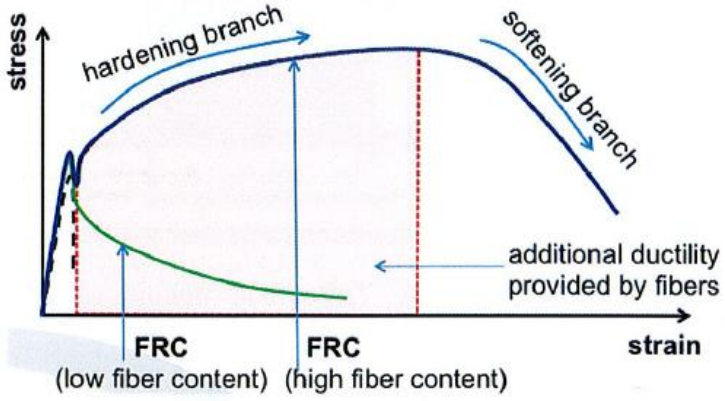

Figure 2-14. Strain softening and hardening behaviors (ACI.544.4R-18)

2.2.1 Steel Fiber Reinforced Concrete (SFRC)

Steel fibers are mostly used in industrial flooring with limited applications in concrete pavements. Since 2017, MnDOT has used steel fibers in concrete bridge decks to control cracking. Figure 2-15 shows various geometries of commonly available commercial steel fibers. As shown in Figure 2-16, steel fibers with a hooked end enhance the resistance to pullout from the concrete matrix (Komatska and Wilson, 2016).

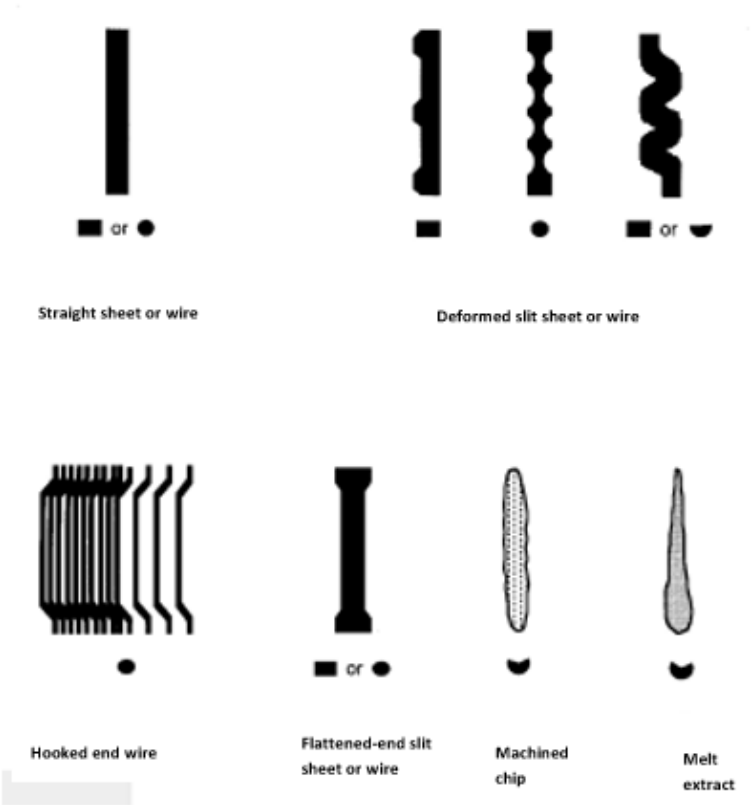

Figure 2-15. Various steel fiber geometries (Komatska and Wilson 2016)

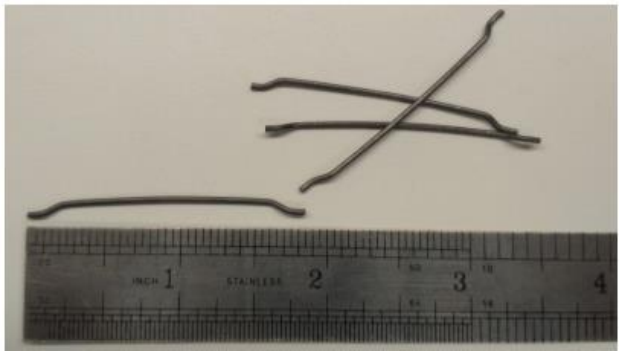

Figure 2-16. Steel fibers with hooked end (Barman, 2018)

Generally, the volume fraction of steel fibers varies from 0.25% to 2% in a concrete mixture. The workability of SFRC is reduced when the fiber volume fraction is greater than 2%, and there is an uneven distribution of fibers in the concrete mixture (Komatska and Wilson, 2016). Uniform dispersion of fibers reduces the path of bleeding water, thus lowering the potential of water movement to the surface. Acikgenc et al. (2013) observed that slump value reduced as the fiber dosage increased (Figure 2-17**)**. The study also showed tha mixture compactibility was linearly related to steel fibers aspect ratio (ratio of length to diameter) and fiber volume fraction (Acikgenc et al., 2013).

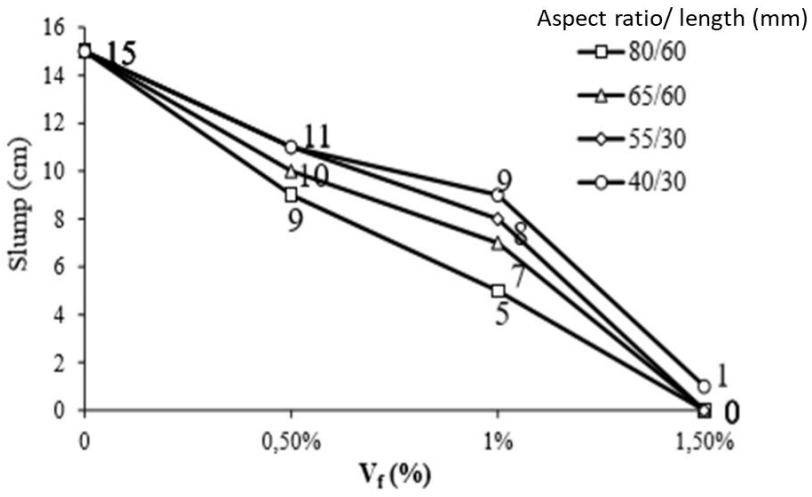

Figure 2-17. Slump test output (Acikgenc et al., 2013)

It has also been found that fiber-reinforcement has little to no impact on the free drying shrinkage of fresh concrete (Komatska and Wilson, 2016). Nevertheless, steel

fibers slow down the fracture of restrained concrete during shrinkage and enhance the creep characteristics of concrete (Komatska and Wilson, 2016). Steel fibers in SFRC cause more cracks due to internal stresses, but the crack widths are much narrower compared to conventional concrete.

The Louisiana Transportation Research Center (LTRC) investigated the fatigue and toughness characteristics of FRC prepared from polypropylene fibrillated, polypropylene macro, carbon, and steel fibers in concrete pavements (Kevern et al., 2016). The properties of fibers are provided in Table 2-1. Figure 2-18 shows pictures of different fibers used in that study. In general, it was found that polypropylene fibers performed better than steel fibers against fatigue when used in correct dosages. Regarding the toughness of the concrete, this study suggests that fibers with high tensile strength results in better residual load carrying capacity and carry a greater load at larger deflections.

Figure 2-18: Fibers used in the (Kevern et al., 2016) study: polypropylene fibrillated fiber (left), polypropylene macro fiber (left middle), carbon fiber (right middle) and steel fiber (right)

Table 2-1. Properties of fibers in Kevern et al. (2016) study

Properties of reinforcing fiber			
Fiber Type	**Specific Gravity**	**Length (in.)**	**Tensile Strength (ksi)**
Polypropylene Fibrillated	0.91	1.50	83-96
Polypropylene Macro	0.91	2.25	83-96
Carbon	1.70	4.00	600
Steel	7.85	2.00	152

The fatigue property of the concrete was studied by applying cyclic load on the pre-notched beam specimens as per RILEM procedure developed by Jenq and Shah

(1985). Pre-notched fatigue testing showed that both the tensile strength and length of fibers influence the fatigue properties of fibers. This study provided the following conclusions: (i) polypropylene fibrillated fibers offered increased fatigue performance but did not offer any significant post-crack performance, (ii) polypropylene macro fibers used at a dosage between 7.5 lb/yd^3 and 10.5 lb/yd^3 provided the highest fatigue, toughness, and pre-notch fatigue performance, and (iii) the use of fiber reinforcement resulted in a reduced pavement thickness.

Komatska and Wilson (2016) concluded that compared to concrete without steel fibers, the addition of 1.5% by volume of steel fibers increased the tensile strength and flexural strength by up to 40% and 150%, respectively. Figure 2-19 (a) indicates that the compressive strength of SFRC decreased beyond 1% fiber volume fraction, possibly due to higher voids in the specimen. It is also observed from Figure 2-19 (b) that longer steel fibers (60 mm) with a larger aspect ratio (80) were more effective in increasing the flexural strength of concrete mixtures.

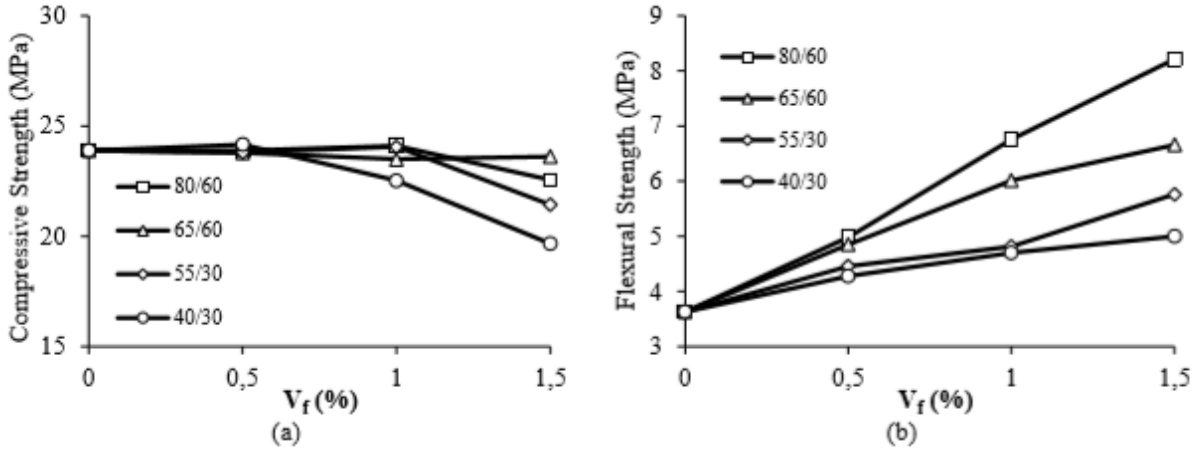

Figure 2-19. SFRC strength at 28-day: a) Compressive strength, and b) Flexural strength (Acikgenc et al., 2013)

Arnold et al. (2005) conducted a joint performance study of SFRC; it was found that an increase in fiber dosage resulted in a decrease in peak differential displacement. Figure 2-20 shows the effect of fiber reinforcement on peak differential displacement. It can be seen that when fiber was used in the concrete mixture, failure occurred at a wider crack width indicating the benefit of fibers in increasing the joint load transfer.

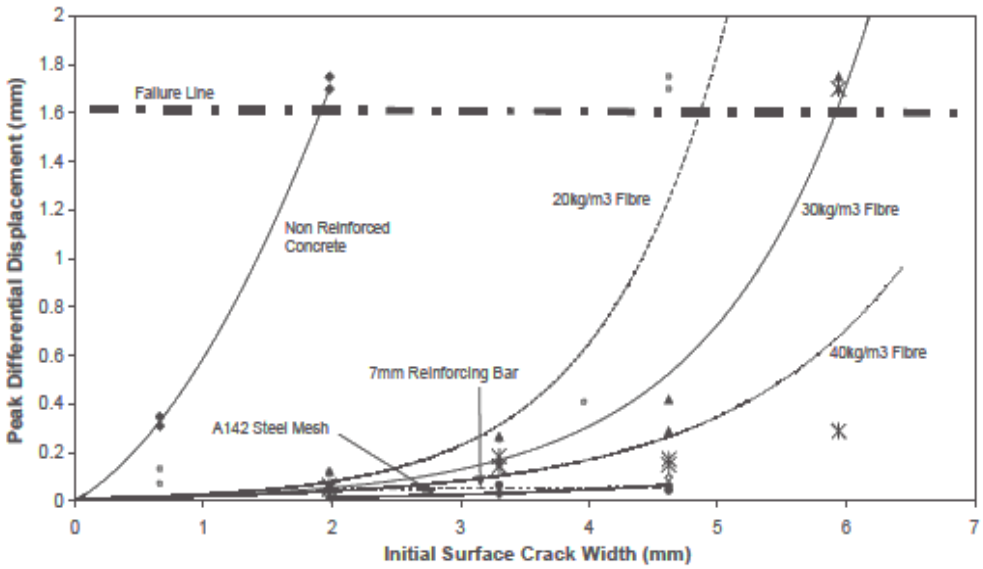

Figure 2-20. Effect of fiber reinforcement in peak differential displacement (Arnold et al., 2005)

Sukontasukkul et al. (2018) found that SFRC showed a more consistent load-carrying capacity and reduced residual strength and toughness with an increase in temperature. The influence of fire on FRC residual strength may be less critical to the pavement, but it is crucial in the context of roadway bridges.

The freeze-thaw durability of SFRC is comparable with that of plain concrete when the SFRC mixture is air-entrained, compacted adequately, and modified to integrate steel fibers (Komatska and Wilson, 2016). The bond between steel fibers and cement matrix can be improved with increased surface roughness or mechanical anchorage and can be protected from corrosion by the alkaline environment in the cement matrix p rovided that the modulus of elasticity is relatively high (Komatska and Wilson, 2016).

2.2.2 Synthetic Fiber Reinforced Concrete (SyFRC)

Synthetic fibers are the most common fiber types used in concrete mixtures. A survey showed that 94% of FRC pavements in the United States included synthetic fibers, and the other 6% included steel fibers (Barman, 2018). Most FRC pavement overlays constructed in recent years have structural synthetic fibers. Several studies exploring the properties and performance characteristics of synthetic FRC were conducted in Illinois (Bordelon, 2011; Roesler et al., 2008; Bordelon, 2005). They considered the impact of

certain factors on the performance of FRCs such as the shape (straight, crimped and twisted), type, dosage, length, diameter, and aspect ratio of fibers. Table 2-2 presents fiber properties and a few hardened concrete test results for the FRC mixtures prepared with three different synthetic fibers in the Roesler et al. (2008) study. The peak flexural load and Modulus of Rupture (MOR) values varied slightly with the dosage, shape, and aspect ratio of the fiber, but a certain trend was not observed. Dosage of 4.5 lb/yd^3 in the straight synthetic fiber category and 4.6 lb/yd^3 in the twisted synthetic fiber category had the highest peak flexural load and MOR values, respectively.

Table 2-2. Properties of structural synthetic fibers and FRC in Roesler et al. (2008) study

Fiber type	**Straight synthetic**				**Twisted synthetic**		**Crimped synthetic**
Cross section	Rectangular				Rectangular		Rectangular
Length (in)	1.57				2.13		2.00
Thickness (in)	0.004				NA		0.03
Width (in)	0.05				NA		0.05
Aspect ratio	90				NA		46
Specific gravity	0.92				0.91		0.91
Volume fraction in the mix (%)	0.19	0.26	0.29	0.58	0.30	0.50	0.40
Dosage used (lb/yd^3)	3.00	4.00	4.50	8.90	4.60	7.70	6.10
Peak flexural load (lb)	6623	5472	9276	8939	8101	6487	8160
Modulus of rupture (psi)	556	456	733	745	675	541	673
Testing age (days)	14	14	14	14	14	14	14

According to Figure 2-21, straight synthetic fibers performed better in terms of MOR values than the other two shapes. Bordelon (2005) found that the post-crack residual load capacity increased with the increase in fiber volume fraction (Figure 2-22). It was also observed that FRC with 0.58% fiber volume fraction had a greater residual load capacity than the mixture with 0.26% volume fraction.

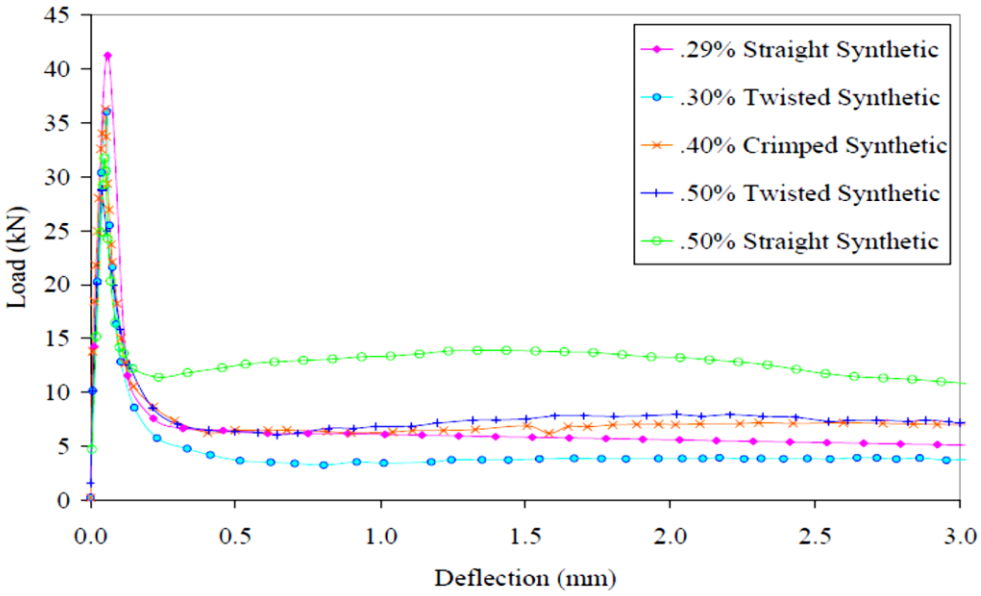

Figure 2-21. Residual load characteristics of different shaped structural synthetic fibers (Bordelon, 2005)

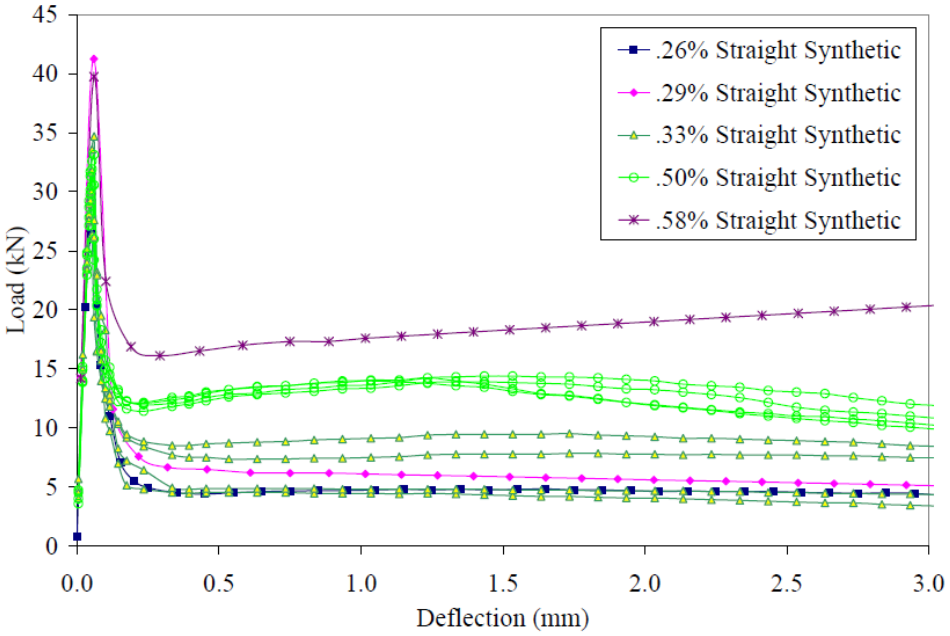

Figure 2-22. Residual load capacities of FRC vs. fiber volume fraction for synthetic fibers (Bordelon, 2005)

Macro-fibers, also called structural fibers, form a mechanical bond with concrete due to friction. They are used to extend joints or produce jointless concrete slabs to

reduce the maintenance cost of a concrete structure during its design life. Recently, a synthetic polyolefin-based macro-fiber was developed that creates chemical bonds in concrete (Attiogbe, 2014; Komatska and Wilson, 2016). Synthetic macro-fibers, with a volume fraction of 0.2 to 1% of concrete, enhance the concrete drying shrinkage crack control. Alhassan and Ashur (2012) reported that certain benefits of adding fibers in bridge overlays include reduction in shrinkage cracking, increase in toughness, additional post-crack strength, and increase in crack resistance. They also found that drying shrinkage was 17% lower in FRC mixtures than the plain concrete mix. Figure 2-23 shows the results of shrinkage vs. curing time for various combinations of plain and fiber reinforced concrete mixes.

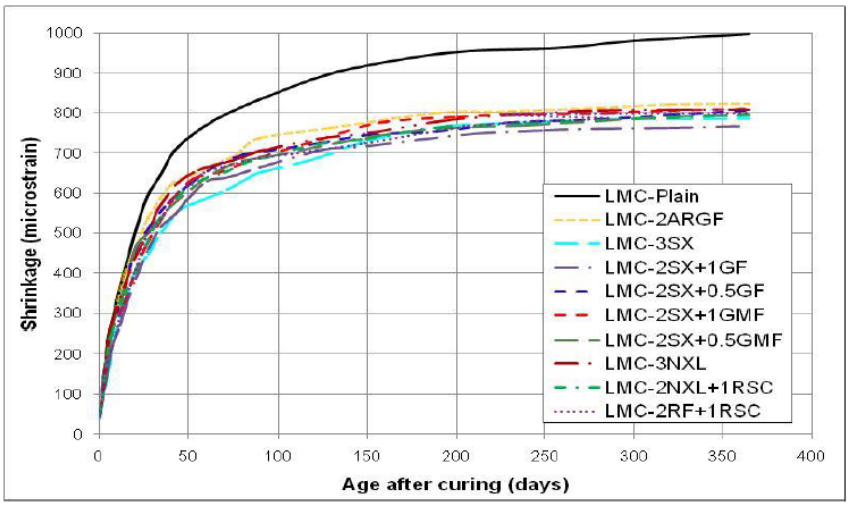

Figure 2-23. Shrinkage vs. curing time for plain and FRC mixes in Alhassan and Ashur (2012) study (LMC = latex modified concrete; ARGF = alkali resistant glass fiber; SX= microtype polyolefin fiber; GF = micro type 100% virgin; NXL = macrotype polyolefin fiber; RSC = microtype polyvinyl alcohol fiber; RF = macrotype polyvinyl alcohol fiber).

The study recommended a synthetic fiber content of 3 lb/yd^3 for bridge overlays. At fiber contents near 3 lb/yd^3, drying shrinkage was reduced by 15% and flexural strength increased due to internal confinement. It was also recommended that fibers should be held between 0.75 inches and 1.75 inches in length.

Synthetic macro fibers affect the hardened concrete mechanical properties in various ways depending on the type of synthetic fiber used in the mixture. The key impact of using synthetic macro fibers in hardened concrete is the increase in flexural

toughness, which is defined as the measure of energy absorption capacity (Komatska and Wilson (2016). This effect also improves the fatigue and shatter resistance of FRC and decreases crack propagation. The impact of synthetic fibers on the post-crack performance of concrete is an important factor for their use in concrete pavements and overlays. Acrylic fibers enhance the post-crack toughness and ductility, aramid fibers improve the resistance to creep, static, and dynamic fatigue, and nylon fibers improve toughness, tenacity, and elastic recovery (Komatska and Wilson, 2016). At a higher dosage of synthetic fibers (1.5% volume fraction), there maybe be negligible effect on the hardened concrete compressive strength. However, the tensile strength can be improved by 80% (Barman and Hansen, 2018).

Issa (2017) studied the effect of early-age properties of FRC on the fatigue damage of concrete pavements. It was found that the synthetic fibers did not have a significant influence on the compressive strength and flexural strength of concrete mixes. However, flexural toughness increased with an increase in fiber dosage. The authors also observed that the fibers with embossed and deformed texture provided better bonding within the concrete mix. Relative dynamic modulus (RDM) tests were also performed, and it was concluded that fibers did not contribute significantly towards concrete durability against freeze-thaw cycles. ASTM C666 specify a minimum RDM of 60% for concrete with good freeze-thaw durability. It was also noticed that the mixes with a higher dosage of synthetic fibers showed increased resistance to scaling by a higher degree.

Barman and Hansen (2018) conducted a comprehensive laboratory study with nine different synthetic fibers of different geometries, lengths, aspect ratios, and stiffness values (Table 2-3).The effect of low, intermediate, and high dosages (0.25, 0.50, and 0.75 percent volume fraction) for each fiber type was studied.

Table 2-3.Summary of fiber details from Barman and Hansen (2018) Study

Fiber Serial Number	Geometry / Type	Length (inch)	Aspect ratio, specific gravity, modulus of elasticity (ksi), tensile strength (ksi)
Fiber 1	Straight / Synthetic	1.5 or 2	*94, 0.91, N/A, 70
Fiber 2	Straight / Synthetic	1.5 or 2	*100, 0.91, N/A, 70
Fiber 3	Straight / Synthetic	1.55	90, 0.92, 1378, 90
Fiber 4	Straight / Synthetic	*1.63	96.5, 0.91, N/A, 70
Fiber 5	Twisted Straight / Synthetic	2	74, 0.92, 1380, 87-94
Fiber 6	Continuously Crimped / Synthetic	2.0	*60, 0.91, N/A, N/A
Fiber 7	Embossed / Synthetic	2.1	70, 0.91, N/A, 85
Fiber 8	Embossed / Synthetic	1.89	*66, 0.90-0.92, 1450, 93
Fiber 9	Embossed / Synthetic	2.1	70, 0.91, N/A, 85

**Measured, not found in manufacturer's sheet.*

It is observed from Figure 2-24 (a) and (b) that the compressive strength and modulus of elasticity of synthetic FRC were minimally influenced by the increase in the Reinforcement Index (RI). The reinforcement index is the product of the aspect ratio (AR) and volume fraction (V_f) of fibers. Figure 2-24 (d) shows that the modulus of rupture varied inconsistently with the change in fiber property and V_f.

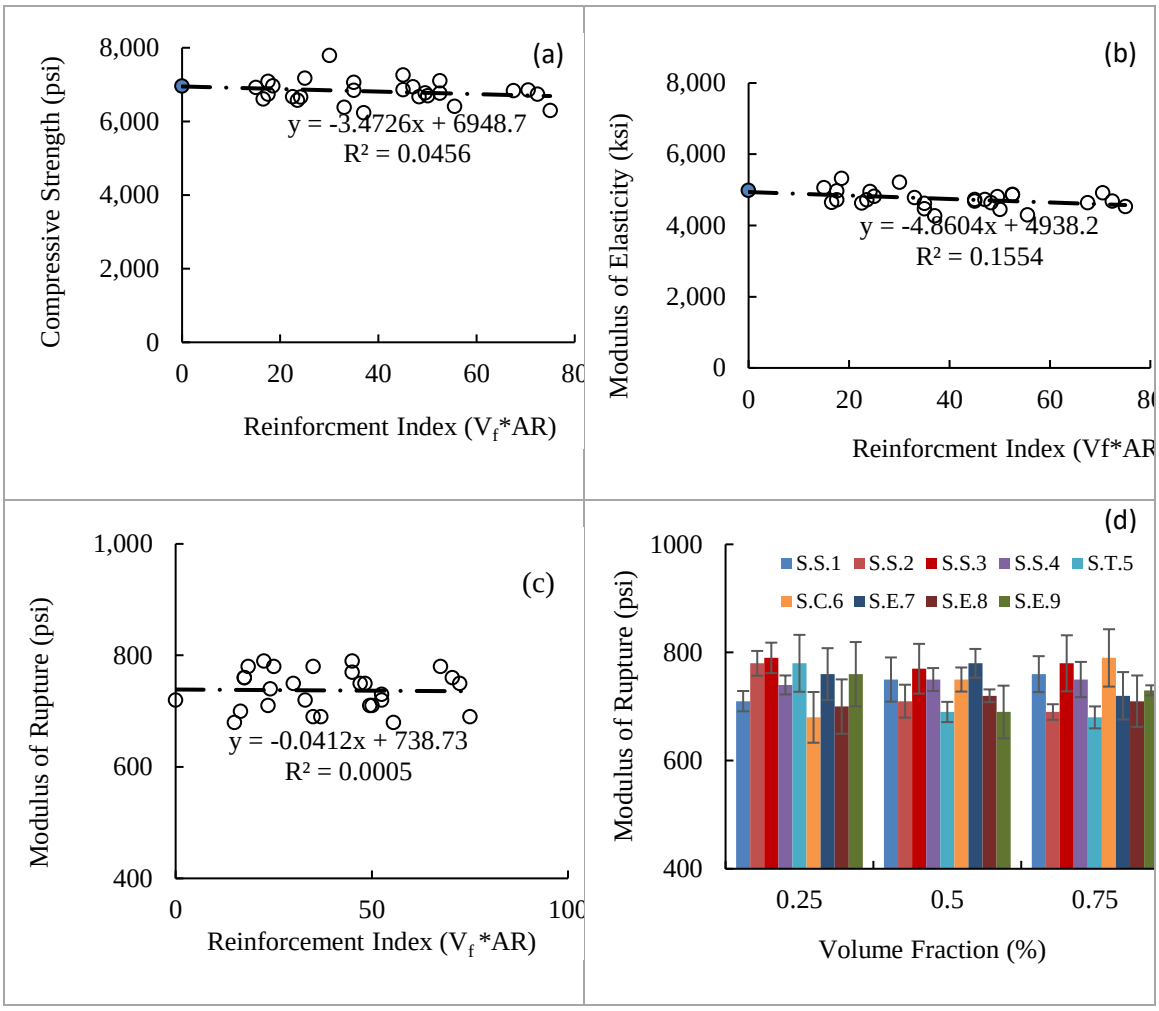

Figure 2-24. (a) Compressive strength, (b) Modulus of elasticity, and (c) and (d) Modulus of rupture as a function of reinforcement index and fibers' volume fraction.

It can be seen from Figure 2-25 (a) that the Residual Strength Ratio (RSR) increased greatly with an increase in V_f for all fiber types. Overall, the RSR and V_f had an excellent correlation ($R^2 = 0.86$). It was concluded that embossed, twisted, and crimped fibers have better RSR and Residual Strength (RS) values than straight synthetic fibers (Figure 2-25 (d)).

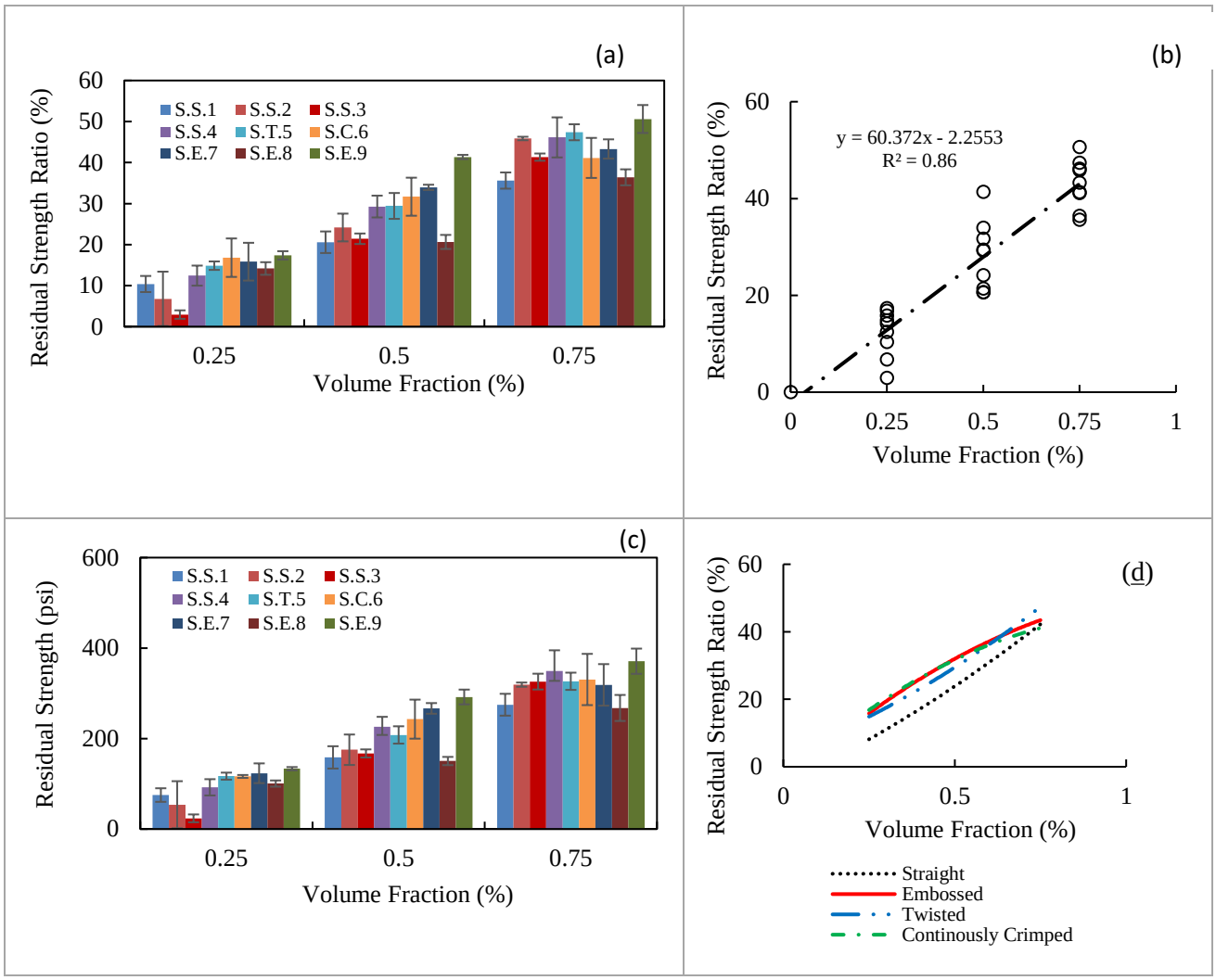

Figure 2-25. (a) RSR vs. Vf, (b) Correlation between RSR and Vf, (c) RS vs. Vf, (d) RSR as a function of Vf and fiber geometry.

Load Transfer Efficiency (LTE) measures the ability of concrete to transfer loads across adjacent slabs to reduce interlayer debonding. Barman and Hansen (2018) found that FRC made with 5.25 to 6.5 lb/yd^3 structural synthetic fibers transferred 20% more load than plain concrete slabs. However, the LTE of FRC decreased with the increase in crack width and number of load applications due to abrasion of crack faces. Nevertheless, structural synthetic fibers did not experience significant fatigue even after millions of load repetitions (Barman, 2014).

Minimal research has been done to understand the freeze-thaw resistance of SyFRC. Similar to SFRC, SyFRC must be air-entrained and consolidated as it is

susceptible to concrete degradation due to freeze-thaw damage (Vondran, 1987; Barman, 2014). Barman et al. (2019) stated that the inclusion of synthetic fibers in the concrete mixture could improve pavement durability against surface spalling.

The addition of synthetic fibers decreases the workability (slump) of a concrete mix. Although less workability is an issue in achieving required consolidation, a reduction in workability may increase the cohesiveness of concrete under the paver, which can improve slip-form characteristics (Ludirdja and Yougn, 1992).

Barman and Hansen (2018) found that the addition of certain synthetic fibers had a significant effect on the failure mode of specimens in various test procedures. For example, compressive strength specimens failed in a ductile manner and rarely exhibited explosive failure.

2.3 CONCLUSION

This chapter provided an introduction to PEM design procedure and fibers for FRC, along with fresh and hardened concrete properties of FRC. The literature review discussed the key engineering parameters (aggregate durability, fluid transport property, cold weather resistance, shrinkage, strength, and workability) in PEM design procedure and the properties (geometry, strength, durability, and physical characteristics) of steel and synthetic fibers. When discussing PEM, it was found that maintaining water to cementitious materials ratio (w/cm) between 0.40 and 0.45 reduces capillary pores volume, using the Tarantula Curve yielded the optimum aggregate gradation, including air-entraining admixture (AEA) stabilizes spherical air voids and avoid aggregates that are prone to ASR or ACR or fracture/dilation. On the other hand, the addition of fibers in concrete reduces workability while improving post-crack performance. Also, laterally stiff fibers with irregular geometry provide a better residual capacity to concrete and longer steel fibers are more effective in increasing the concrete structure flexural strength. The literature review found limited information on implementing the PEM design procedure for producing FRC and target value for PEM test parameters. This study will design FRC according to PEM design procedure and establish target values of the test parameters for FRC.

CHAPTER 3: RESEARCH METHODOLOGY

This research includes four main tasks, as shown in Figure 3-1. Task 1 is a comprehensive review of previous research studies. Task 2 is the laboratory investigation that includes material collection and testing. Tasks 3 consists of data analysis, discussion, and interpretation of the results and finaly the Task 4 was writing this thesis. In addition, data for one plain concrete (Field_PC) and one fiber reinforced concrete(Field_FRC) field mixes that were not designed in accordance with PEM requirements were included for comparison. The key difference between the PEM design and the Field mixes is the designed water/cement (w/c) ratio. The two field mixes were designed with a w/c ratio of 0.44.

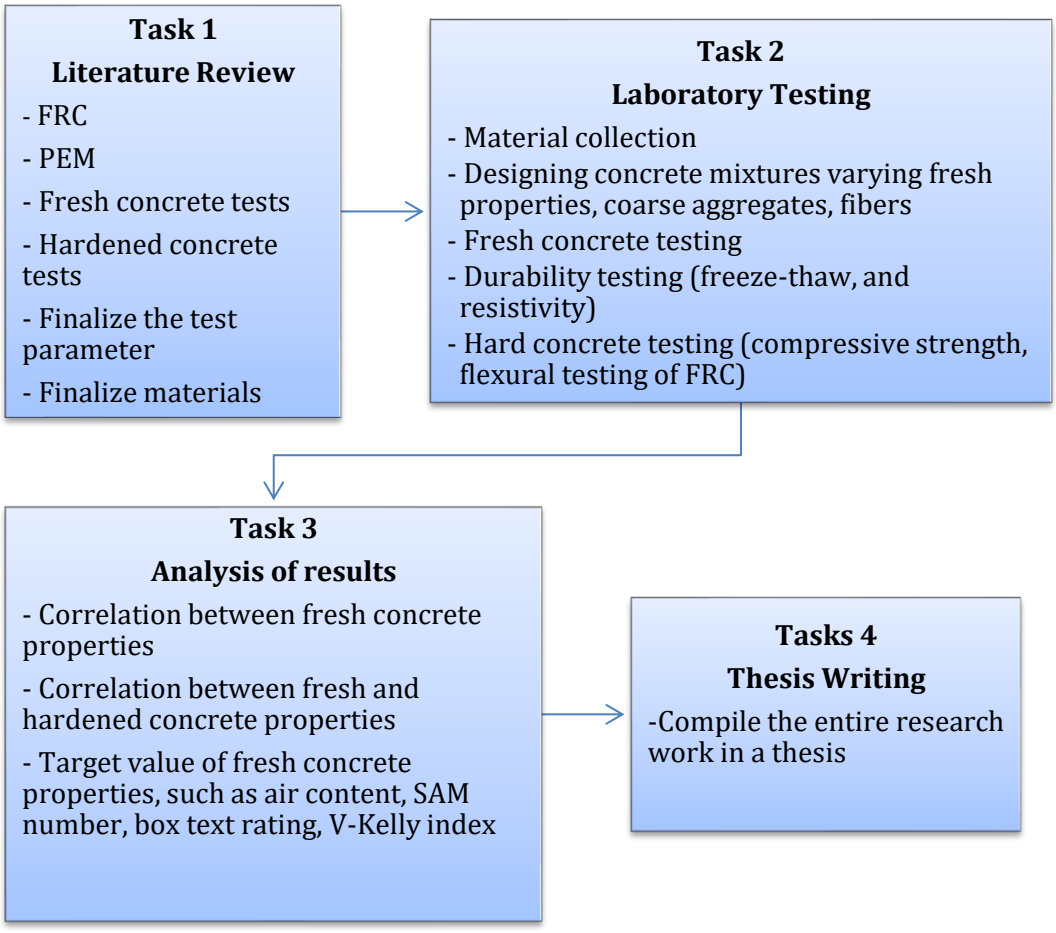

Figure 3-1. Flowchart of work conducted

For the laboratory investigation (Task 2), concrete ingredients (aggregates, cement, fly ash, fibers, and admixtures) were collected from different parts of Minnesota. An FRC mixing procedure was developed for all mixtures to ensure consistency. Aggregate characterization tests were conducted on the different aggregates to determine their specific gravities, unit weight, and absorption. A total of 24 concrete mixes were prepared varying air contents (4%, 6%, 8%), coarse aggregate types (Class A and B), fiber types (synthetic twisted geometry and embossed geometry) and and fiber dosages (0.26 and 0.50 volume fractions (V_f)). At times, multiple batches were prepared for the single mix because to achieve the right concrete mix.

Fresh concrete tests such as Slump test, Box test, V-Kelly test, and Super Air Meter (SAM) test were conducted for each mix. The mixtures produced for fresh concrete tests were also tested for their durability. Hardened concrete test (Cylindrical and Beam) specimens were tested for hardened properties such as compressive strength (ASTM C39), modulus of elasticity (ASTM C469), beam flexural strength (ASTM C1609), freeze-thaw resistivity (ASTM C666), and surface/electrical resistivity (AASHTO TP95). The rapid freeze-thaw test was performed to study the resistance of concrete against the freeze-thaw cycles. The electrical surface resistivity test assesses the durability of concrete against the passage of water and aggressive fluids (e.g., chloride ions), and the FRC flexural strength test assesses the post-crack behavior of fiber-reinforced concrete. All beams and cylindrical specimen used for testing was stored/cured in an environmental chamber at a 95% relative humidity and a temperature of 21.1℃. The correlation between fresh and hardened concrete properties will be used to establish the target range of fresh concrete properties. Table 3-1 provides a list of tests, including a test matrix.

Table 3-1. Tests to be considered in the study.

Test parameters	Test specification	No. of coarse agg. type	No. of fiber type	No. of fiber dosage	No. of air content
Compressive strength	ASTM C39	2	2	2	3
Beam flexural test	ASTM C1609	2	2	2	3
Rapid freeze-thaw	ASTM C666	2	1	2	2
SAM and fresh air content	AASHTO TP 118	2	2	2	3
Bucket Test		2	2	2	2
Box test	AASHTO PP-84	2	2	2	3
Slump test	ASTM C143	2	2	2	3
V-Kelly test	AASHTO TP 129	2	2	2	3
Surface/electrical resistivity	AASHTO TP 95	2	2	2	3
Mixture Type					
Plain Concrete		2	NA	NA	2
Fiber Reinforced Concrete		2	2	2	3
Field_PC		1	NA	NA	1
Fireld_FRC		1	1	1	1

**Note: NA = Not Any*

3.1 CONCLUSION

This chapter discussed how the thesis work was conducted through the completion of several tasks, which include a comprehensive literature review, experimental laboratory testing, data analysis and compiling the entire research work in a thesis. The laboratory investigation described in this chapter includes a collection of concrete ingredients (aggregates, cement, fly ash, fibers, and admixtures), development of an FRC mixing procedure and aggregate characterization tests. Finally, the laboratory investigation plan details the scope of work conducted in this study, which includes fresh concrete tests (slump, box, V-Kelly, and super air meter (SAM)) and hardened concrete tests (compressive strength, modulus of elasticity, beam flexural test, rapid freeze-thaw test, and surface/electrical resistivity) for all the mixes.

CHAPTER 4: MATERIALS AND TESTING

This chapter describes the properties of ingredients used in the laboratory investigation. Properties of fibers, cement, supplementary cementitious materials (SCM), aggregates (characteristics and gradations), and admixtures (air entrainer and water reducer), are discussed in this chapter. A detailed description of concrete mixture proportioning, batching, and mixing procedure is also provided. Different tests conducted in this study are briefly introduced in this Chapter as well.

4.1 FIBERS

The polypropylene-based macro synthetic fiber is the most common variety of fiber used in concrete pavements. The two fibers used in this research were synthetic fibers with different manufacturers, lengths, and geometries. More information about the fibers used is given in Table 4-1. Two different fiber dosages were considered in terms of volume fractions, i.e. 0.26 % (4 lb/yd^3) and 0.5% (7.6 lb/yd^3) of the concrete volume. Fiber 1 is twisted and bundled, which unfurl during the concrete mixing; therefore, its effective diameter and aspect ratio is not uniform in the concrete mixture, unlike Fiber 2, which does not breakdown in the concrete mixture.

Table 4-1. Description of fibers investigated in this task.

Fiber Designation	Fiber 1	Fiber 2
Geometry	Twisted	Embossed
Length (in)	2.25	2.1
Aspect Ratio	Varies	70
Tensile Strength (ksi)	85	85
Specific Gravity	0.91	0.91

4.2 CEMENT

The chemical composition of cement and supplementary cementitious materials (SCM) can affect the concrete strength gained over time and the electrical conductivity of hardened concrete. A singular cement variety was used to prepare the concrete mixtures in this research. ASTM C150 Type-I Ordinary Portland cement and ASTM C618 Class-F fly ash were used. Class-F Fly-ash was collected from Boral Resource (coal creek station)

located in Duluth, MN. The fly-ash replaced 20% of the Type I cement. More information about the composition of Class-F fly-ash is provided in Table 0-2 in the APPENDIX.

4.3 AGGREGATE

The coarse aggregates comprised of granite (Class A) and limestone (Class B) with aggregate sizes of ¾-inch and 1 ½-inch and specific gravity between 2.70 to 2.75. The details of the two different classes of coarse aggregates are provided in Table 4-2.

Table 4-2. Aggregate's characteristics

Coarse Aggregate	Absorption	Bulk Specific Gravity
Granite 3/4" - Class A	0.35%	2.70
Granite 1.5" - Class A	0.25%	2.70
Limestone 3/4" + Class B	0.83%	2.74
Limestone 3/4" - Class B	1.08%	2.73
Fine Aggregate		
River Sand	1.70%	2.68

As shown in Figure 4-1 and Figure 4-2 , Class A aggregates were angular and smooth, and Class B aggregates were angular and sub-rounded, respectively. As a result, Class B aggregates enable a better and easier compaction process. They also have a higher dry rodded unit weight (103.8 lb/yd^3) than Class A aggregates (101.4 lb/yd^3) due to their angular shape. The aggregates were quarried and processed to obtain desired aggregate sizes.

Figure 4-1. ¾" and 1 ½" Granite Class A Aggregates

Figure 4-2. ¾" plus and ¾" minus Limestone Class B Aggregates

Fine aggregate (river sand), as shown in Figure 4-3, was collected from a concrete plant located in Duluth, MN. The concrete mixture produced in this study has approximately 40 - 45% fine aggregate. Gradation information of the aggregates used is given in Table 4-3 and Figure 4-4.

Figure 4-3. Fine aggregates (river sand)

Table 4-3.Sieve analysis results of the aggregates used

	Fines Aggregates	Class B 3/4" minus	Class B 3/4" plus	Class A 3/4"	Class A 1.5"
No.	**% Passing**	**% Passing**	**% Passing**	**% Passing**	**% Passing**
2"	100%	100%	100%	100%	100%
1.5"	100%	100%	99.81%	100%	91.77%
1"	100%	100%	62.93%	100%	36.99%
3/4"	100%	91.00%	18.07%	99.71%	6.57%
1/2"	100%	53.03%	0.97%	53.40%	0.69%
3/8"	100%	32.42%	0.56%	21.15%	0.63%
#4	99.60%	2.91%	0.56%	1.34%	0.62%
#8	82.80%	0.60%	0.55%	0.50%	0.61%
#16	60.90%	0.58%	0.54%	0.49%	0.59%
#30	37.45%	0.55%	0.53%	0.46%	0.56%
#50	13.80%	0.50%	0.51%	0.40%	0.49%
#100	2.65%	0.45%	0.47%	0.33%	0.38%
#200	0.60%	0.35%	0.40%	0.21%	0.23%
Pan	0.00%	0.00%	0.00%	0.00%	0.00%

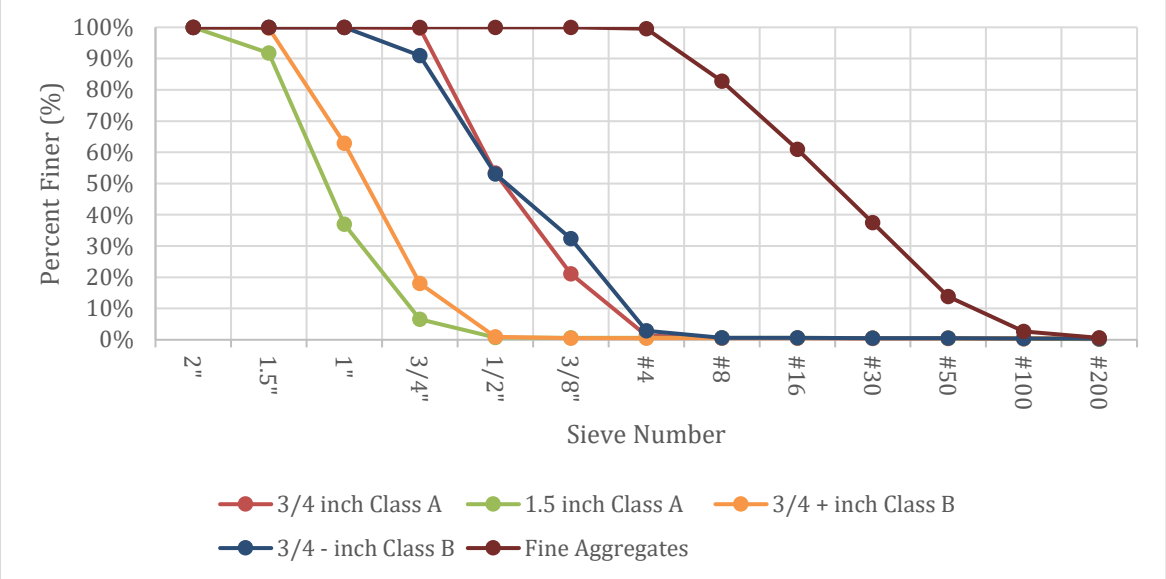

Figure 4-4. Gradation curves of the aggregates used

The tarantula aggregate gradation curve is used to determine the optimum aggregate gradation for concrete mixtures. Figure 4-5 shows the aggregate gradation curve of each mixture. Mixtures with granite and limestone aggregates are referred to as Mixture A and Mixture B, respectively. An aggregate gradation fitting the tarantula curve possesses good workability characteristics.

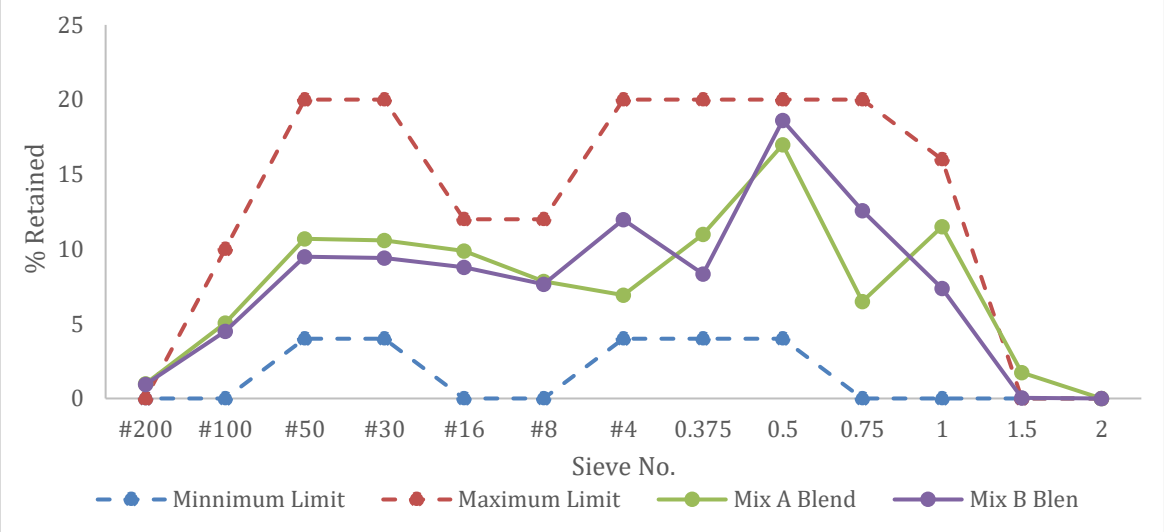

Figure 4-5. Combined aggregate gradation on a tarantula curve.

Several trial batches were prepared before finalizing the base mixture design. The trial batches were made with different dosages of Air Entraining Admixture (AEA) and Water Reducer (WR) to ensure the air content and slump range (≤5") within the acceptable range of target values. Three different target air content values (4%, 6%, and 8%) were used. These air contents were decided based on the possible ranges of the air contents in the paving mixtures. It shall be noted that Minnesota's allowable range of the air contents for the concrete pavement mixtures is between 5.5 and 9% (MnDOT, 2017).

4.4 CONCRETE MIXTURE

Concrete mixtures produced in this study contained a constant amount of cementitious material, 550 lb/yd^3, matching with the typical amount of cement used in concrete pavements in Minnesota recently. The concrete mixture had a water/cement ratio of 0.42. Table 4-4 provides batch weight values for the granite Type A mixture and limestone Type B mixture with 4%, 6%, and 8% air content. The aggregate proportion was decided on the basis of particle size distribution and gradation limits in the tarantula curve. The paste volume, comprised of cement, water, and air, varied from 27-32%.

Table 4-4. Summary mixture design for concrete mixes used in this study

Component (lb/cy)	Type A 4% Air	Type A 6% Air	Type A 8% Air	Type B 4% Air	Type B 6% Air	Type B 8% Air
Water	231	231	231	231	231	231
Cement (Type I)	550	550	550	550	550	550
Coarse Aggregate 1	1109	1078	1047	1314	1278	1249
Coarse Aggregate 2	685	666	647	657	639	621
Coarse Aggregate Total	1794	1744	1694	1971	1917	1870
Fine Aggregate	1467	1427	1386	1314	1278	1241
Air entrainer Type	BASF MasterAir® 400					
Water reducer Type	MasterPolyheed® 1020					
Paste content, % vol. of concrete	28.07	30.07	32.07	28.07	30.07	32.07

4.4.1 Mixture Designation

The mixture designation describes each mixture with respect to the coarse aggregate type, design air content, fiber number, and fiber dosage. For example, a 6A1.50 mixture represents a mixture with 6% air content (‘6’), Granite Class A Aggregate (‘A’), fiber with a serial number of ‘1’ (Table 4-5), and a fiber dosage of 0.50 percent. A 6A1.50-2 mixture represents the 2nd batch of 6A1.50 mixture. A 2nd batch was made because the measured air content was higher/lower than the target air content and belonged to a category for which a mixture was already made.

Table 4-5. Nomenclature for mixture designation

Air content (%)	Coarse Aggregate type	Fiber Number	Fiber Dosage (V_f %)
4	Granite (A)	1	0.26
6	Limestone (B)	2	0.50
8	-	-	PC (Plain Concrete)

4.4.2 Mixing Procedure

A mixing procedure was developed to ensure efficient and consistent production of fiber reinforced concrete with the required air content and slump values. As fibers tend to ball up and mat when they are not dispersed properly, the developed mixing procedure involved proper dispersion of fibers to avoid fiber balling. A conditioning butter batch is conducted prior to mixing the full batch. The butter batch is proportionally identical (including admixture) to the full mixture. The purpose of the butter batch is to coat the inner wall of the concrete mixer as well as the wheelbarrow. Figure 4-6 shows the concrete mixer used for this research. The mixing procedure for the butter batch is as follows:

i. All the materials were placed into the mixer and mixed for three minutes while changing the tilt of the drum to thoroughly coat the inside of the mixer.

ii. The butter batch was dumped into the wheelbarrow used for this research to coat the inside of the wheelbarrow.

iii. Dispose of the concrete.

The mixing procedure for the final batch is as follows:

I. Fine aggregates and AEA were added to the mixer with 1/3rd of the mixing water and mixed for 2 minutes. This ensured the generataion of air bubbles in air-entrained concrete.

II. Coarse aggregates were added to the stopped mixer.

III. The mixer was turned ON, and fibers were added with care pulling apart any balls or mats. The mixer was run for a total of 3 minutes.

IV. With the mixer still spinning, cement, remaining water, and water reducer were added to the mixer and mixed for 3 minutes.

V. The mixer was stopped, and the mixture was allowed to rest for 3 minutes.

VI. Finally, the mixer was run for two more minutes.

Figure 4-6. Concrete mixer used.

4.5 FRESH CONCRETE TESTS

This section describes the tests conducted to determine various fresh concrete properties.

4.5.1 Slump Test

Slump test is conducted to determine the workability of concrete mixtures. Following the completion of the concrete mixing procedure, a slump test was performed on the fresh concrete mixture in accordance with ASTM C143. Even though a constant water-cement ratio was maintained for all the mixtures, the slump of the concrete varied between 1 and 5 inches. This is not surprising as the concretes produced in this study contained different dosages of air-entraining admixtures to produce concretes with three different air contents (4, 6, and 8%). An appropriate amount of water reducer was added at times to improve the workability of the concretes, especially which had lower air contents. Figure 4-7 shows a slump test conducted on fresh fiber reinforced concrete.

Figure 4-7. Slump test on FRC mixture

4.5.2 Air Content and Super Air Meter (SAM) Test

SAM test was performed in accordance with AASHTO TP 118 to determine air content (%) and SAM number. The SAM number determines the air void size and spacing factor and provides an assessment of the resistance of concrete mixture against freeze-thaw-related distresses (Ley, 2015). The results from this test have been used to study the influence of adding fibers in the concrete mixture on SAM number.

Figure 4-8. Ongoing SAM test

4.5.3 Box Test

The Box test is conducted to investigate the thixotropic property of concrete mixtures, which is defined as the impact of vibration on the concrete mixture and its ability to hold an edge after vibration (Cackler et al., 2017). Box test, as shown in Figure 4-9, was performed in accordance with AASHTO PP84 after the mixture was tested for the slump. Figure 4-10 depicts the surface air voids ranking system, which is based on the assessment of the air voids on the sides of the concrete sample during the box test. The visual inspection is conducted to determine the suitability of the concrete mixture for slip-form paving. A Box test rating of 2 is ideal for slipform paving (Cook et al., 2014), which corresponds to 10 to 30 percent surface voids.

Figure 4-9. Box test in progress

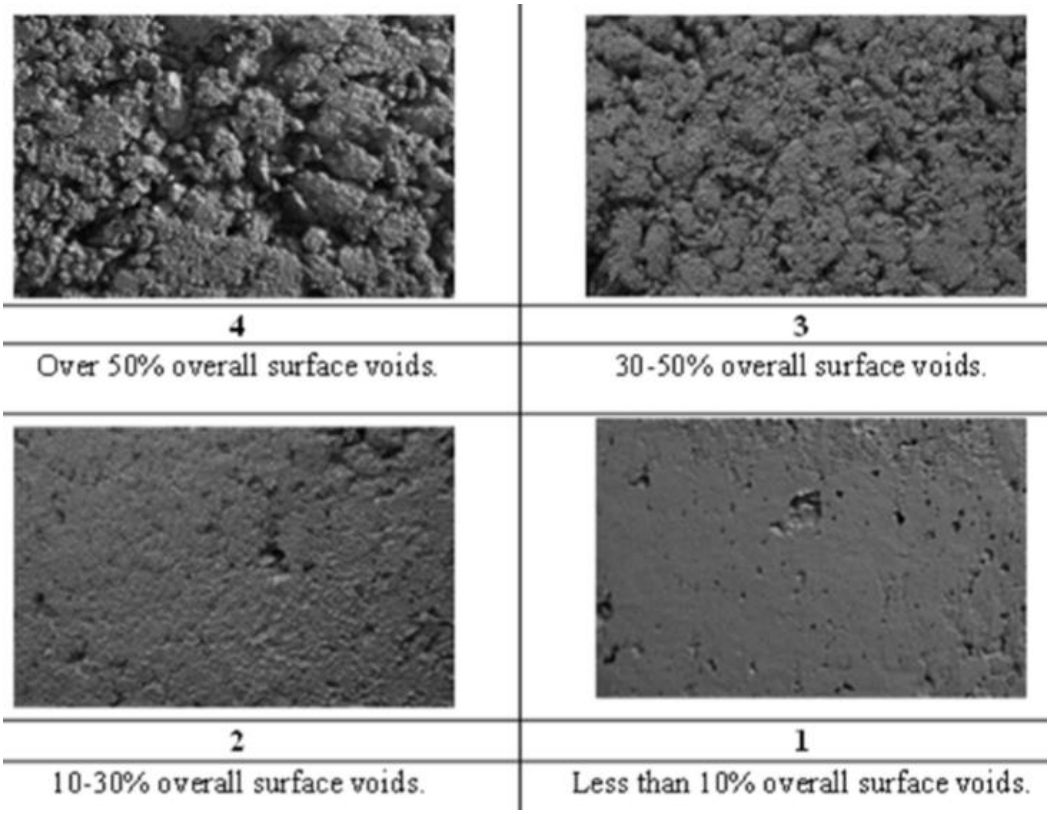

Figure 4-10. Surface air voids ranking system for box test (Cook et al. 2016)

4.5.4 Vibrating Kelly Ball Test (V-Kelly Test)

The Vibrating Kelly Ball (V-Kelly) test was performed in accordance with AASHTO TP 129. V-Kelly test examines the workability of concrete mixture and its response to vibration. The first part of the V-Kelly test, prior to turning ON the vibrator, is known as the Static Test. The second part, after switching the vibrator ON, is known as the Dynamic Test. The static test provides a measure of the concrete consistency and the dynamic test provide provides the concrete response to vibration. V-Kelly index.

Figure 4-11. Vibrating Kelly Ball Test (V-Kelly Test)

4.6 HARDENED CONCRETE TESTS

This section describes the laboratory tests conducted to determine different hardened concrete properties such as compressive strength, modulus of elasticity, flexural strength, resistance to distresses caused by multiple freeze-thaw cycles, and surface/electrical resistivity. Specimens were stored/cured in an environmental chamber at a 95% relative humidity and a temperature of 21.1°C. All tests were performed at room temperature.

4.6.1 Compressive Strength Test

The compressive strength test was conducted per ASTM C39, using 6-inch (diameter) × 12-inch (height) cylindrical specimen. For every mixture type, four

cylinders were cast and tested for their compressive strength 28-day from casting and the average compressive strength of the samples was used to evaluate the compressive load the hardened concrete could bear before fracturing.

Figure 4-12. Compressive strength test

4.6.2 Electrical/Surface Resistivity Test

The electrical surface resistivity test assesses the durability of concrete against the passage of water and aggressive fluids (e.g., chloride ions). Hard concrete is a poor conductor of electricity in comparison to concrete with fluid-filled pores. Therefore, the resistivity of concrete is lower when the volume and connectivity of the pore system is higher (Cackler et al., 2017). Reducing the transport of aggressive unwanted fluids into the concrete will allow hardened concrete to survive harsh climate conditions.

The electrical/surface resistivity test method was performed in accordance with AASHTO TP95 on 6-inch (diameter) × 12-inch (height) cylindrical specimens by using a four-point Werner probe array (AASHTO TP95, 2014) and generating a current flow by applying an AC potential difference in the outer probes of the array. The inner probes measured the difference in the current flow. Three specimens were tested for each

mixture after 28-day at room temperature and the average was used to assess the durability of concrete against the passage of water and aggressive fluids (e.g chloride ions).

Figure 4-13. Surface resistivity test

4.6.3 Flexural Strength Test

The flexural strength test was performed in accordance with ASTM C 1609 on three 21-inch (length) × 6-inch (wide) × 6-inch (depth) beam specimens with a loading span length of 18 inches. The average flexural strength of the specimens was used to assess the mixture's flexural performance, toughness and equivalent flexural strength ratio. Figure 4-14 illustrate an ongoing flexural performance test. Figure 4-15 shows fibers bridging a crack during a flexural performance test. The test data include the first peak strength (load supported before cracking), peak strength, and residual strength (load withstood by fibers after a mid-span displacement of 0.12 inches was reached). The test results were used to determine the Modulus of Rupture (MOR), Residual Strength (RS),

Residual Strength Ratio (RSR), and toughness of hardened concrete. RSR, also called equivalent flexural strength ratio, is given by equation (1).

$$RSR = 100 * \frac{f_{e,3}}{MOR} \quad (1)$$

Where, $f_{e,3}$ is the residual strength (RS) at mid-span for a deflection equal to 120 mils. The area under the load vs displacement graph was used to determine the toughness of concrete.

Figure 4-14. Four-point flexural bending test as per ASTM C 1609

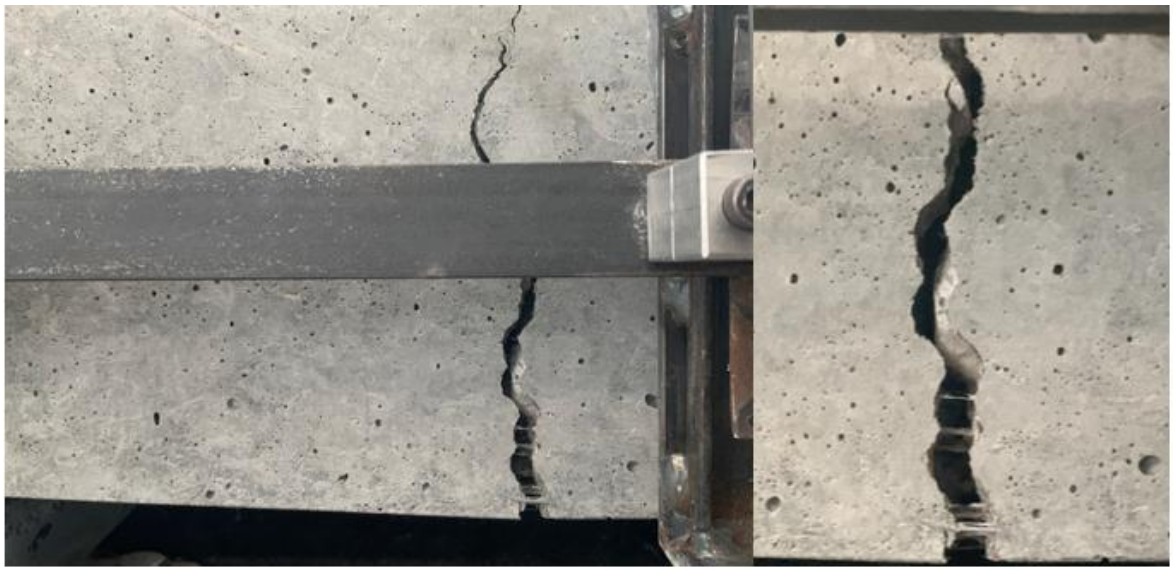

Figure 4-15. Fibers bridging a crack during an ongoing four-point flexural bending test.

4.6.4 Formation Factor Bucket Test

The formation factor bucket test evaluates the ability of concrete to prevent fluid transport through its pores. The test was conducted in accordance with AASHTO TP 119-15 on two 4-inch (diameter) × 8-inch (height) cylindrical specimens that were covered with wet burlap for 24-hours before demolding. Immediately after demolding, the specimens were immersed in a 5-gallon bucket with calcium hydroxide saturated simulated pore solution (consisting of 7.6g/L NaOH, 10.64g/L KOH, and 2g/L Ca $(OH)_2$). The specimens were kept in the solution for seven days before testing them using the Werner probe array, as described in Section 4.6.2 . The specimens were tested at room temperature and the average test result of the specimens was used to assess the mixture's ability to prevent fluid transport through its pores.

4.6.5 Modulus of Elasticity Test

The static modulus of elasticity test, also known as chord modulus or young's modulus of elasticity test, was performed on one 6-inch (diameter) × 12-inch (height) cylindrical specimen. This test was conducted in accordance with ASTM C469M to examine the stiffness of hardened concrete. After the modulus of elasticity test, cylindrical specimens were tested for ultimate compressive strength in accordance with ASTM C39.

Figure 4-16.Modulus of Elasticity test

4.6.6 Rapid Freeze-Thaw Test

The rapid freeze-thaw test was performed in accordance with ASTM C666 to study the resistance of concrete to distresses caused by multiple freeze-thaw cycles (ASTM C666, 2008). This test evaluates the durability of concrete against shrinkage and expansive damages due to variations in temperature or weather conditions.

Three beam specimens were exposed to freeze-thaw cycles inside a freeze-thaw chamber. The specimens were covered with wet burlaps for 24-hours before demolding and cured for 14 days prior to testing. The beams were put in aluminum containers surrounded by water and placed in the freeze-thaw chamber as per the test specification. The Relative Dynamic Modulus of Elasticity (RDME) was calculated at every 30 freeze-thaw cycles until 300 cycles were completed for each specimen. The average RDME of the specimens after 300 cycles was used to assess the durability of the concrete against

distresses caused by multiple freeze-thaw cycles. The RDME was calculated using equation (2).

$$P_C = \frac{{n_C}^2}{{n_0}^2} * 100 \qquad (2)$$

Where: P_c is the RDME corresponding to 'c' number of freeze-thaw cycles (%), n_c is the fundamental transverse frequency after 'c' number of freeze-thaw cycles (ksi), and n_0 is the fundamental transverse frequency after 0 freeze-thaw cycles (Hz).

The durability factor was calculated using equation (3).

$$DF = \frac{P_N}{300} \qquad (3)$$

Where: DF is the durability factor (%), P is the RDME at N number of freeze-thaw cycles (%), and N is the number of freeze-thaw cycles.

Figure 4-17.Freeze-Thaw Chamber

4.7 CONCLUSION

Detailed in this chapter is information related to the materials, mixing procedures, and concrete testing procedures used in this research. The materials used in this study include two types of coarse aggregates, one type of fine aggregate, two types of fiber, cement, fly ash, and admixtures. The fresh concrete tests conducted in this study are slump, box, V-Kelly, and SAM tests. The hardened concrete tests conducted in this study are compressive strength, modulus of elasticity, beam flexural test, rapid freeze-thaw test, and surface/electrical resistivity test.

CHAPTER 5: RESULTS AND DISCUSSIONS

This chapter presents the findings of the fresh and hardened concrete tests performed under the scope of this research project. The summary of the fresh concrete test results are given in Table 5-1. Along with the test results for mixes prepared in the lab, results for one plain and one fiber reinforced concrete field mixes are also provided. The two field mixes (Field.PC & Field.FRC) were used in a MnROAD pavement project. These mixes were not designed according to the PEM requirements, are also included in Table 5-1.

Table 5-1. Fresh Concrete Properties

Mixture	Slump (in)	V-Kelly Slump (in)	V-Kelly Index (in/√s)	Air (%)	SAM Number	Box Rating
A.PC	2.00	0.8	1.03	4	0.16	3
4A1.26	2.00	0.9	0.79	4.9	0.21	2
6A1.26	1.25	0.4	0.82	6	0.11	2
8A1.26	2.00	0.8	0.81	8.1	0.4	2
4A1.50	1.25	0.5	0.46	2.9	0.84	4
6A1.50-1	1.75	0.4	0.71	5.9	0.3	3
6A1.50-2	1.75	1.3	0.69	6.9	0.23	3
8A1.50	1.50	0.3	0.26	7.5	0.2	4
4A2.26	2.25	1.0	0.41	4.4	0.24	2
6A2.26	2.25	0.7	0.8	7	0.16	3
8A2.26-1	3.75	1.0	0.69	7.7	0.11	1
8A2.26-2	3.25	0.9	0.57	7.6	0.14	1
4A2.50	0.25	0.5	0.42	2.8	0.74	4
6A2.50	3.25	1.1	0.62	6.3	0.15	2
8A2.50-1	3.75	1.3	0.28	8.9	0.12	1
8A2.50-2	3.00	0.6	0.46	8.2	0.17	1
B.PC-1	3.00	2.8	1.03	5.4	0.21	1
B.PC-2	3.50	2.7	0.98	5.6	0.19	1
4B1.26	2	1.5	0.61	3.5	0.67	3
6B1.26	1.75	1.8	0.88	6.9	0.18	2
8B1.26	4.00	2.5	0.79	8.5	0.14	1
4B1.50	1.00	0.6	0.35	4	0.72	3
6B1.50	3	1.5	0.47	6.4	0.24	2
8B1.50	2.50	1.9	0.61	8.9	0.12	1
Field_PC	5.50	-	-	7.8	0.09	-
Field_FRC	-	-	-	5.7	0.44	-

(Note: Designations provide information about the fiber and aggregate. Example: A1.50vf represents a mixture with Granite Class A Aggregates (A), a fiber with a serial number of 1 (Fiber 1) and a fiber

dosage in terms of volume fraction of 0.50%;Field_PC represents Field Plain Concrete and Field_FRC represent Field Fiber-Reinforced Concrete)

The summary of the hardened concrete test results is given in Table 5-2 and Table 5-3. The modulus of elasticity values obtained from the laboratory tests and the ACI equation are provided in Table 5-3.

Table 5-2. Hardened Concrete Properties

Mixture	28-Day Compressive Strength (psi)	28-Day Surface Resistivity (kOhm-cm)	MOR (psi)	Toughness (in-lb)	L/150		Deflection Peak load in ASTM C1609 test (mil)
					Residual Strength (lbf)	RSR (%)	
A.PC	5891	20	717	20	0	0	3.94
4A1.26	4535	20	684	351	130	19	3.88
6A1.26	4378	21	619	272	94	15	3.73
8A1.26	4242	20	618	279	119	19	3.90
4A1.50	5195	17	746	484	234	32	4.40
6A1.50-1	4466	19	630	406	240	39	3.67
6A1.50-2	4628	19	669	456	277	41	4.09
8A1.50	3954	22	605	359	161	26	3.63
4A2.26	5878	21	753	291	93	12	4.41
6A2.26	6271	23	735	367	156	21	4.64
8A2.26-1	4525	24	674	409	149	22	4.38
8A2.26-2	5196	24	708	342	133	19	4.36
4A2.50	6629	19	817	467	213	26	4.75
6A2.50	5558	20	634	369	164	26	4.48
8A2.50-1	4932	23	664	452	219	33	4.88
8A2.50-2	4947	23	682	537	294	44	4.82
B.PC	5795	20	776	107	0	0	4.32
4B1.26	6928	18	809	339	91	11	4.83
6B1.26	5738	19	800	341	103	13	4.85
8B1.26	5074	19	647	306	83	13	4.74
4B1.50	5744	20	777	427	171	22	4.85
6B1.50	4857	19	760	462	210	28	4.83
8B1.50	4770	20	696	433	189	27	4.84
Field_PC	4367	11	601	15	0	0	3.49
Field_FRC	4687	9	577	435	232	40	3.37

Note: 1 mil = 1/1000 inches.

Table 5-3. Hardened Concrete Properties continued

Mixture	Elasticity (x10^6 psi)		Poisson Ratio	Average Density (lb/ft^3)
	Lab Test	ACI Equation		
A.PC	5.94	4.2	0.25	153
4A1.26	4.05	3.93	0.22	150
6A1.26	4.08	3.87	0.23	149
8A1.26	4.21	3.59	0.25	148
4A1.50	4.77	4.01	0.21	152
6A1.50-1	4.38	3.77	0.2	148
6A1.50-2	3.75	3.79	0.23	147
8A1.50	3.45	3.52	0.21	147
4A2.26	2.71	4.4	0.13	154
6A2.26	4.16	4.45	0.22	152
8A2.26-1	2.14	3.83	0.1	147
8A2.26-2	4.92	3.96	0.4	149
4A2.50	3.13	4.67	0.06	154
6A2.50	4.68	4.26	0.26	154
8A2.50-1	2.06	4.15	0.09	148
8A2.50-2	2.77	3.97	0.16	147
B.PC	4.35	4.25	0.19	151
4B1.26	4.80	4.75	0.26	154
6B1.26	4.32	3.91	0.24	151
8B1.26	4.34	3.95	0.22	149
4B1.50	4.80	4.32	0.2	20
6B1.50	4.04	3.92	0.22	19
8B1.50	4.70	3.95	0.22	20
Field_PC	3.84	3.83	0.21	148
Field_FRC	4.00	3.82	0.2	148

5.1 ANALYSIS AND DISCUSSION OF RESULTS

This section interprets and evaluates the experimental findings and discusses the influence of fiber on key engineering properties of fresh and hardened concrete properties.

5.1.1 Discussion of Fresh Concrete Properties

5.1.1.1 SAM Test

A SAM number of 0.20 (corresponding to a spacing factor of 0.008 inches and durability factor of 70%) or below is recommended for plain concrete mixtures subjected to harsh weather conditions, including freezing and thawing (Ley, 2015). The SAM number results presented in Figure 5-1 show that an increase in entrained air content decreases the SAM number (R^2= 0.62), and a large set of SAM numbers are close to 0.20, the recommended SAM number value for plain concrete. It also appears that the SAM number can be very high when the concrete mixture has less than 4% air voids, irrespective of the fiber type and dosage.

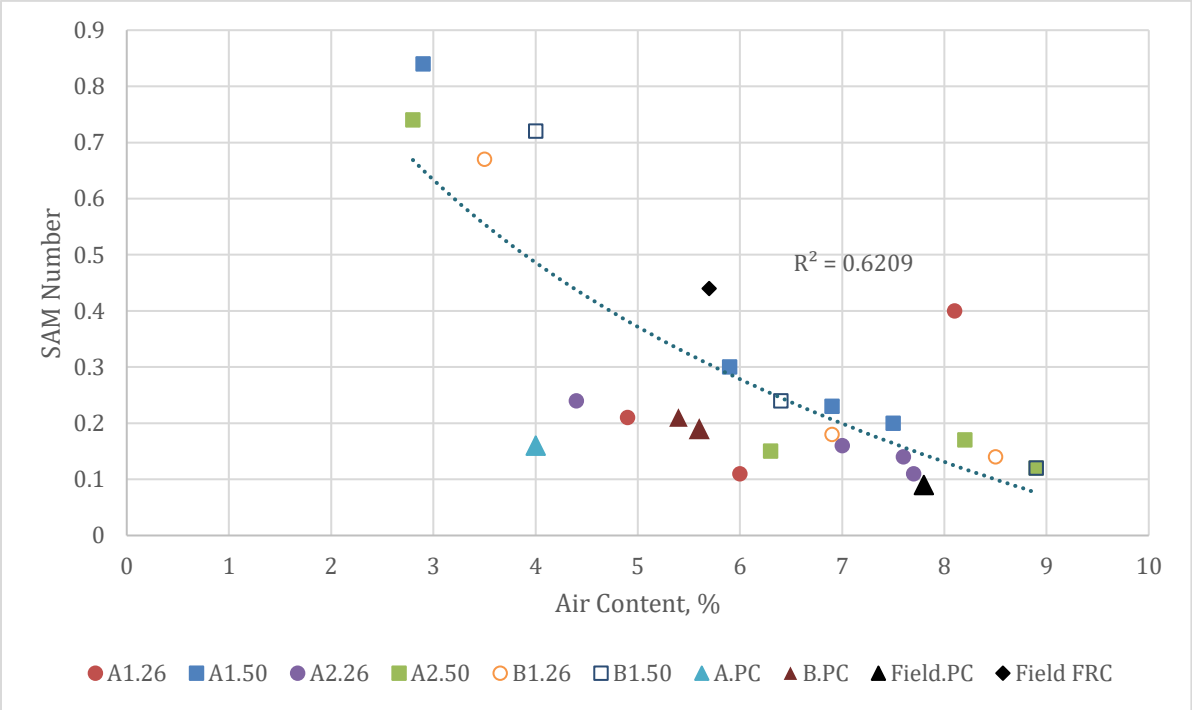

Figure 5-1.SAM number vs Air content

To verify the influence of fiber dosage on SAM number, the average SAM number was calculated for all mixes with air content above 4%. Mixes with less than 4% air content were not included because they are not suitable for resistance against freeze-thaw related distresses and are not used in Minnesota climate. Figure 5-2 shows the average SAM numbers based on fiber dosage. The average SAM numbers for mixes with

no fiber, 0.26 volume fraction, and 0.50 volume fraction were 0.185, 0.188, 0.191, with standard deviations of 0.035, 0.091, 0.063, respectively.

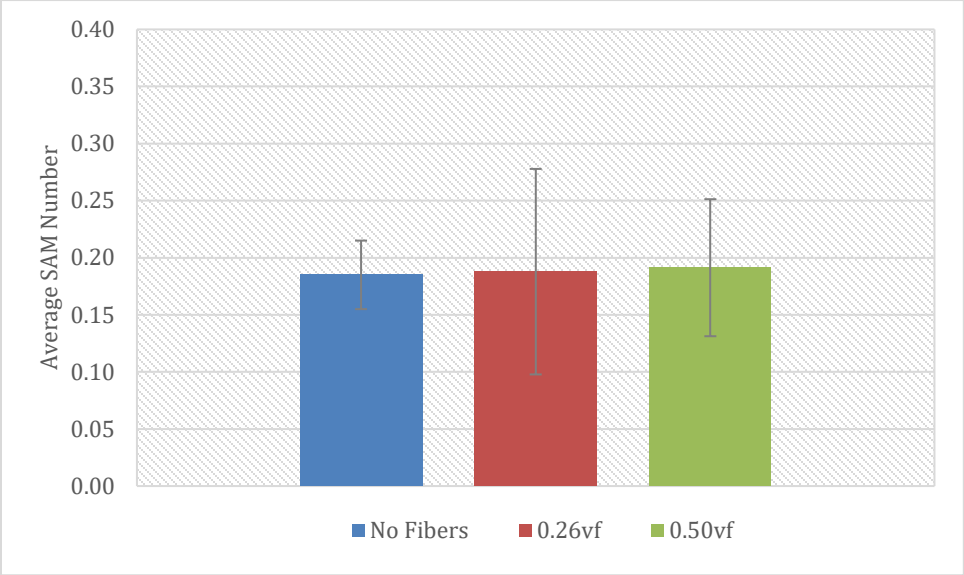

Figure 5-2.Influence of fiber dosage on SAM Number

Figure 5-3 shows SAM number values for each fiber type and dosage (only for aggregate Class A). It is observed from the figure that mixtures with Fiber 1 (twisted geometry) have high SAM numbers than the mixtures with Fiber 2. It is important to note that the mixture containing Fiber 1 had a lower average air void content than the mixture with Fiber 2 for different fiber dosages.

Figure 5-3 also depicts that the SAM number for Fibers 1 and 2 is not influenced significantly by a change in fiber dosage. Also, concrete mixtures with no fibers and Fiber 2 have similar SAM numbers.

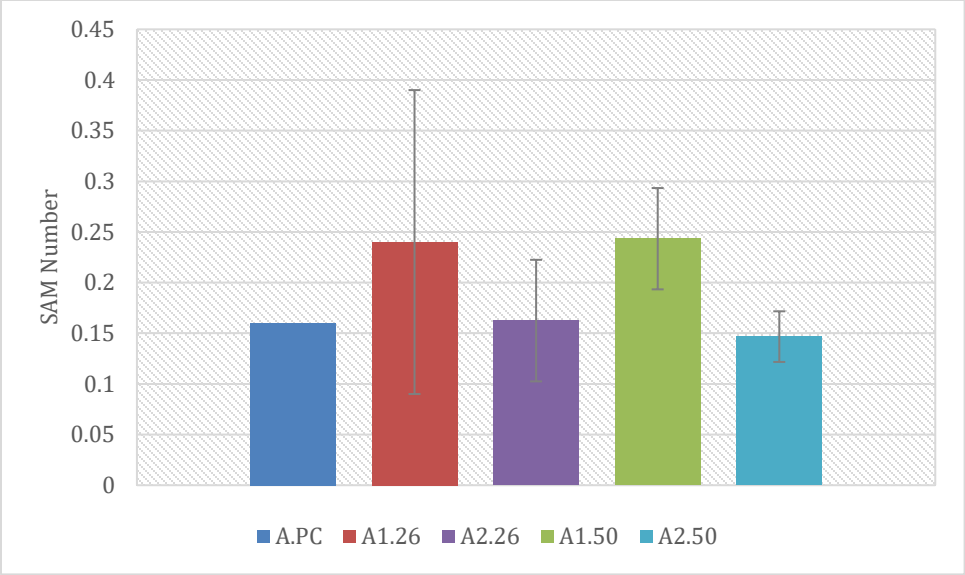

Figure 5-3.Influence of fiber type on SAM Number

Figure 5-4 shows that for aggregate type A, the average SAM number is slightly higher for mixtures with fibers. However, there is no impact of a change in fiber dosage. In comparison, the average SAM number is slightly lower or similar when fibers were added to the mix containing Aggregate type B; also, similar to the Aggregate type A, the fiber dosages did not play a significant role in the SAM number.

It can be concluded that the limited fiber dosage variation adopted in this study did not significantly influence the SAM number. However, it seems that the fiber type may play a role. The twisted fibers used in this study can increase the SAM number compared to the plain concretes or concretes with embossed fibers. Further study with additional fiber dosages and types is recommended for a more reliable conclusion.

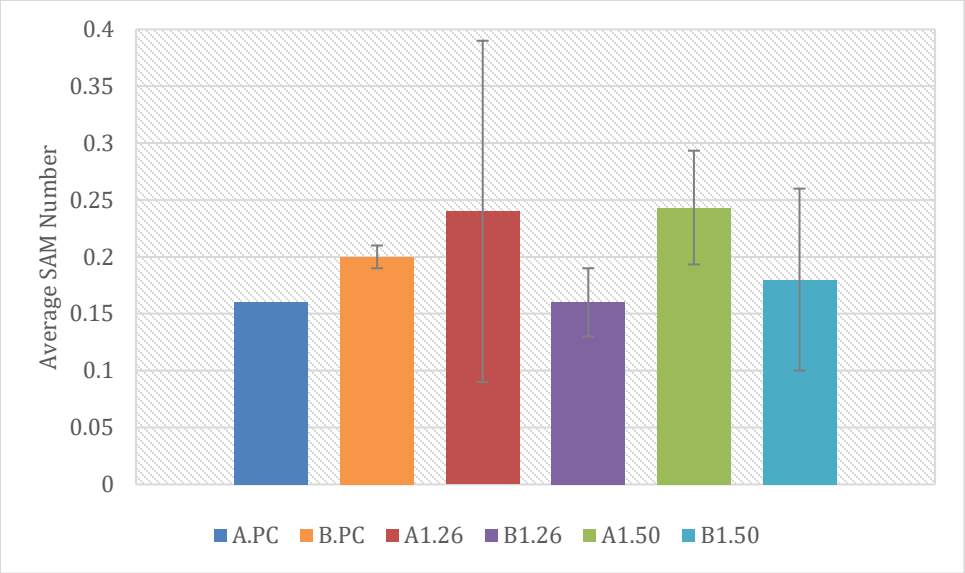

Figure 5-4.Influence of aggregate type on SAM Number

5.1.1.2 Box Test

As discussed in Section 4.5.3 , a Box test rating of 2 is ideal, which corresponds to 10 to 30 percent surface voids. A higher rating indicates more surface voids. Figure 5-5 and 5-6 show the relationship of the Box Test rating with the entrained air content (R^2= 0.47) and slump values (R^2= 0.66), respectively. Both these figures indicate the box test visual rating has an inverse relationship with the air content and slump values. As shown in Figure 5-7, the increase in fiber dosage increases the Box Test rating for a given water-cement ratio, indicating more voids on the surface. Some concrete mixtures with 0.5% vf had visual ratings of more than 2. The results make sense as the box test rating depends on mixture workability (slump value), and fiber usually decreases the workability.

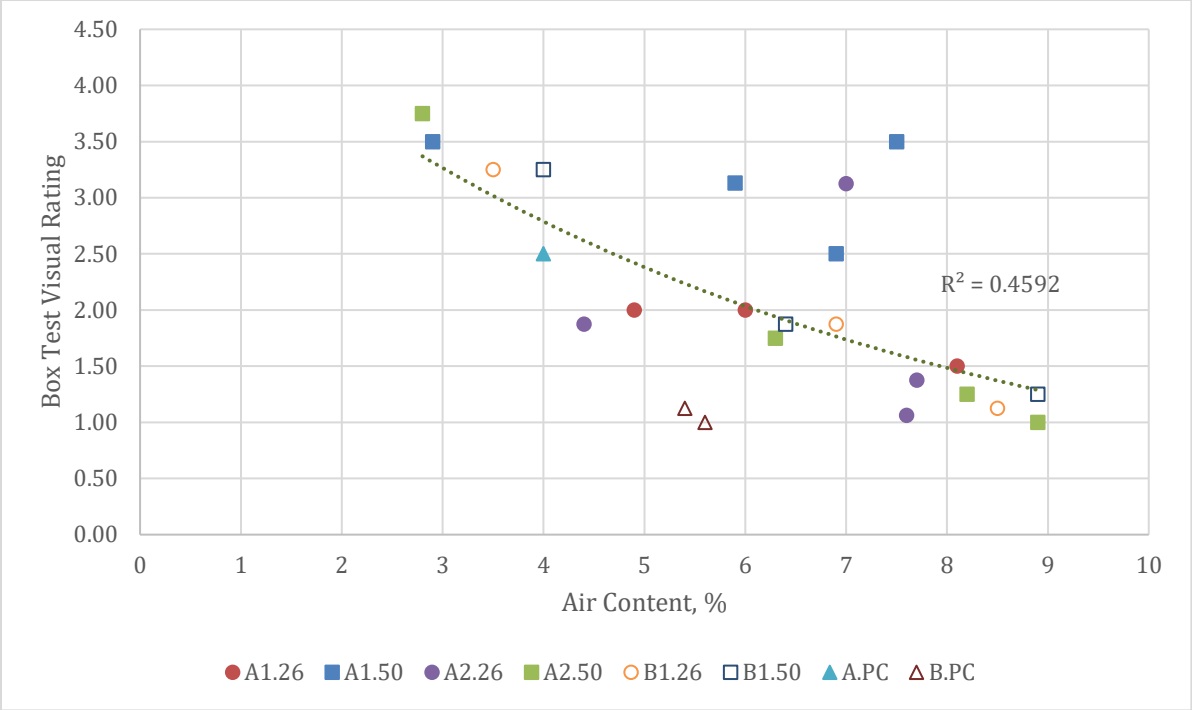

Figure 5-5.Box test rating vs Air content

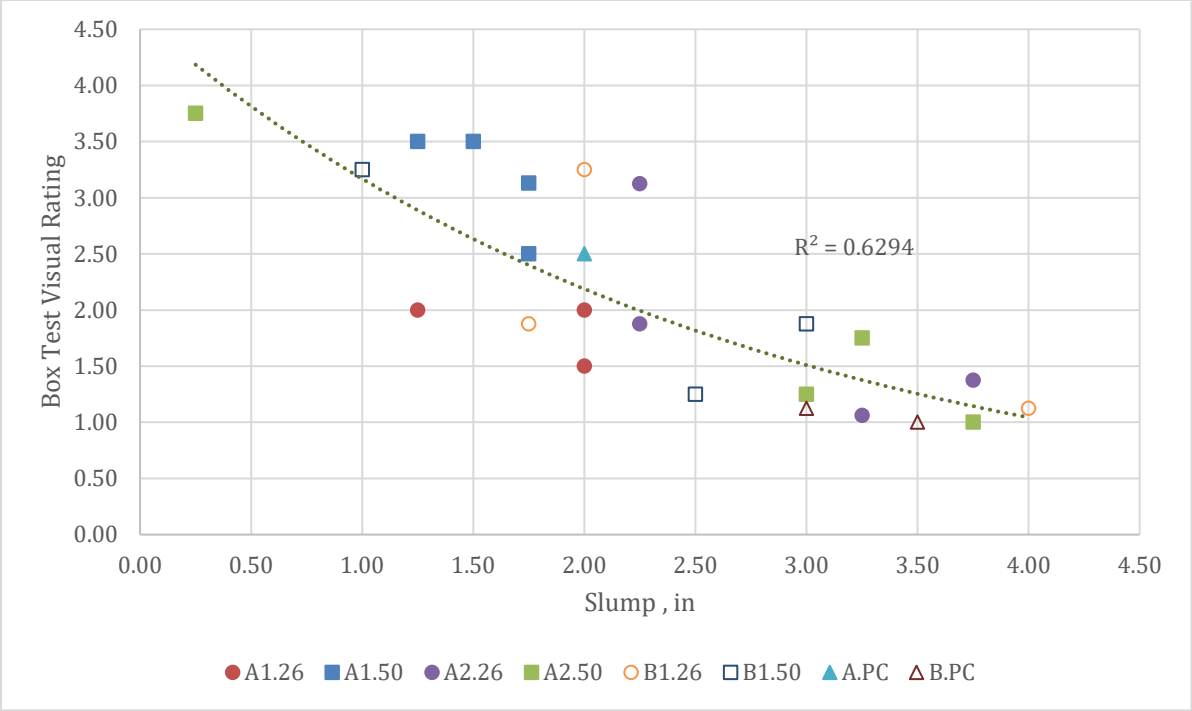

Figure 5-6.Box test rating vs Slump

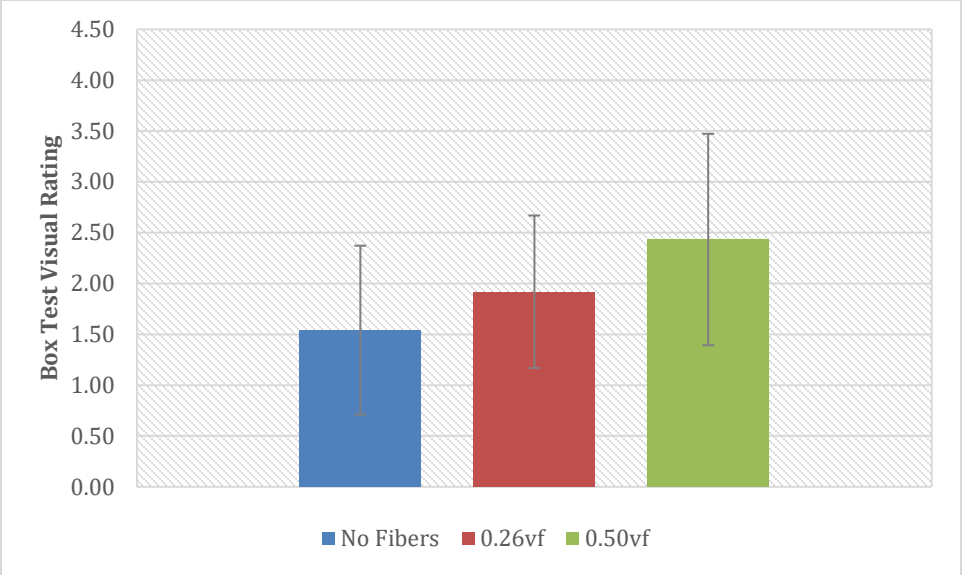

Figure 5-7.Influence of fiber dosage on box test rating

5.1.1.3 V-Kelly Test

Figure 5-8 compares V-Kelly slump and regular slump test results. It can be seen that the V-Kelly slump and regular slump test results (both are based on a static test) have a direct correlation ($R^2 = 0.35$). However, as neither the V-Kelly slump nor regular slump test results actually quantify the workability of the concrete under vibration, the V-Kelly index result is more meaningful for investigating the influence of the fiber on the workability of the pavement concrete. The V-Kelly index obtained from the dynamic V-Kelly test gives more information about the thixotropic nature of concrete mixture than the static slump test. This is pronounced in Figure 5-9, which shows that the V-Kelly index has a poor correlation with the regular slump test result. This finding indicates that concrete with a good regular slump value may not be workable enough for the slip-form paving. A V-Kelly Index between 0.8 to 1.2 in/√s is recommended for the plain concrete mixture to be used for slip-form paving.

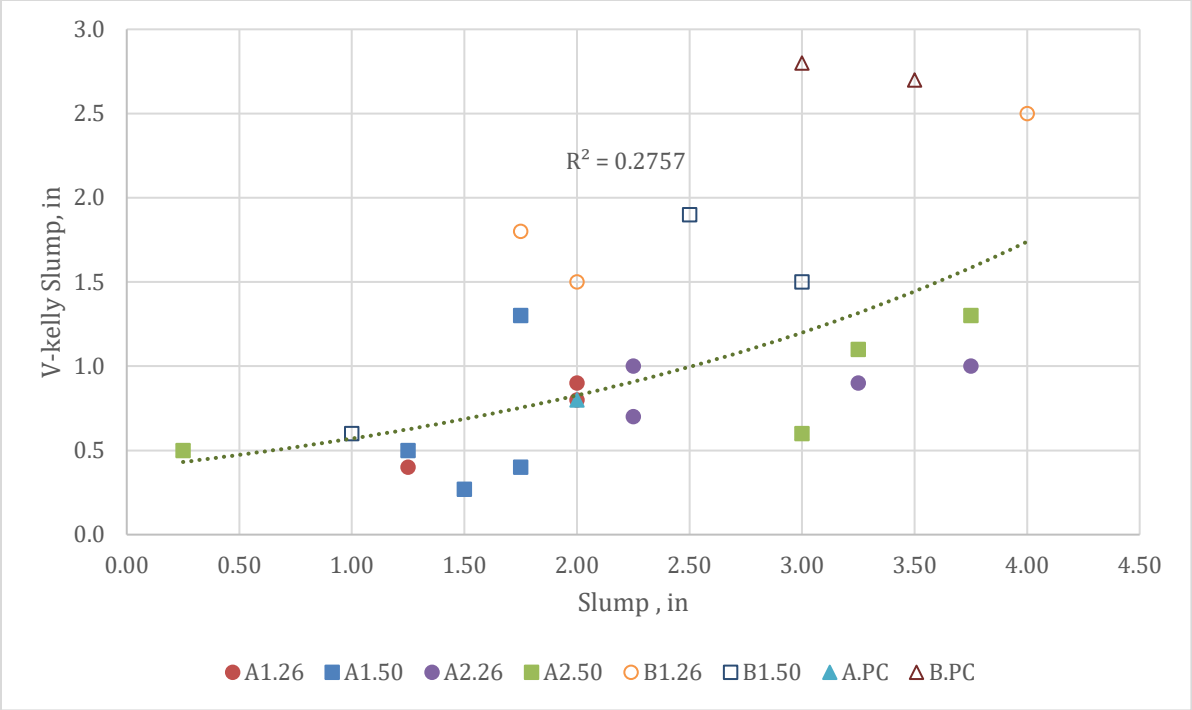

Figure 5-8.V-Kelly slump values vs slump test results

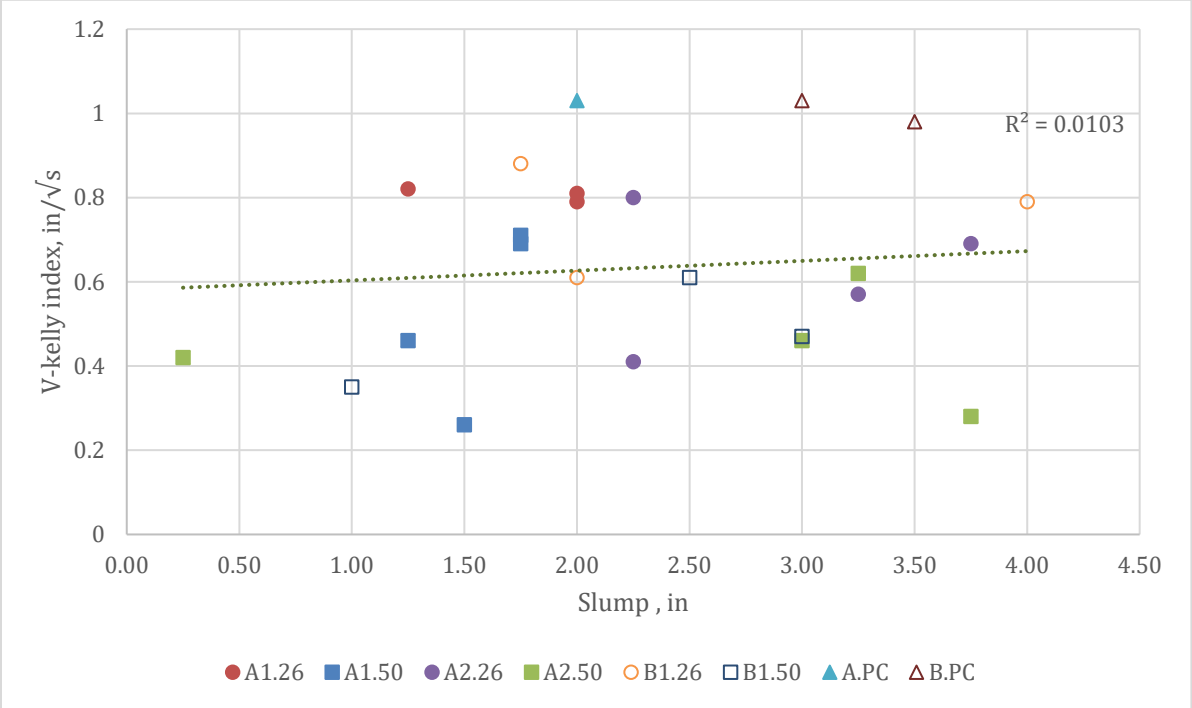

Figure 5-9. V-Kelly index vs slump test results

Figure 5-10 shows that an increase in entrained air content does not have any influence on the V-Kelly index (R^2= 0.0). Also, a large set of V-Kelly index values for mixtures with fibers are below the 0.8 in/√s recommended range for plain concrete. The V-Kelly index for plain concrete with granite class A and limestone class B aggregates was 1.03 and 1.01 in/√s, respectively, which is within the recommended range. The V-Kelly index for mixtures with fiber dosage of 0.26% vf are slightly below 0.8 in/√s, and mixtures with fiber dosage of 0.50% vf are further below. This indicates that the addition of fiber in the mixture significantly influences the V-Kelly index and workability of the concrete under vibration in the slip-form paving.

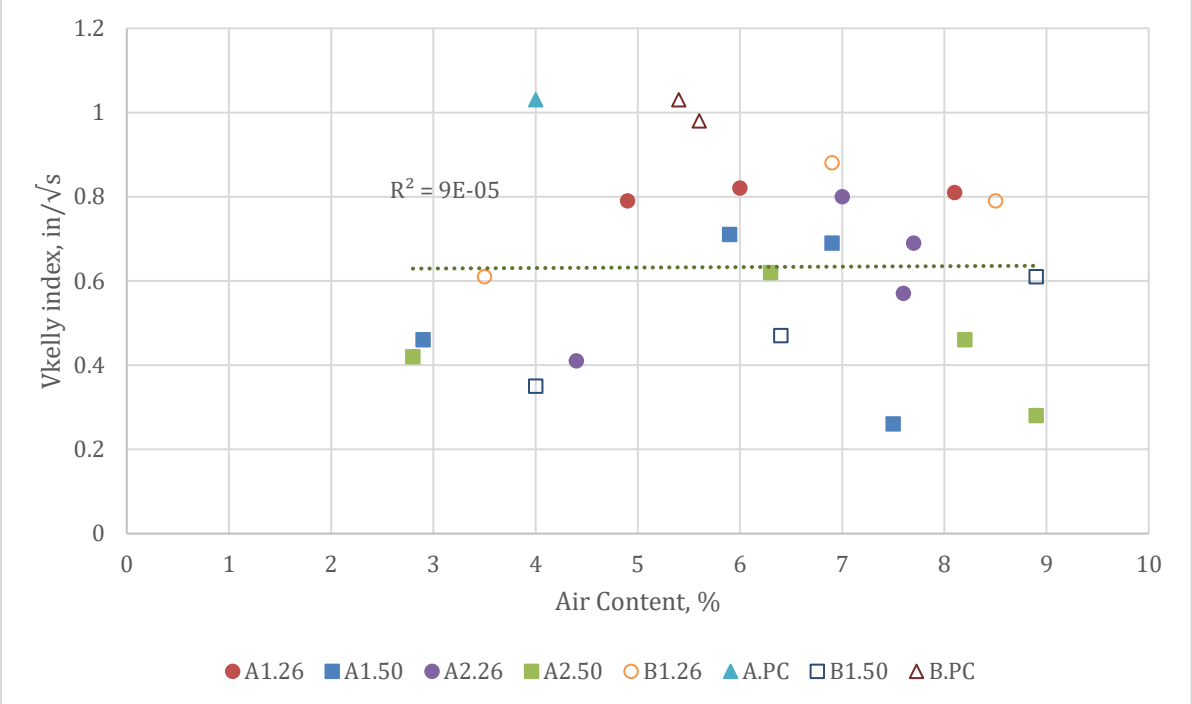

Figure 5-10.V-Kelly Sump vs Air Content

Figure 5-11 and Figure 5-12 show that the V-Kelly index and V-Kelly slump decrease with an increase in fiber dosage. This was evident during mixing as the mixture became stiffer with the increase in fiber dosage due to a decrease in mixture workability.

Therefore, it can be stated that when fibers are used in the mixtures, additional effort shall be given to improve the workability of the concrete so that the V-Kelly index can be improved to meet the target V-Kelly index of 0.8 in/√s. It may also happen that FRC does not need to meet the 0.8 in/√s criterion, but that can be confirmed from the hardened concrete test results. However, it may also be cautioned that the slip-form paving may not work with the concrete that has a V-Kelly index value below 0.8 in/√s.

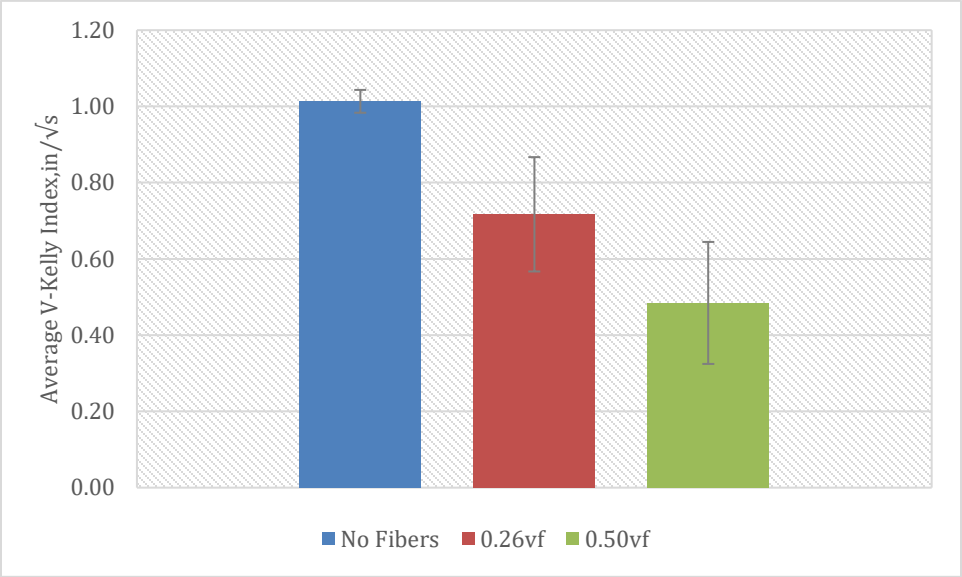

Figure 5-11.Influence of fiber dosage on V-Kelly index

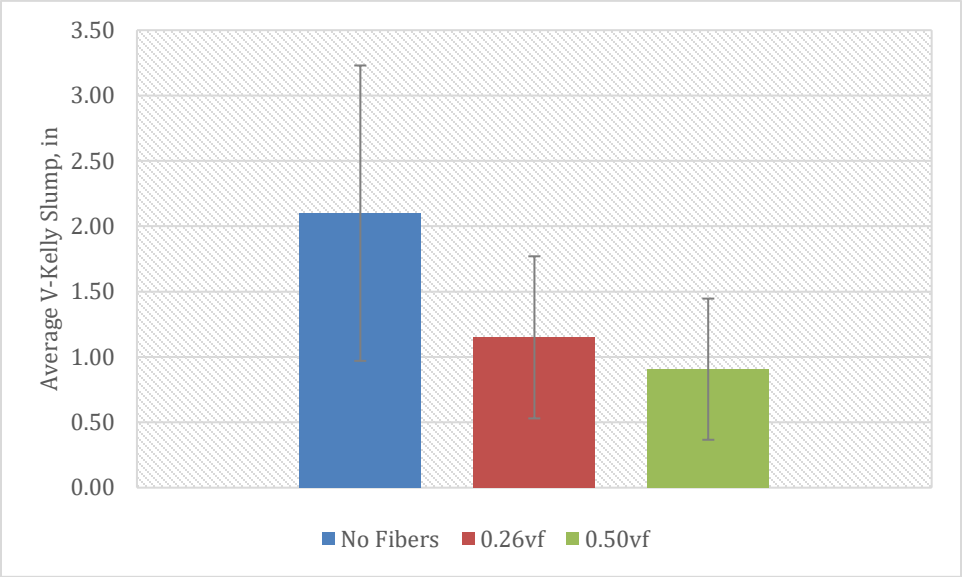

Figure 5-12.Influence of fiber dosage on V-Kelly Slump

Figure 5-13 shows the influence of the fiber type and dosage on the V_Kelly index. The figure illustrates that in addition to fiber dosage, fiber type has a significant influence on the V-Kelly index. In average, the plain concrete resulted in higher V-Kelly index values than the fiber mixes. Between the two types of fibers, concretes with Fiber 2 resulted in lower value V-Kelly index values.

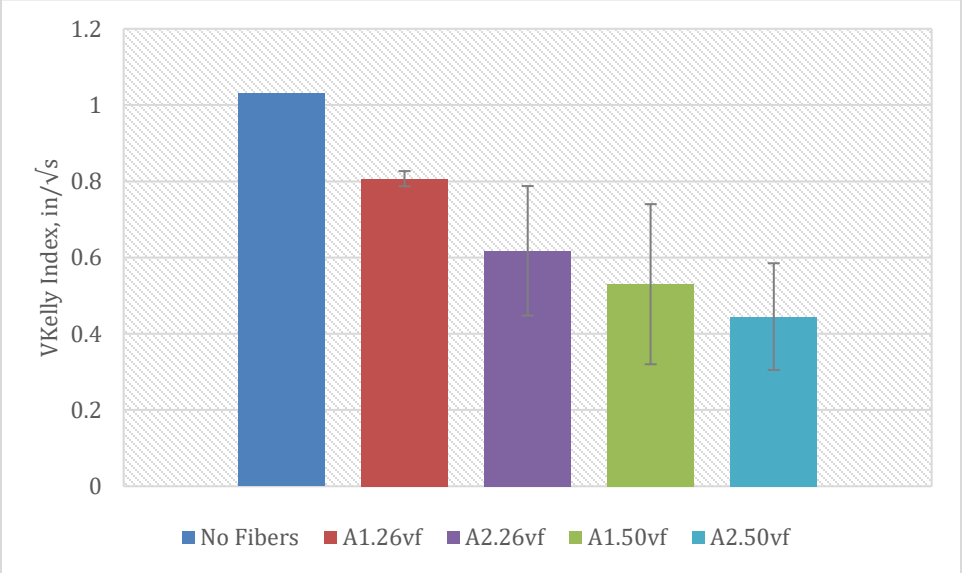

Figure 5-13.Influence of fiber type on V-Kelly index

Figure 5-14 shows that the V-Kelly index is almost identical for plain concrete with aggregate types A and B. For FRC mixes, V-Kelly index for aggregate type A is slightly higher than aggregate type B at a similar fiber dosage. The two types of aggregates have a similar influence on the V-Kelly index, possibly due to the similar size and gradation of both aggregates.

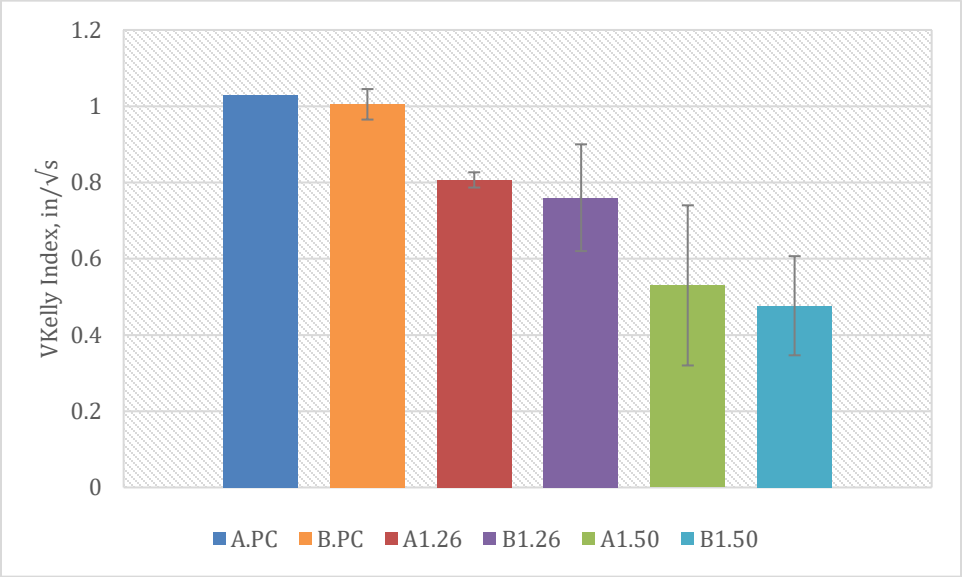

Figure 5-14. Influence of aggregate type on V-Kelly index

5.1.2 Discussion of Hardened Concrete Properties

5.1.2.1 Compressive Strength

All the concrete mixes produced in this study met MnDOT's 28-day minimum compressive strength of 4,000 psi for concrete pavement projects. Figure 5-15 shows that an increase in air content slightly reduces compressive strength. This finding is consistent with results from Ley (2015), according to which concrete compressive strength decreased by approximately 500 psi for every 1% increase in air content.

Figure 5-16 indicates that the addition of macro synthetic fiber into the concrete mixture can decrease the compressive strength. Figure 5-17 and Figure 5-18 show the compressive strength of mixtures with different types of fibers and aggregates, respectively. Mixtures containing Fiber 2 have a higher compressive strength than

mixtures containing Fiber 1, possibly due to the embossed geometry of Fiber 2, and a higher stiffness and aspect ratio than Fiber 1.

It is noticed from Figure 5-18 that mixtures with aggregate B have a higher compressive strength than mixtures with aggregate A. This observation can be attributed to a higher aggregate to cement ratio in mixtures with aggregate B (with 60% coarse aggregates) than those with aggregate A (with 55% coarse aggregates). Erntroy and Shacklock (1954) found that at a constant water-cement ratio, concrete mixtures with more coarse aggregates per volume had higher strength. Neville (1996) concluded that the higher strength is due to less water per volume of concrete.

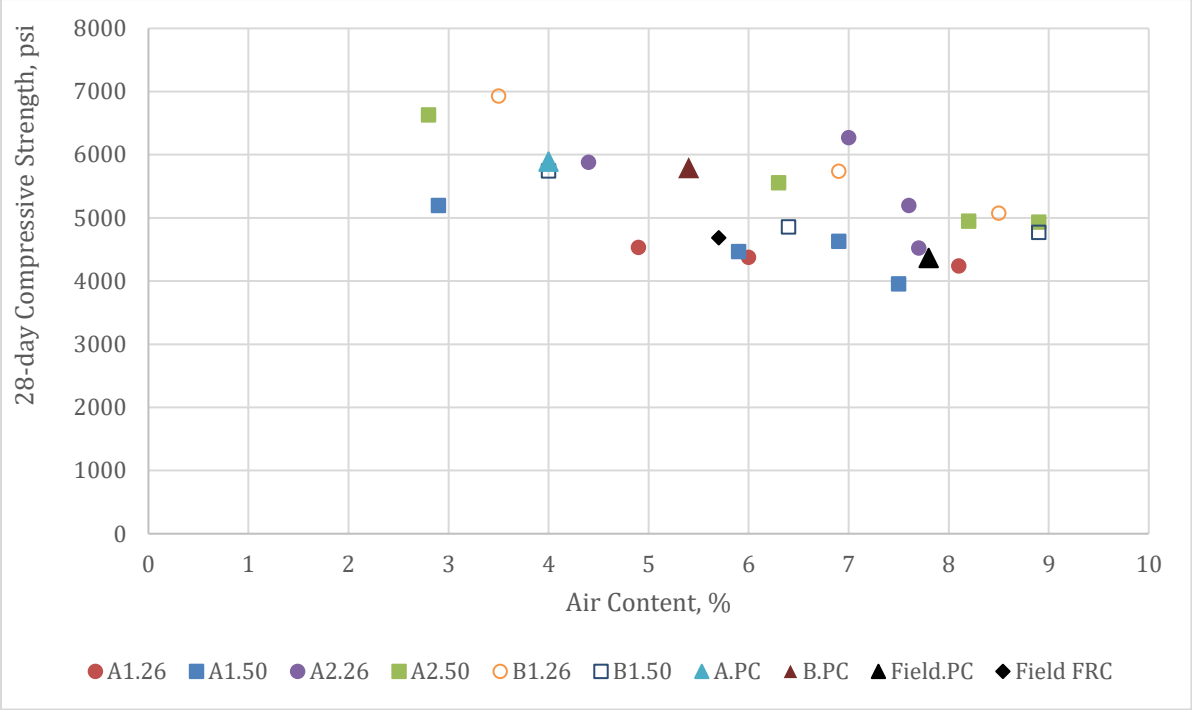

Figure 5-15. Compressive strength vs Air content

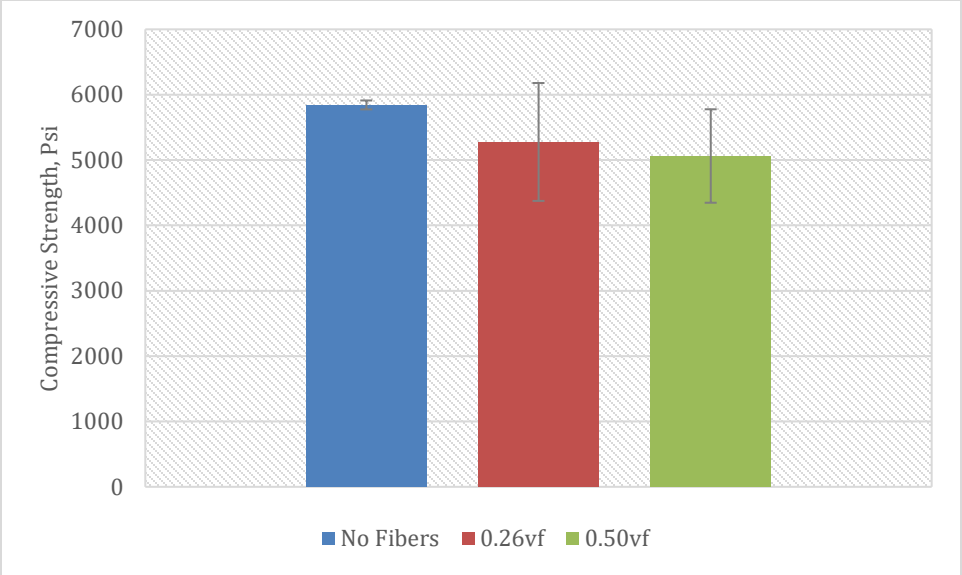

Figure 5-16. Influence of fiber on compressive strength

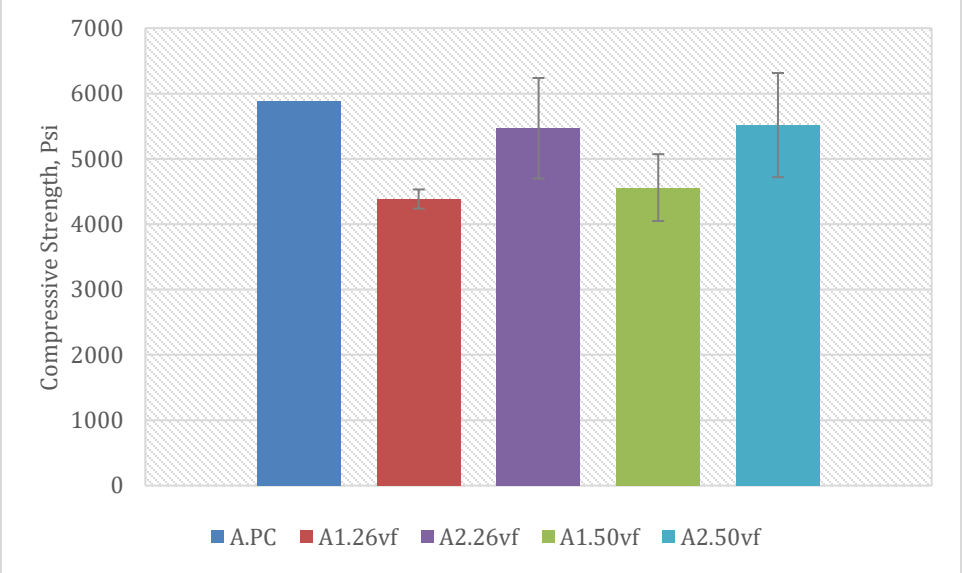

Figure 5-17.Influence of fiber type on compressive strength

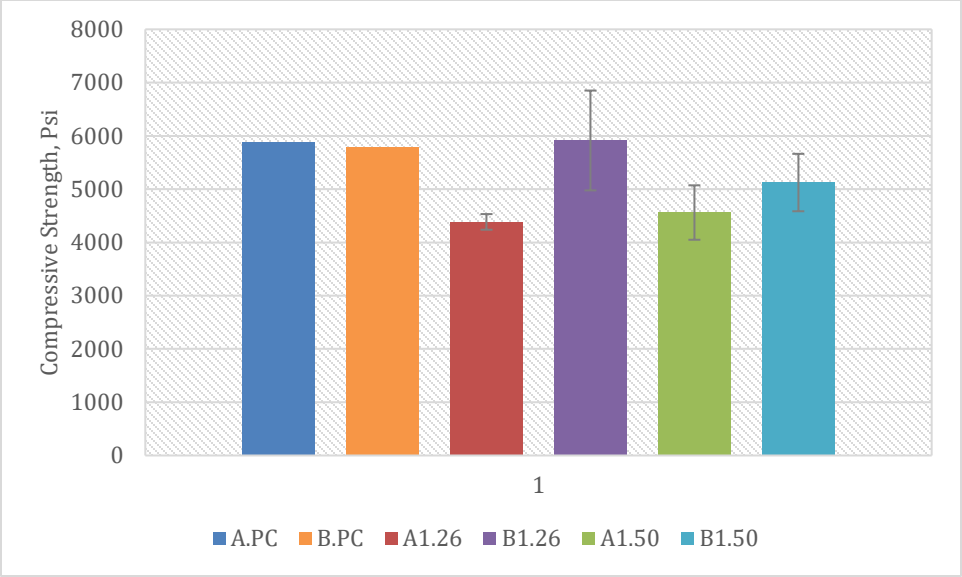

Figure 5-18.Influence of aggregate type on compressive strength

5.1.2.2 Modulus of Elasticity

Figure 5-19 shows that the inclusion of fiber into the concrete mixture lowers the modulus of elasticity of hardened concrete. Also, as observed from Figure 5-20**,** increasing the fiber dosage from 0.26% to 0.50% vf does not significantly influence the modulus of elasticity. The concrete mixture with Fiber 1 shows a higher average modulus of elasticity than the mixture with Fiber 2 (Figure 5-21). Some of the results for Fiber 2 are surprisingly very low. The mixture with granite class A aggregate has a lower elasticity than the mixture with limestone class B aggregate (Figure 5-22).

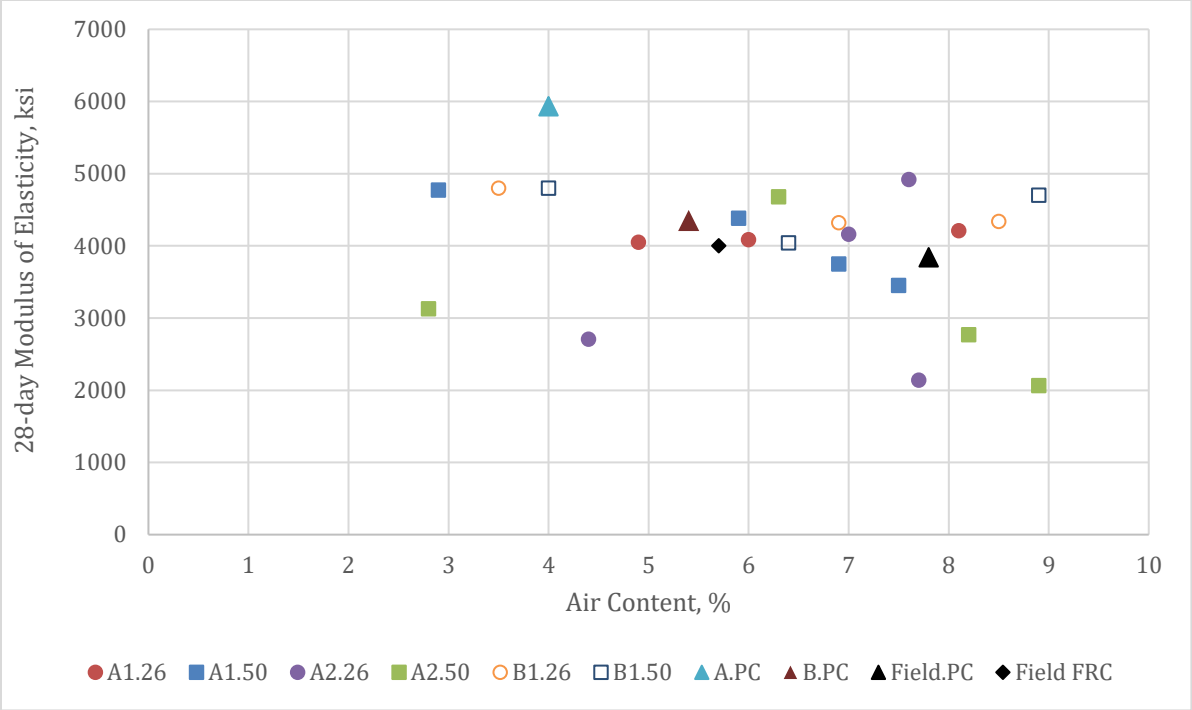

Figure 5-19. Modulus of elasticity vs Air Content

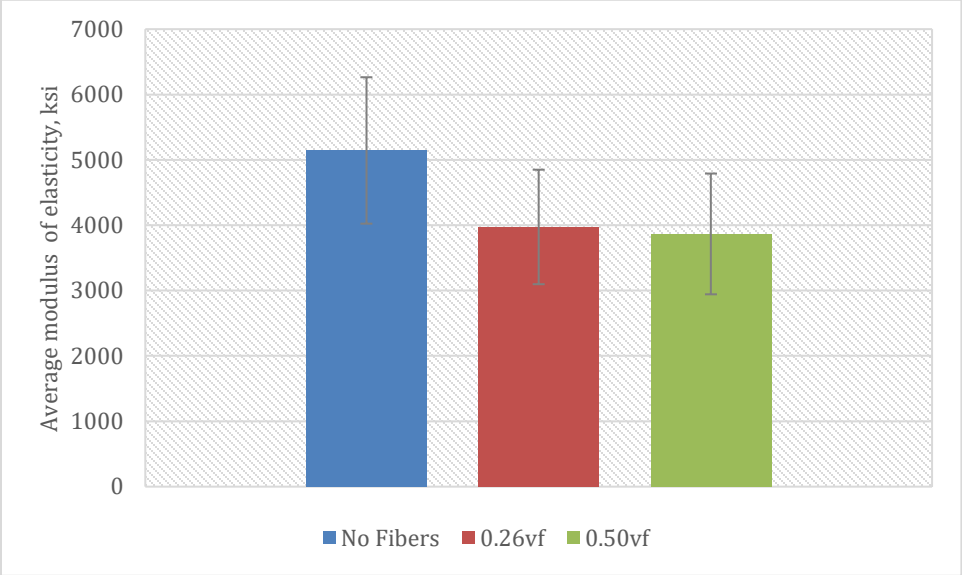

Figure 5-20.Influence of fiber dosage on the modulus of elasticity

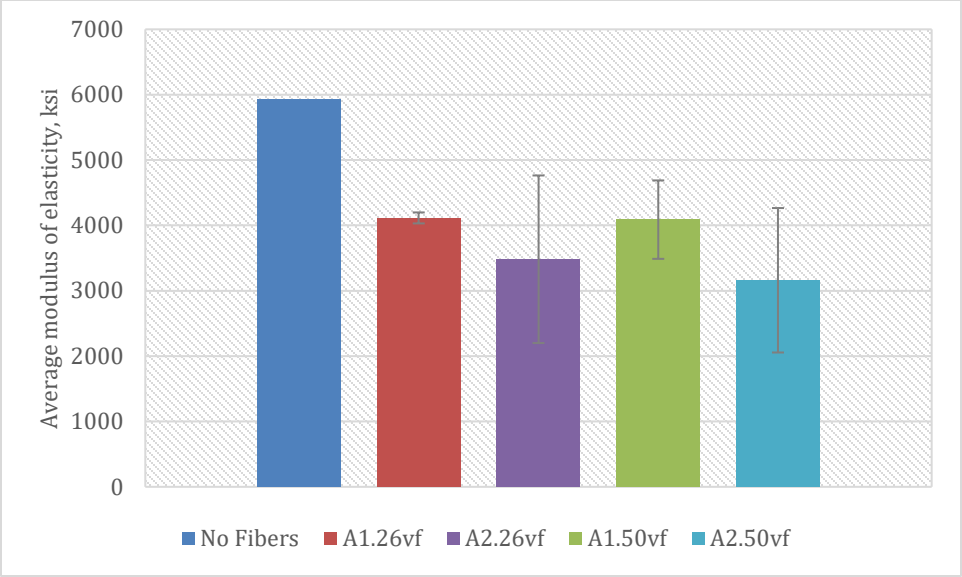

Figure 5-21. Influence of fiber type on the modulus of elasticity

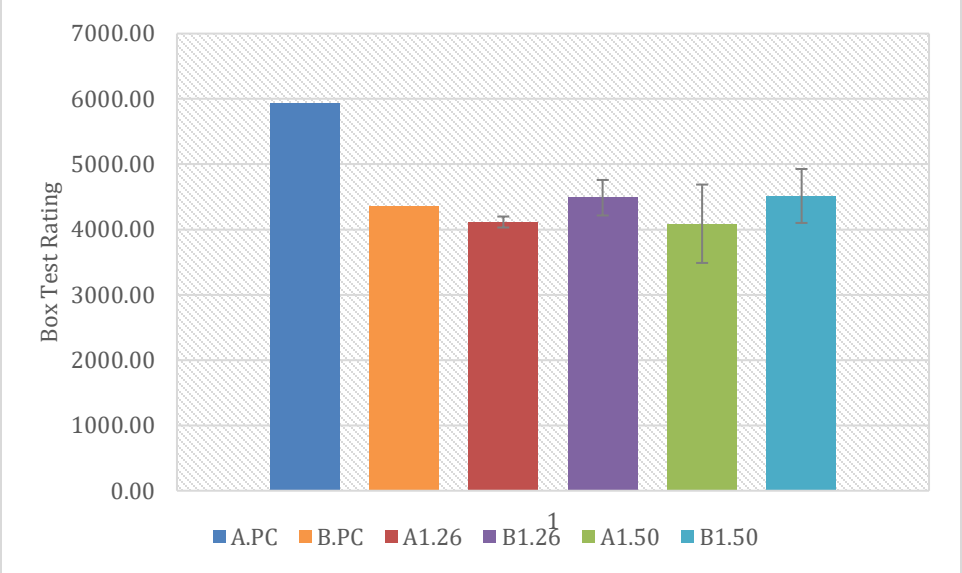

Figure 5-22.Influence of Aggregate type on the modulus of elasticity

5.1.2.3 Flexural Strength

MnDOT requires a minimum flexural strength of 500 psi for concrete pavement slabs less than seven inches thick for opening to construction and general traffic. For slab thickness greater than seven inches, minimum require flexural strength ranges from 350 to 480 psi. From the results of Modulus of Rupture (MOR) test shown in Figure 5-23, it

can be seen that plain concrete and FRC mixes that were designed in accordance with PEM design requirements have a higher MOR than field mixes (not designed in accordance with PEM guidelines). Figure 5-23 also shows a decrease in MOR as the air content increases.

As shown in Figure 5-24, the MOR value is not influenced significantly by the addition of fibers. The slight decrease in MOR with the increase in fiber volume fraction can be attributed to the difference in air content. The average air content of plain concrete and concrete mixtures with 0.26% and 0.50% vf of fiber was 4.7%, 6.46%, and 6.25%, respectively. This finding agrees with Barman et al. (2018) study, which concluded that MOR remained minimally influenced by the volume fraction of macro synthetic fibers.

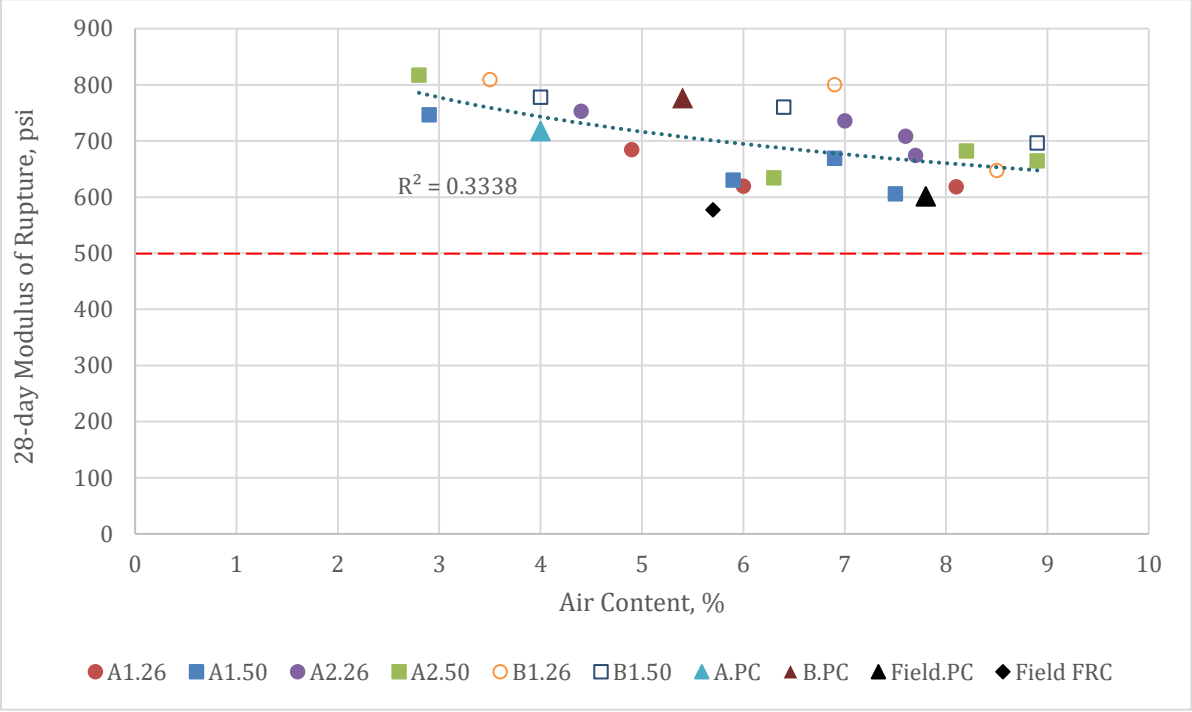

Figure 5-23. MOR vs Air content

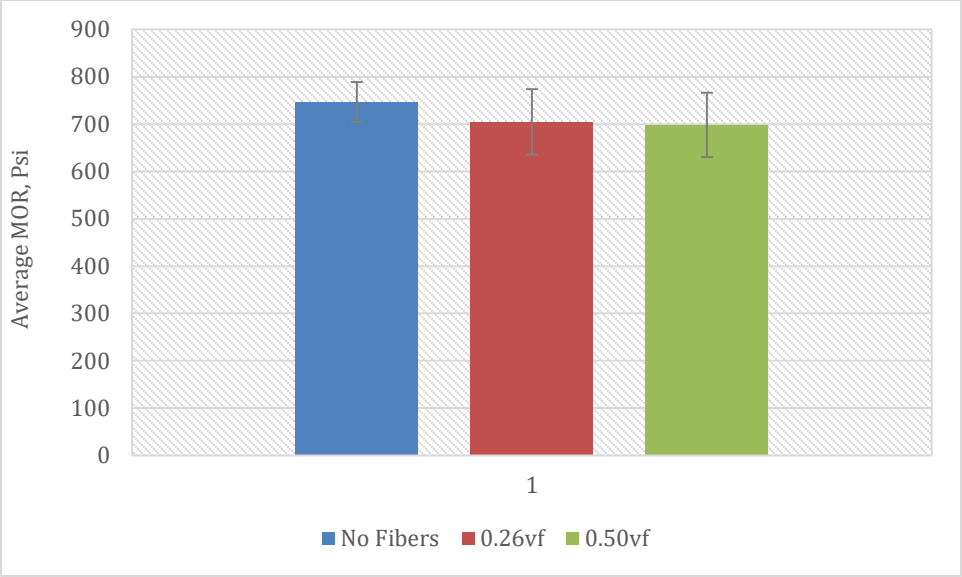

Figure 5-24.Influence of fiber dosage on MOR

As the volume fraction of fiber did not have a significant influence on the MOR of concrete, the effect of fiber and aggregate types was explored. Figure 5-25 shows that mixtures containing Fiber 2 have MOR values almost similar to the plain concrete (for both dosages). However, mixtures containing Fiber 1 have a lower MOR value than plain concrete and mixtures with Fiber 2. Barman et al. (2018) also showed a similar trend for fibers with embossed geometry (Fiber 2) and twisted geometry (Fiber 1). Also, mixtures with Granite Class A aggregates have a lower MOR than mixtures with Limestone Class B aggregates (Figure 5-26).

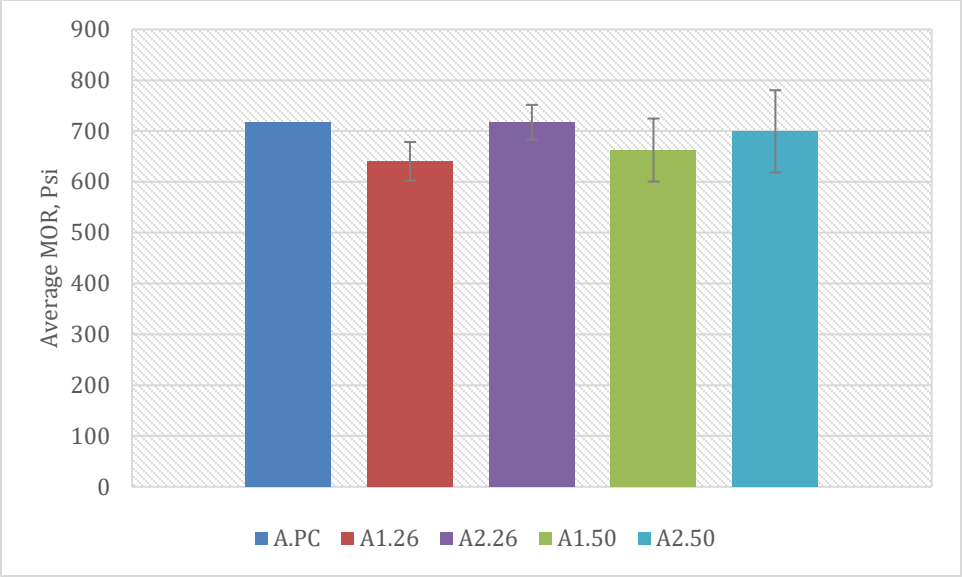

Figure 5-25.Influence of fiber type on MOR

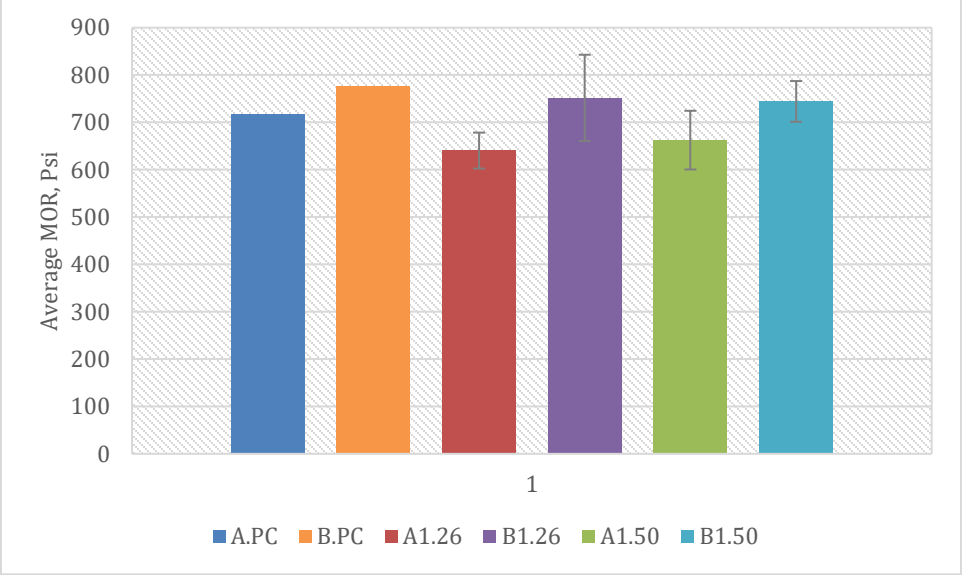

Figure 5-26.Influence of aggregate type on MOR

5.1.2.4 Toughness

Toughness values are computed from the load vs displacement relationships obtained in ASTM C1609 test. Figure 5-27 shows the load vs displacement relationships for three specimens prepared with two dosages (0.26% and 0.50% Vf) of Fiber 1, tested

at 28-day. It can be seen that these specimens continued to sustain loads well after peak load and endure large deformations.

The toughness values are given in Figure 5-28. Although synthetic fibers did not significantly influence the compressive strength and flexural strength of concrete mixtures, the effect of fiber addition on flexural toughness is evident (Figure 5-29). There is an increase of 418% in the toughness of concrete by adding fiber by 0.26% vf. The average toughness improves by 34% by increasing the fiber dosage from 0.26% to 0.50% vf. The improvement in toughness is also apparent in the failure mode of the specimen due to the ability of fibers to enhance the durability of concrete. SyFRC specimens subjected to compressive load failed in a ductile manner and rarely exhibited brittle/explosive failure.

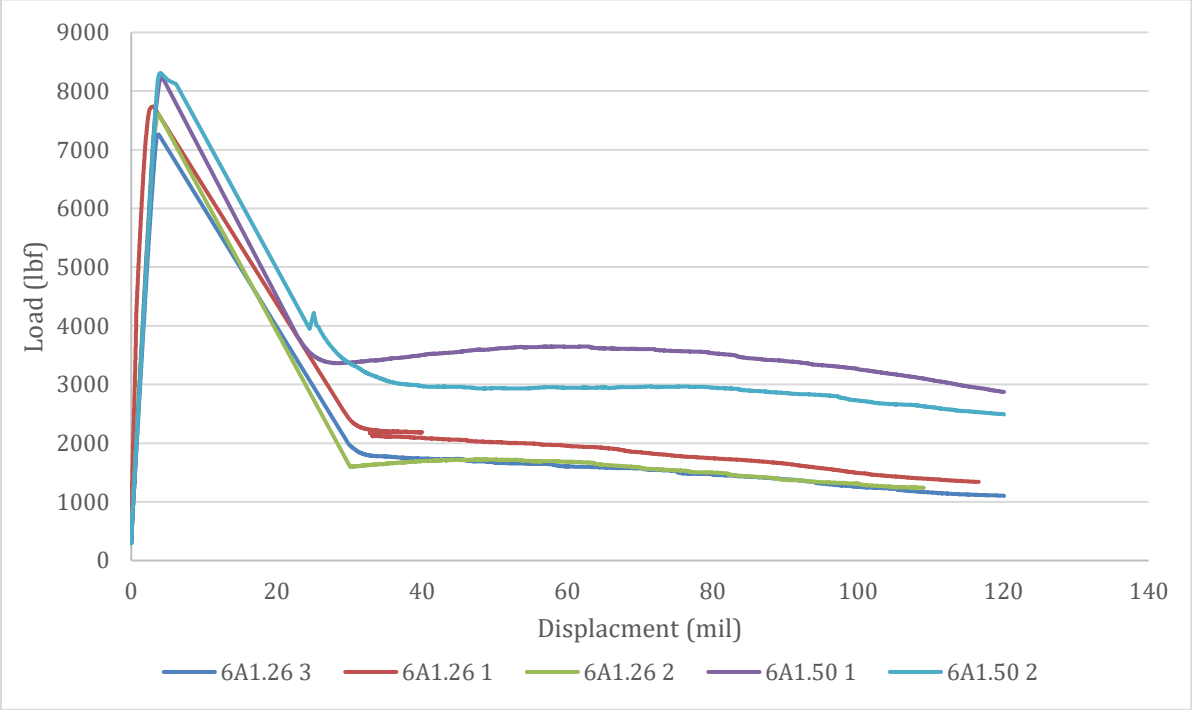

Figure 5-27. Load vs displacement curve for 6A1.26 and 6A1.50

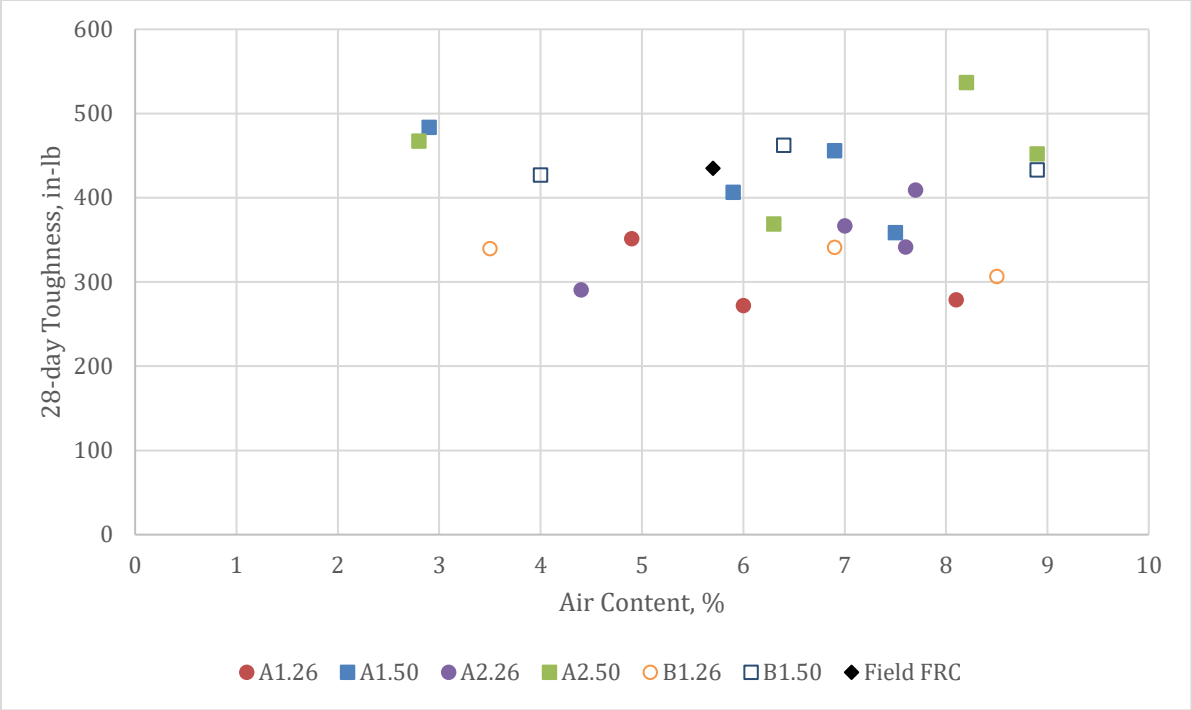

Figure 5-28. Toughness vs Air content

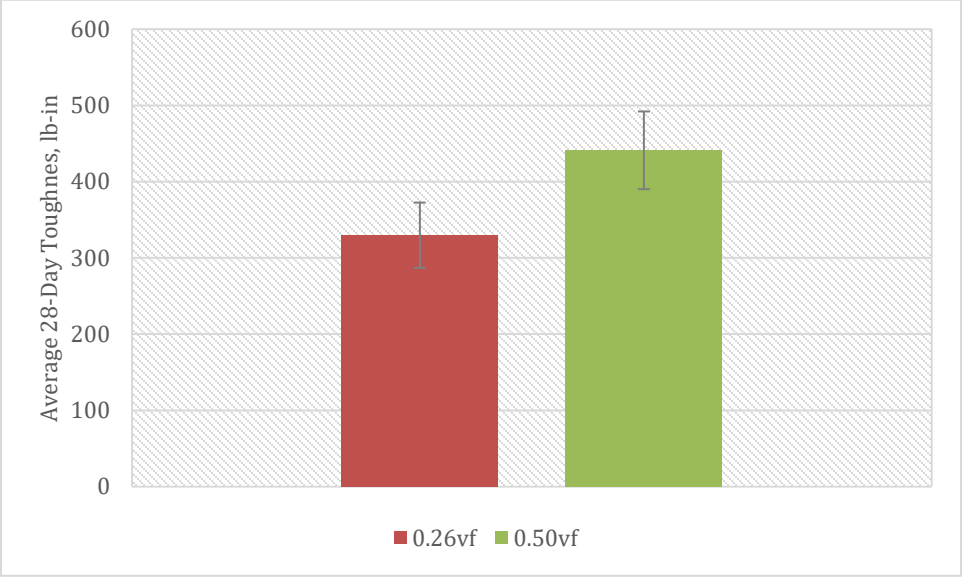

Figure 5-29.Influence of fiber dosage on toughness

It is observed from Figure 5-30 that increasing fiber dosage significantly improves the toughness of concrete. Also, mixtures with Fiber 2 have greater toughness than mixtures with Fiber 1, probably due to their better interfacial bonding with concrete

matrix owing to their embossed and deformed texture. Figure 5-31 shows that the type of aggregate does not significantly influence the toughness, which is obvious, as the toughness in the FRC is provided by the fibers.

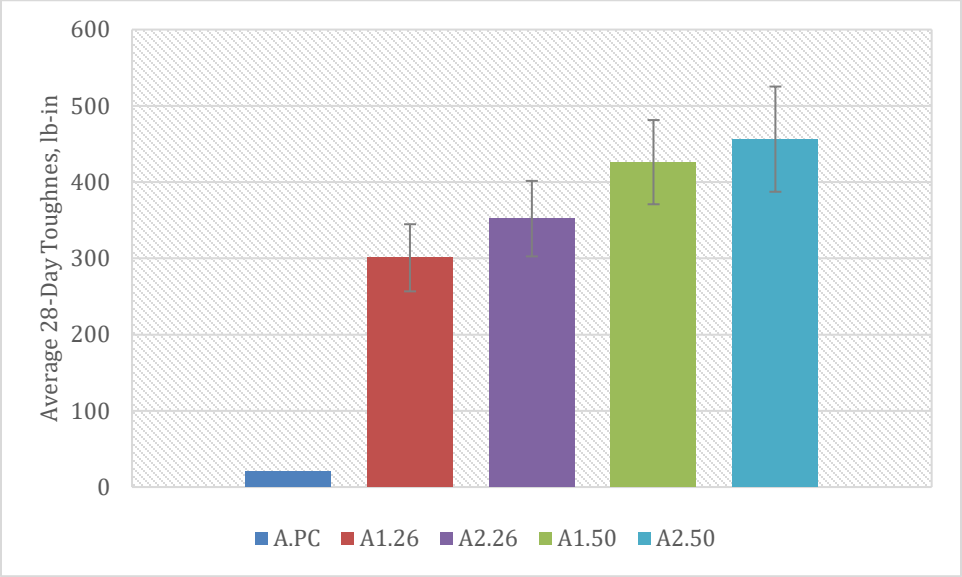

Figure 5-30.Influence of fiber type on toughness

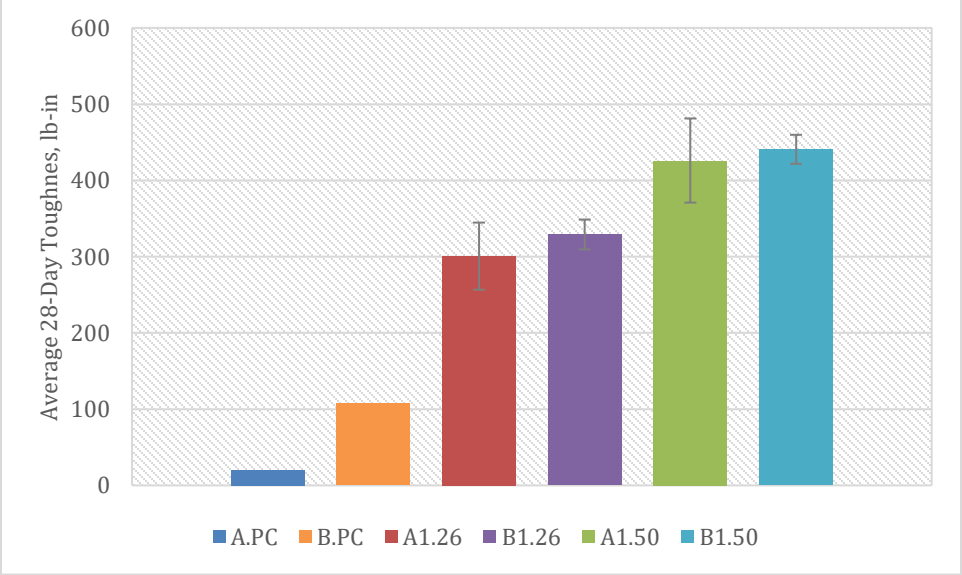

Figure 5-31.Influence of aggregate type on toughness

5.1.2.5 Residual Strength Ratio (RSR)

Figure 5-32 shows that RSR values lie between 11 to 44 percent for all mixes and do not yield a good correlation with air content. Similar to the flexural toughness values of concrete, RSR increased with an increase in fiber dosage (Figure 5-33). This finding is consistent with Barman and Hansen (2018). The average RSR increases from 16 to 31% when the fiber dosage increases from 0.26% to 0.50% vf.

It is observed that fiber type affects the RSR values, as shown in Figure 5-34**.** At a dosage of 0.26% vf, RSR is nearly the same (18%) for both fiber types. Increasing the dosage to 0.50% vf improves the RSR of Fiber 1 and Fiber 2 to 34% and 32%, respectively. Figure 5-35 depicts that mixtures with Granite Class A aggregates have higher RSR than mixes with Limestone Class B aggregates. Increasing the dosage to 0.50% vf improved the RSR of Granite Class A and Limestone Class B mixtures from 18 to 35% and from 12 to 26%, respectively.

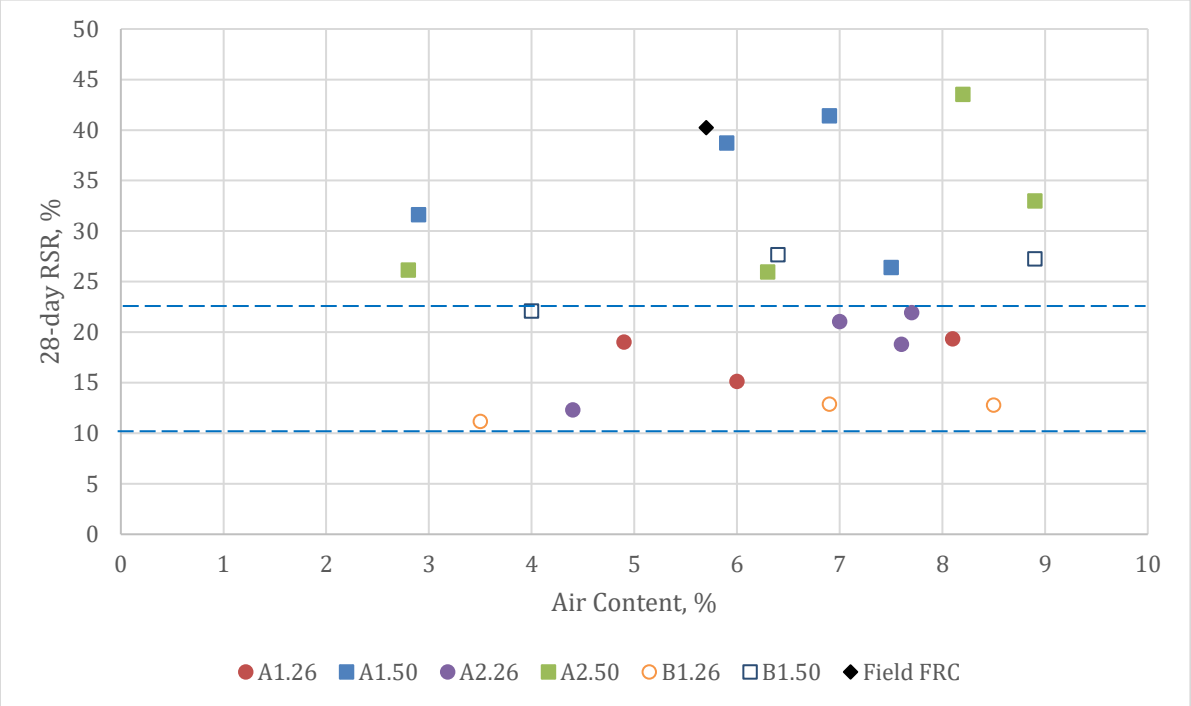

Figure 5-32. RSR vs air content

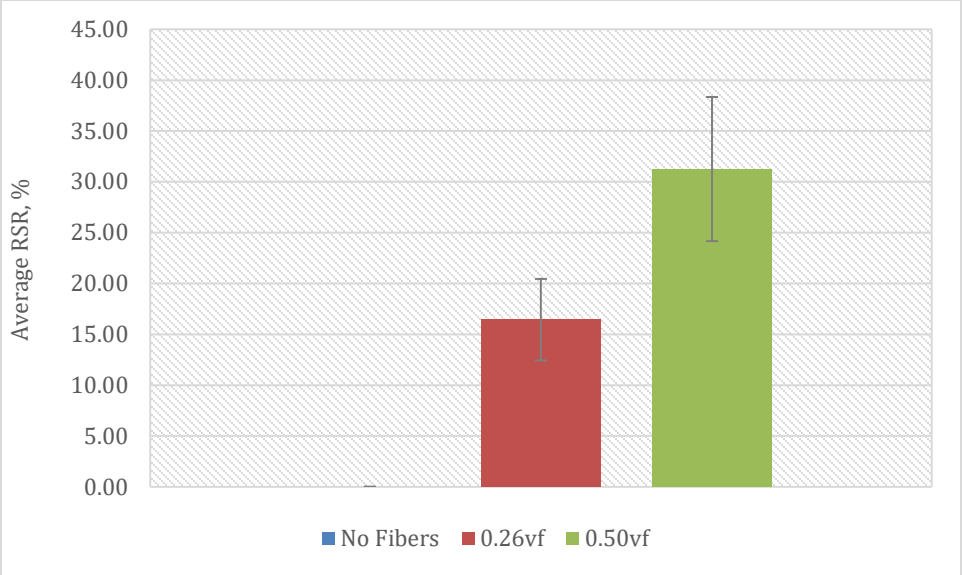

Figure 5-33. Influence of fiber dosage on RSR

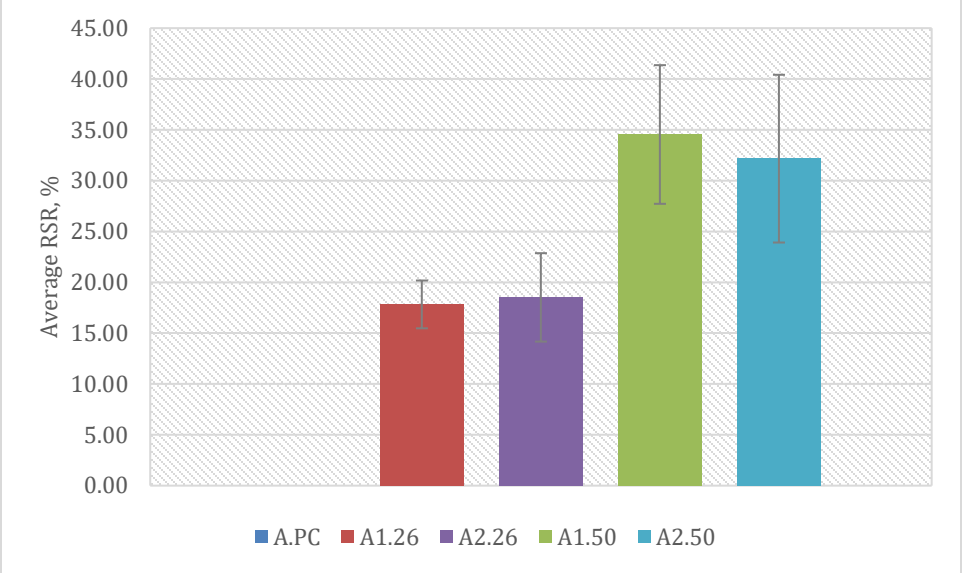

Figure 5-34. Influence of fiber type on RSR

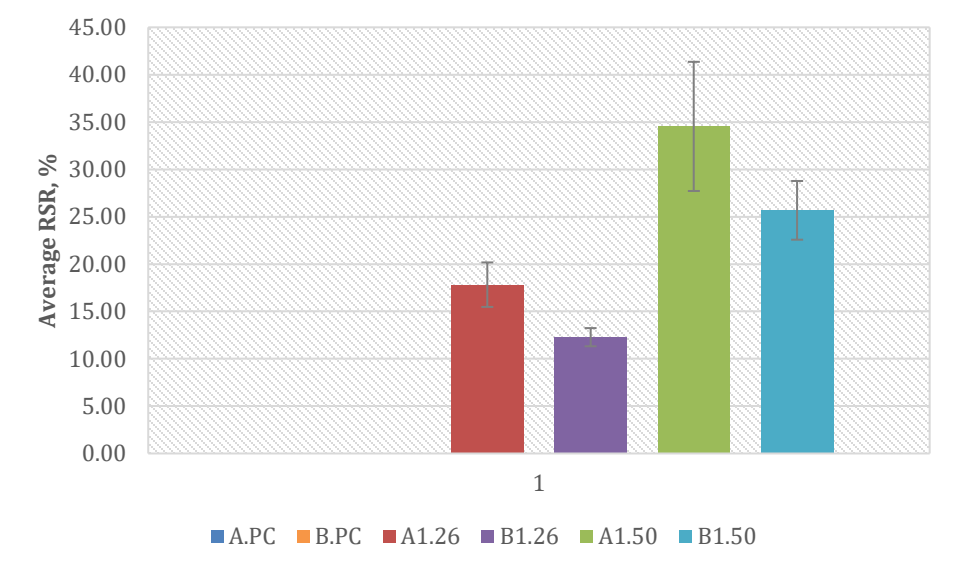

Figure 5-35. Influence of aggregate type on RSR

5.1.2.6 Electrical Resistivity

The electrical resistivity of concrete can assess the resistance of concrete against the penetrability of chloride ions. The factors such as specimen age, geometry, and curing condition can impact the resistivity of concrete. In this study, two different sets of specimens were used to study the electrical resistivity of the concrete: (i) Set A- concrete specimens cured in a calcium hydroxide saturated simulated pore solution for 7-days (referred to as bucket test), and (ii) Set B-concrete specimens cured in a moist room for 28-day (20^0C and 95 relative humidity).

SET-A (CALCIUM HYDROXIDE SATURATED SPECIMEN)

Table 5-4 shows the resistivity limits for a saturated specimen. A specimen is considered fully saturated after it is submerged in a pore solution for a minimum of 6 days. The electrical resistivity values shown in Figure 5-36 are the 7-days resistivity measurements for several mixes, with and without fibers. It is seen that after 7-days, concrete specimens have resistivity readings that correspond to moderate to the low penetrability of chloride ions. Generally, the resistivity of concrete increases as the specimen ages until it reaches a nick point; therefore, it may be anticipated that the electrical resistivity of the concrete will further increase if the specimens were tested at

28-day or later. Alternatively, it can be stated that the concrete mixes tested in this study, either plain or fiber reinforced concrete, will not be vulnerable to chloride ion penetration. The results in Figure 5-36 also indicate that the inclusion of macro synthetic fiber does not influence 7-day bucket test resistivity results, at least for the types and dosages used in this study.

Table 5-4. Performance limits from the Rapid Chloride Permeability Test (RCPT), along with equivalent resistivity values of a saturated system (ASTM C1202)

ASTM C1202 Classification[1]	Charge Passed (Coulombs)[1]	Resistivity (kOhm·cm)[2]
High	>4,000	<5.2
Moderate	2,000–4,000	5.2–10.4
Low	1,000–2,000	10.4–20.7
Very low	100–1,000	20.7–207
Negligible	<100	>207

[1]From ASTM C1202-12.
[2]Calculated using first principles.

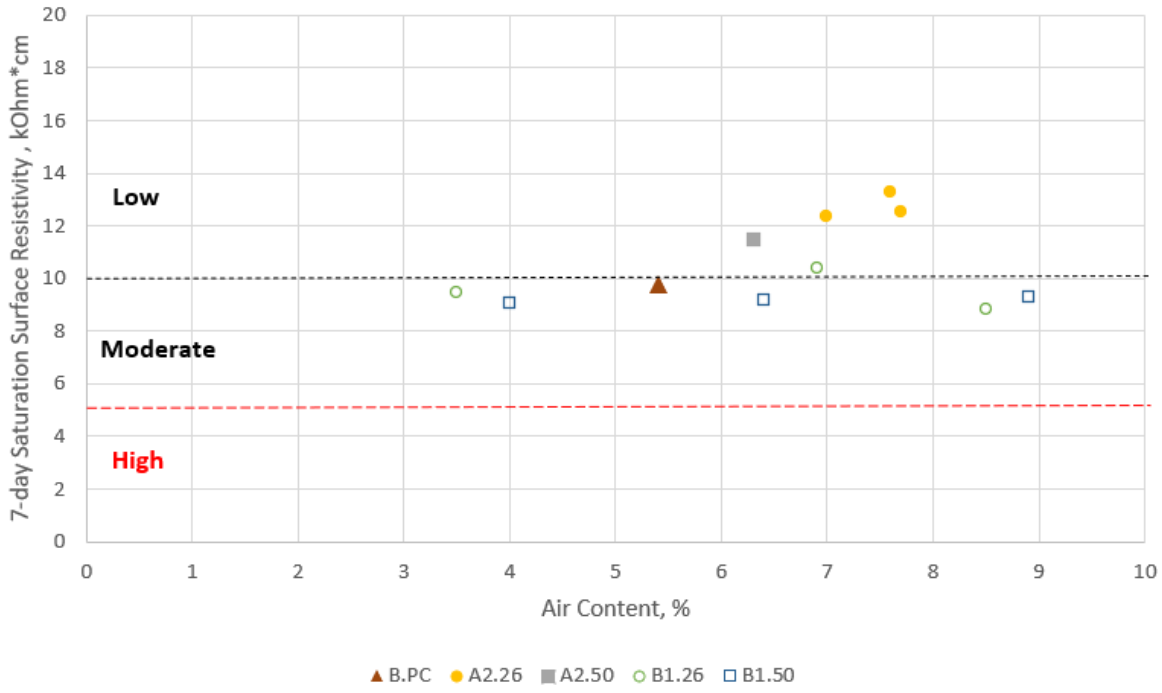

Figure 5-36. Saturation surface resistivity vs Air content

SET-B (MOIST CURED SAMPLES)

Table 5-5 shows the 28-day resistivity classification of chloride ion penetrability of specimens cured in a moist room based on the specimen geometry (AASHTO TP 95). Figure 5-37 shows that the concrete specimens tested in this study, irrespective of plain or fiber reinforced concrete, exhibited low chloride ion penetration. It is observed that the mixes designed in accordance with PEM requirements have better resistance to the penetration of chloride ions compared to the MnROAD samples, which were not designed according to the PEM method. Like the Calcium hydroxide saturated specimen, the resistivity results for the moist cured specimen also indicate that the addition of macro synthetic fibers into the mixture has no significant effect on resistivity readings.

Table 5-5.Chloride Ion Penetration Classification (AASHTO TP 95)

Chloride Ion Penetrability	Surface Resistivity Test	
	4 inch X 8 inch Cylinder (KOhm-cm) a=1.5	6 inch X 12 inch Cylinder (KOhm-cm) a=1.5
High	< 12.0	< 9.5
Moderate	12.0 – 21.0	9.5 - 16.5
Low	21.0 – 37.0	16.5 – 29.0
Very Low	37.0 – 254.0	29.0 – 199.0
Negligible	> 254.0	> 199.0

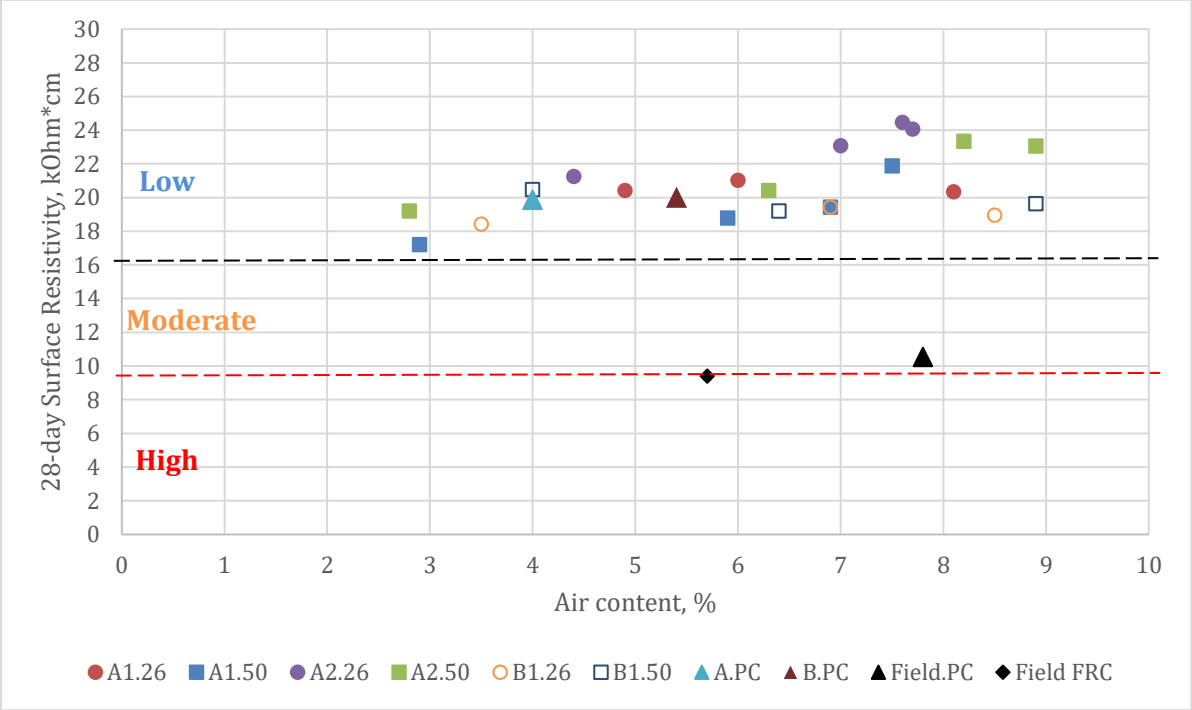

Figure 5-37. Surface resistivity vs Air content

5.1.2.7 Freeze-Thaw Durability

Concrete with Relative Dynamic Modulus (RDM) value greater than 60% after 300 freeze-thaw cycles is considered to have good resistivity against freeze-thaw exposure (ASTM C666). Figure 5-38 depicts that every specimen tested in the current study satisfies the 60% RDM minimum criterion by a large margin, which indicates that the mixes prepared with the PEM method can produce mixes that can offer excellent resistance to freeze-thaw, irrespective of the plain or fiber reinforced concrete.

This finding is in agreement with the results from Komatska and Wilson (2016) study, which states that adding fibers does not compromise the concrete structure freeze-thaw durability, provided that it is air-entrained, compacted adequately, and modified to integrate fibers. One surprising observation from the freeze-thaw test result is that the RDM did not decrease with the freeze-thaw cycles. Al-Assadi et al.,2015 also did not see a decrease in RDM under freeze-thaw testing for the C45 concrete.

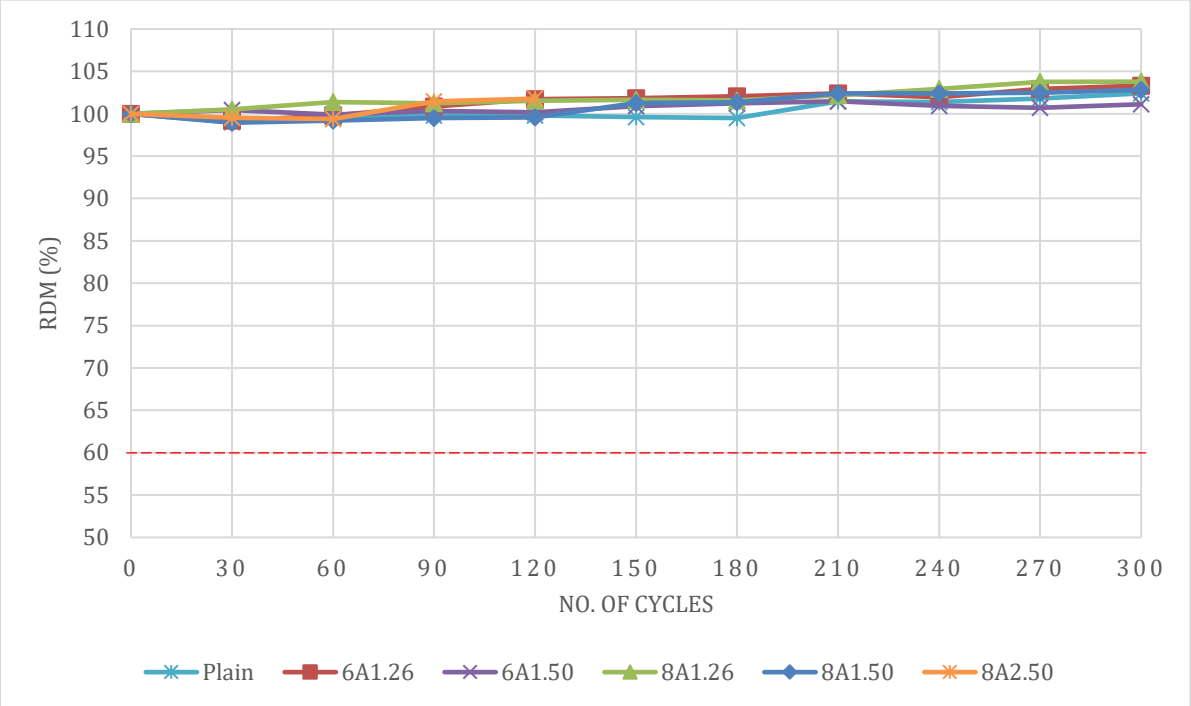

Figure 5-38. Relative dynamic modulus (RDM) vs number of F-T cycles

5.1.3 Correlation Between Fresh and Hardened Concrete Properties

PEM design procedure seeks to produce concretes resistant to climate and material-related distresses, such as durability cracks and concrete-degradation due to chloride-ion penetration. As the key objective of the study is to determine the target fresh concrete properties, it is essential to investigate the influence of the fresh properties on the hardened concrete properties.

5.1.3.1 V-Kelly index vs Harden Concrete Properties

As shown in Figure 5-39 and Figure 5-40, concrete flexural toughness and RSR values decrease as the V-Kelly index increases. This can be attributed to the observation from previous sections that fiber dosage is directly proportional to concrete toughness and RSR and inversely related to the V-Kelly index.

The RDM results slightly decrease as the V-Kelly index increases (as shown in Figure 5-41), but it shall be recalled that the variation of the RDM for all the mixes were not significant. Based on the test results, it appears that the V-Kelly index does not yield any reasonable correlations with MOR (Figure 5-42**)**, compressive strength **(**Figure 5-43**)**, and surface resistivity **(**Figure 5-44) for the laboratory produced concretes and test samples. While this may sound surprising, but as it was seen that the plain and fiber reinforced concretes produced in this study did not differ much in terms of the above mentioned three parameters. It may be stated that the target value of V-kelly index for the pavement concrete shall rather be decided based on the desired workability for the pavement concrete in the field. Because fibers decrease the V-Kelly index, appropriate measures shall be taken to improve the V-Kelly index in order to achieve a proper consolidation of the fiber reinforced concrete under the pavers. It shall be recognized that the consolidation effort which can be applied in the laboratory condition may not differ much between the plain and FRC test specimens, but in the field the same may not be true. A low V-kelly index can create a harsh mix for the paver, and the effective consolidation may be less in the field, resulting in low compressive strength and modulus of rupture.

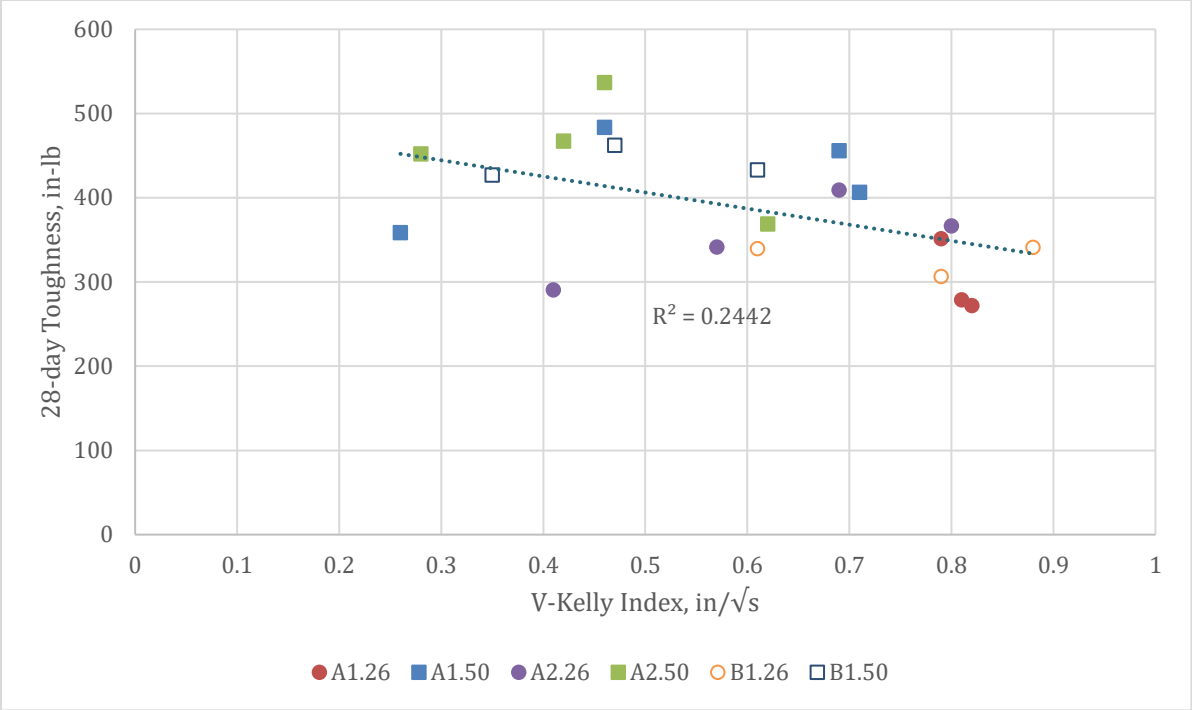

Figure 5-39. Toughness vs V-Kelly index

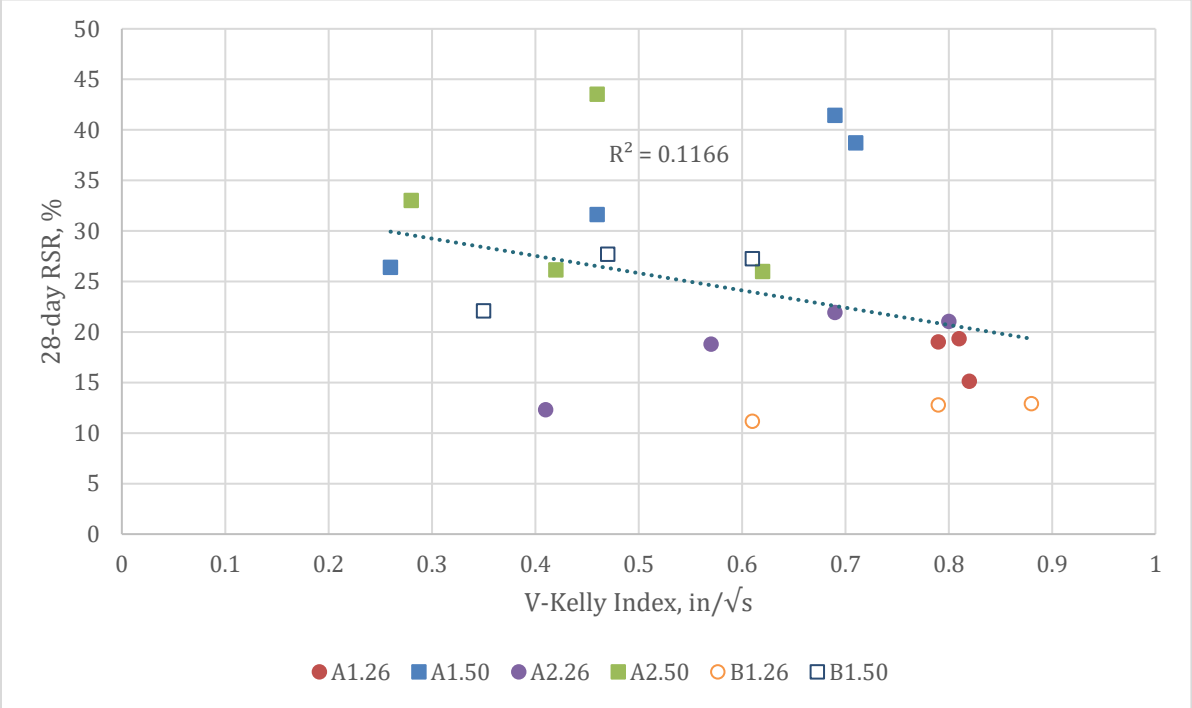

Figure 5-40. RSR vs V-Kelly index

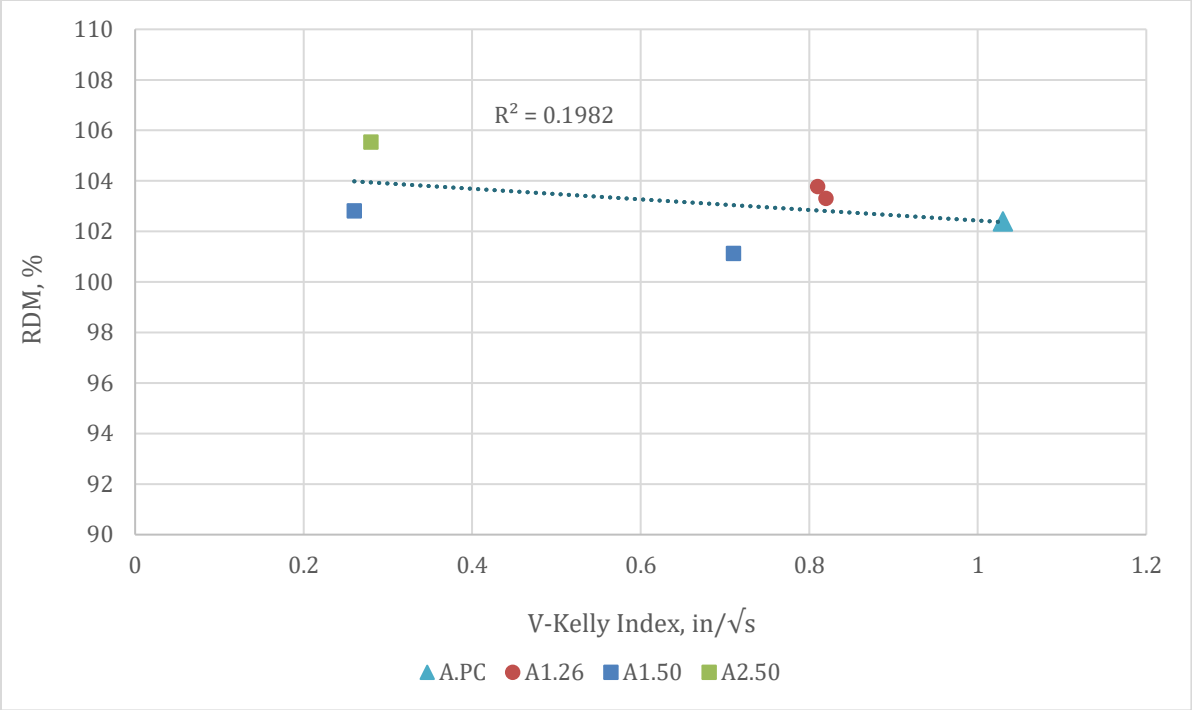

Figure 5-41. RDM vs V-Kelly index

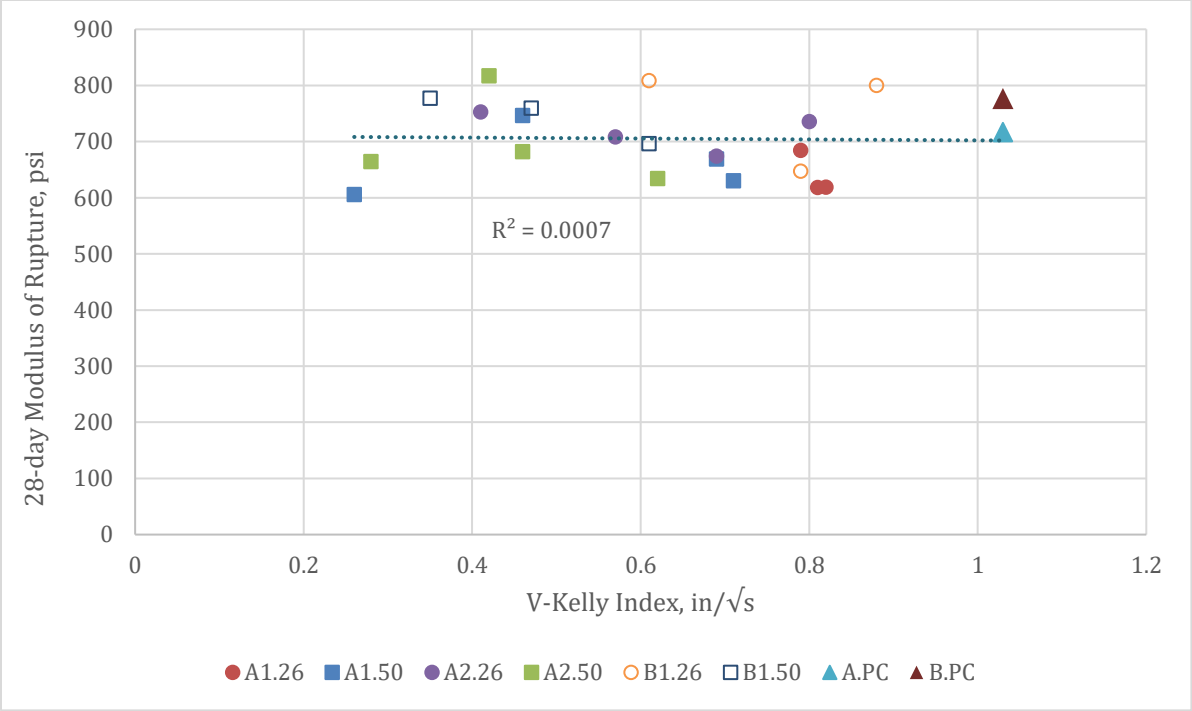

Figure 5-42. MOR vs V-Kelly index

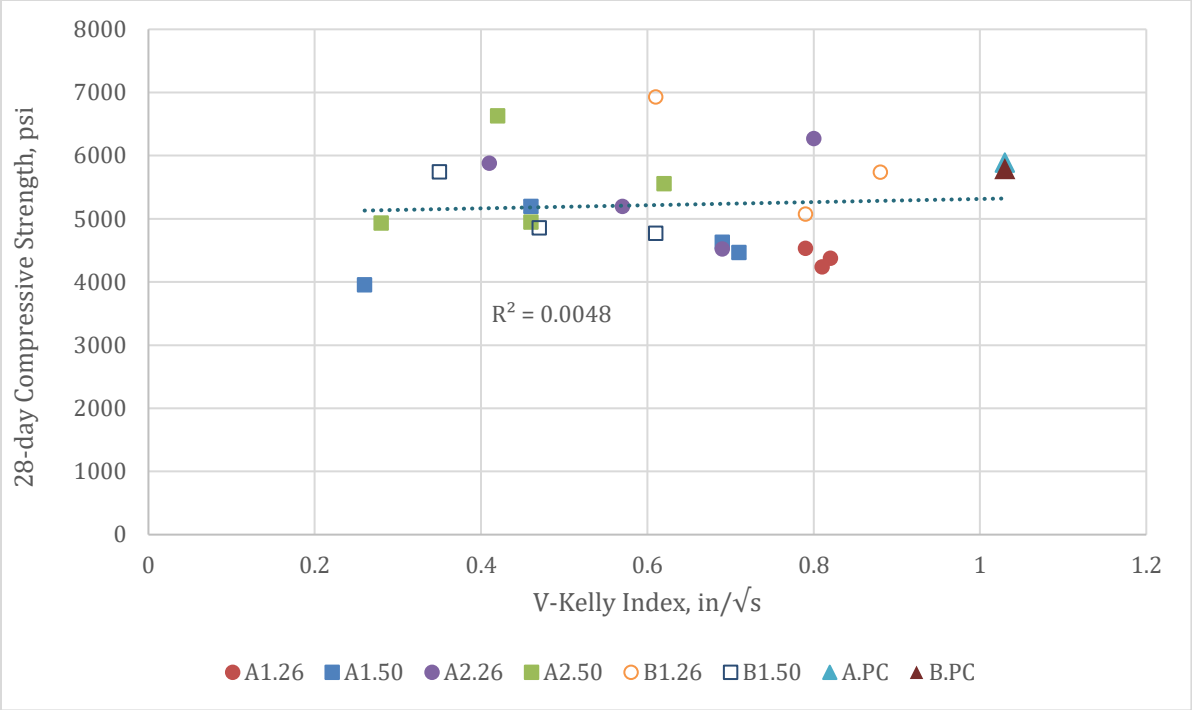

Figure 5-43. Compressive Strength vs V-Kelly index

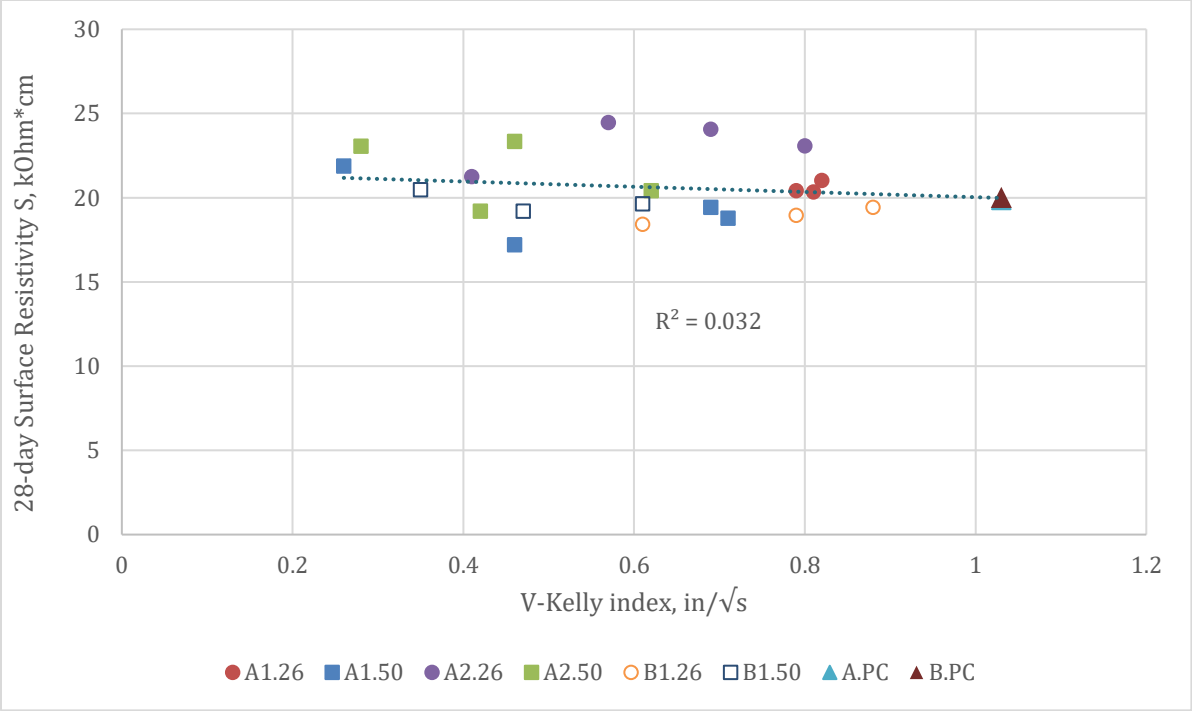

Figure 5-44. Surface Resistivity vs V-Kelly index

5.1.3.2 SAM Number vs Harden Concrete Properties

As shown in Figure 5-45 and Figure 5-46, concrete flexural toughness and RSR did not show any notable correlation with the SAM number. Other harden concrete properties showed poor correlations too as shown in Figure 5-47, Figure 5-48, Figure 5-49 and Figure 5-50. As the SAM number is an indicator for the air content spacing factor, it was expected that the SAM number will have a reasonable correlation with the surface resistivity (Figure 5-50); however this was not the case, probably because of the small data set and less variation in the mixture properties. Based on the above mentioned results, it can be stated the limited change occur in the SAM number because of the fibers' (or because of fiber geometry, dosage, or other properties) may not significantly influence the surface resistivity or the freeze-thaw durability of the concrete. However, further study with more varieties of fibers and additional dosages can provide a better conclusion.

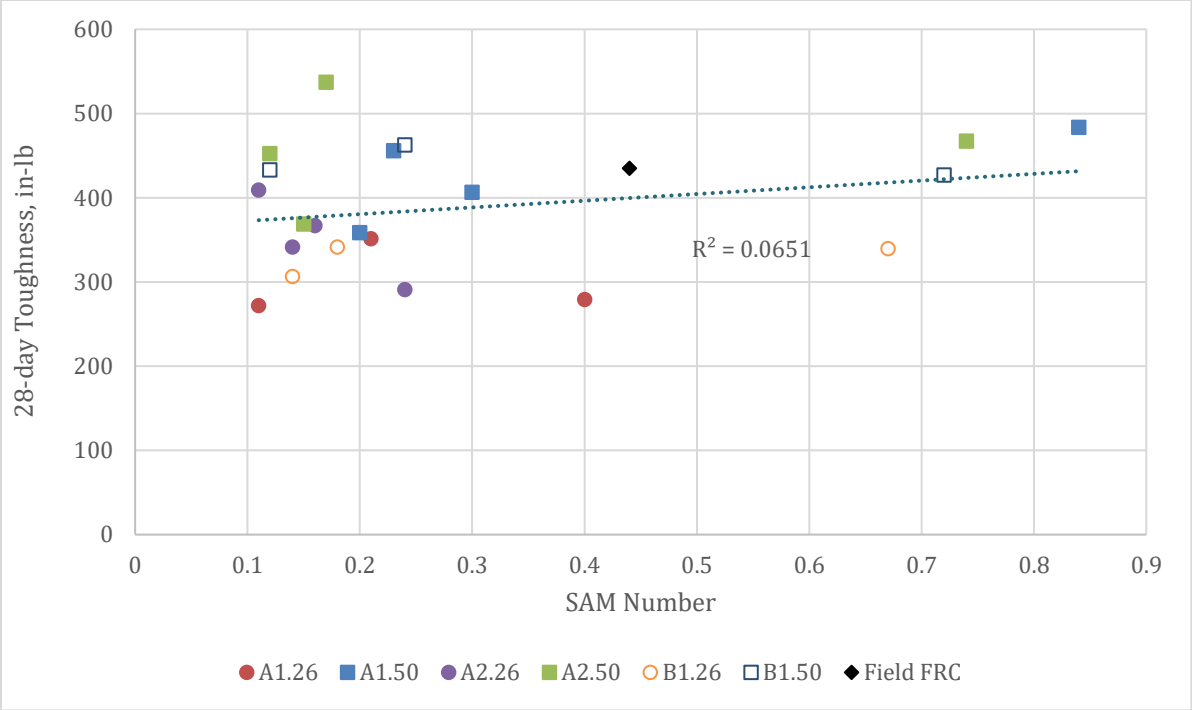

Figure 5-45. Toughness vs SAM number

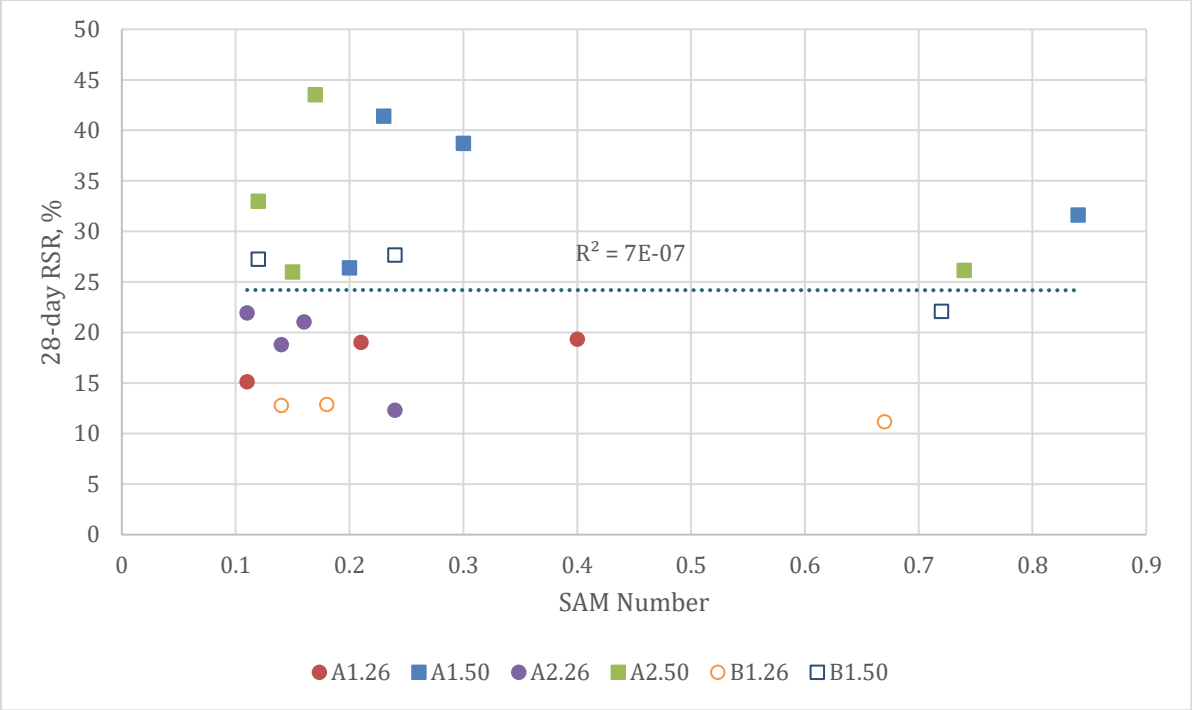

Figure 5-46. RSR vs SAM number

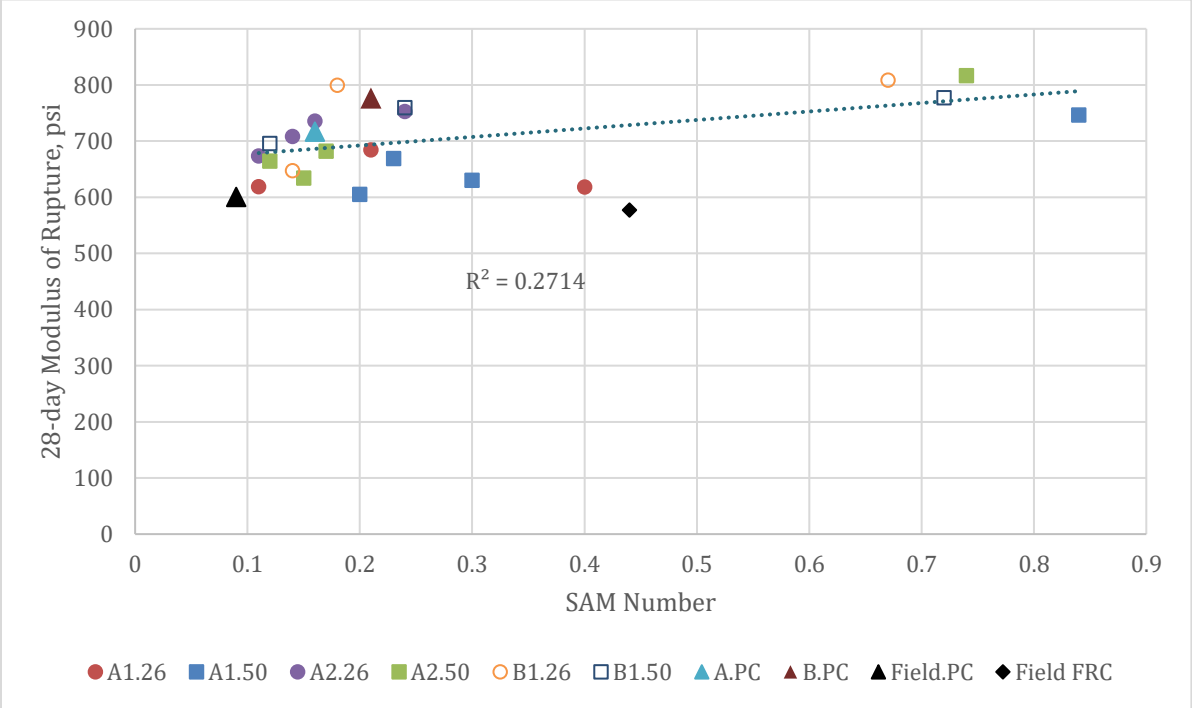

Figure 5-47. MOR vs SAM number

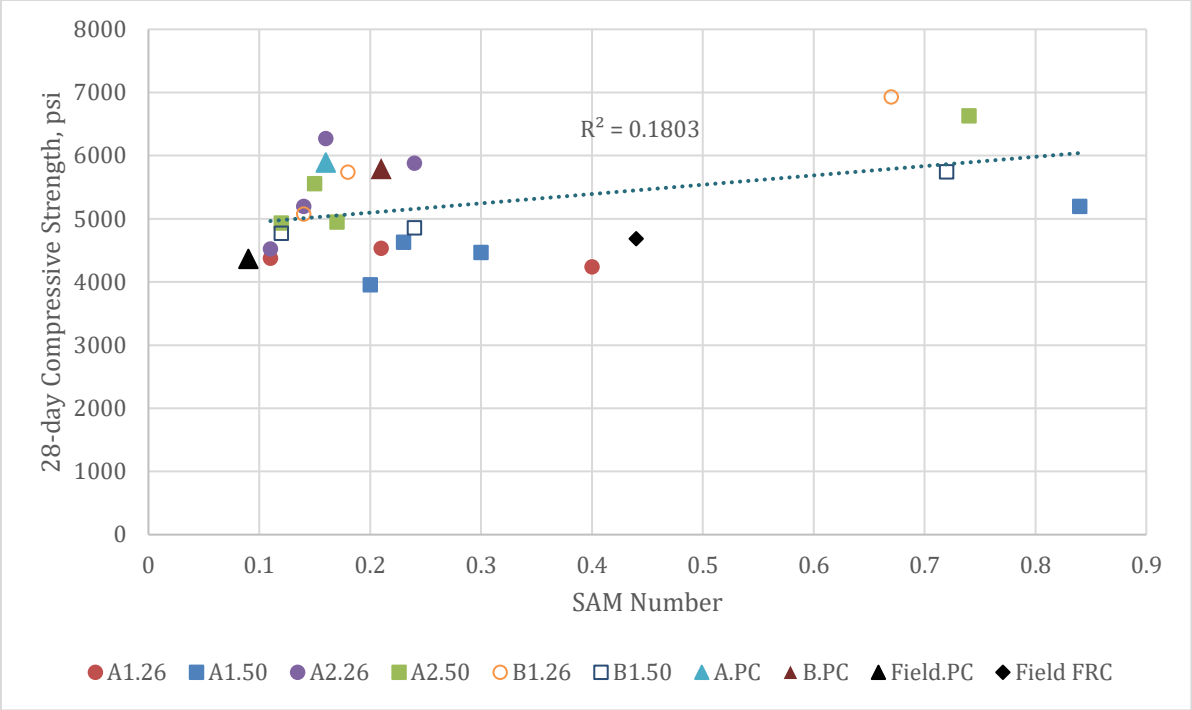

Figure 5-48. Compressive Strength vs SAM number

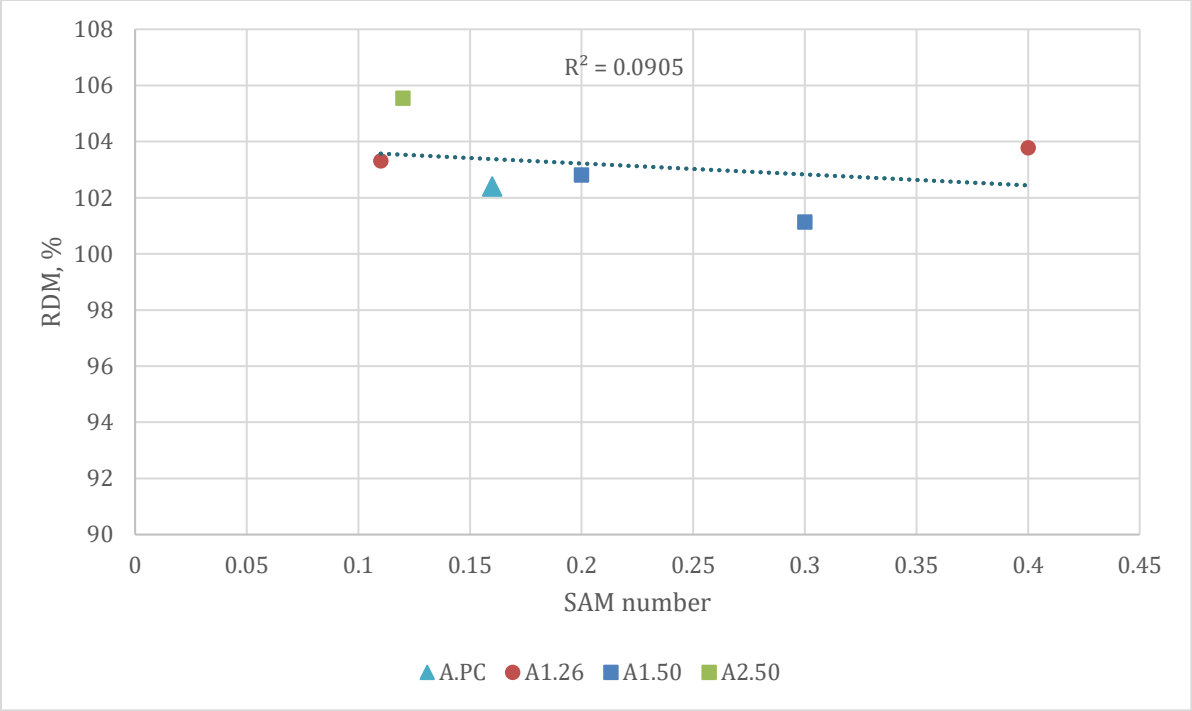

Figure 5-49. RDM vs SAM number

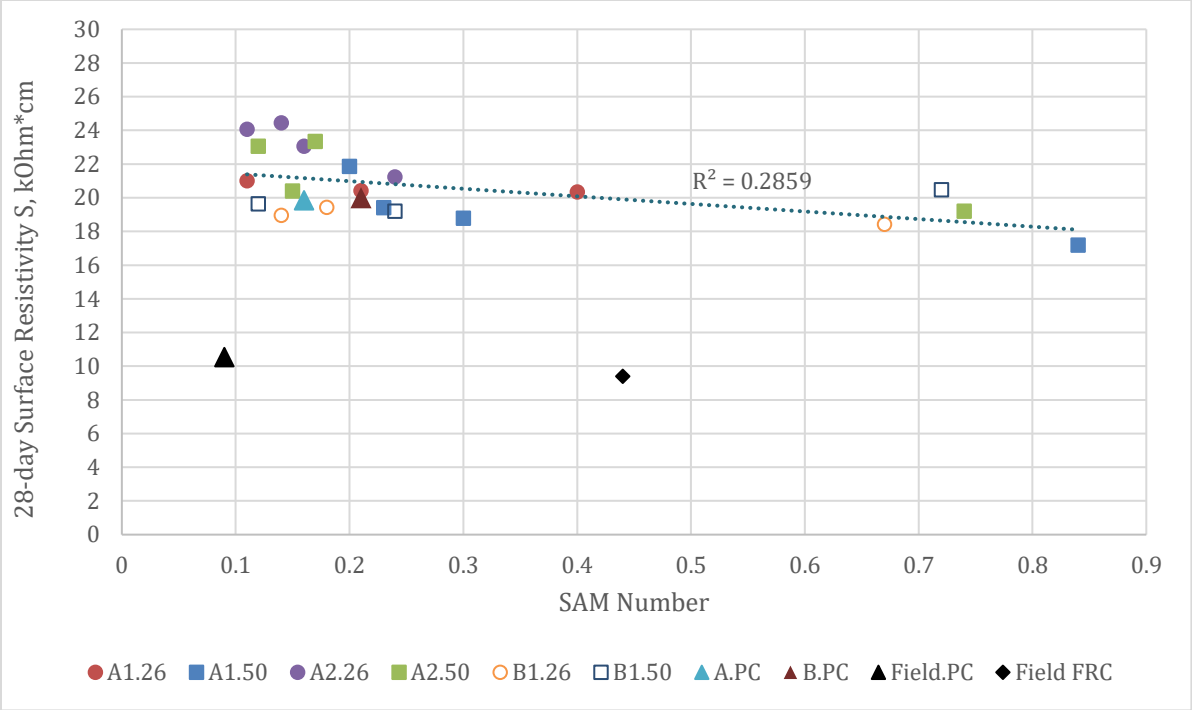

Figure 5-50. Surface resistivity vs SAM number

5.1.3.3 Box Test Visual Rating vs Harden Concrete Properties

Box test visual rating results do not show strong correlation with the ASTM C1609 test results such as toughness and RSR (Figure 5-51 and Figure 5-52). Similarly concrete MOR (Figure 5-53) and compressive strength (Figure 5-54) also showed poor correlation with Box test rating. RDM and Box test rating shows a correlation as can be seen in Figure 5-55; R^2 is equal to 0.69; but again the RDM values are significantly high for all the concrete specimens tested. Surface resistivity showed some correlation with the Box test rating. As anticipated, both the RDM and surface resistivity decreases as Box test rating increases.

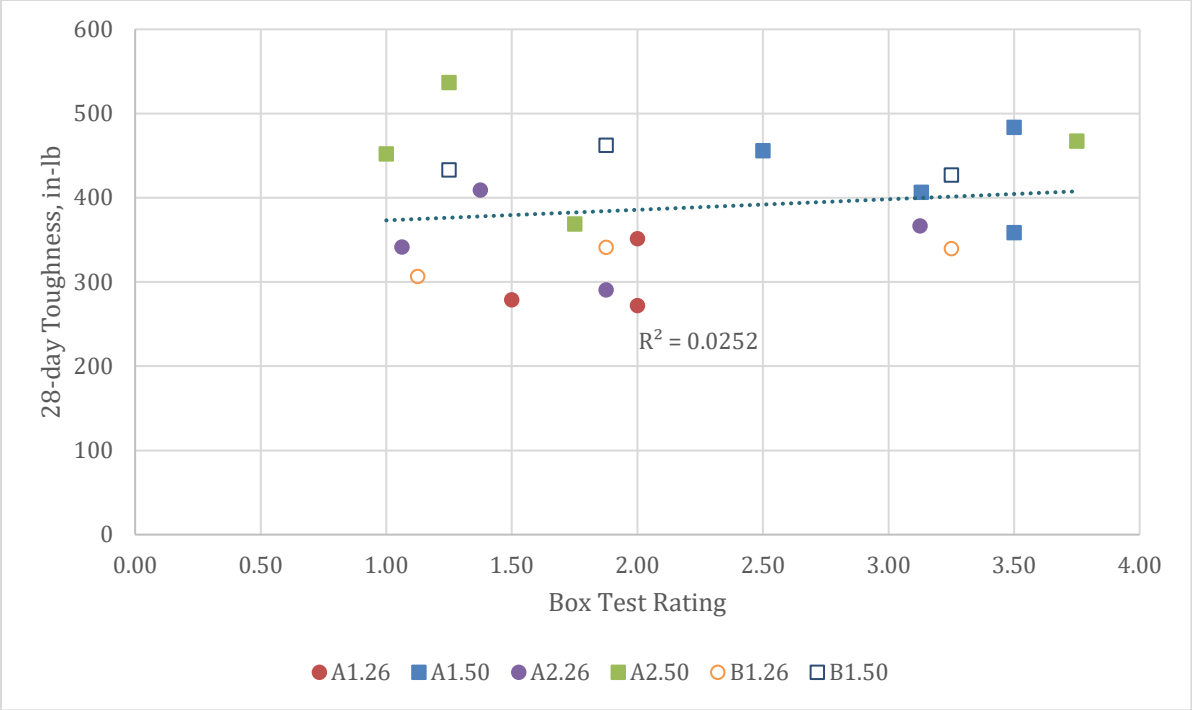

Figure 5-51. Toughness vs Box test rating

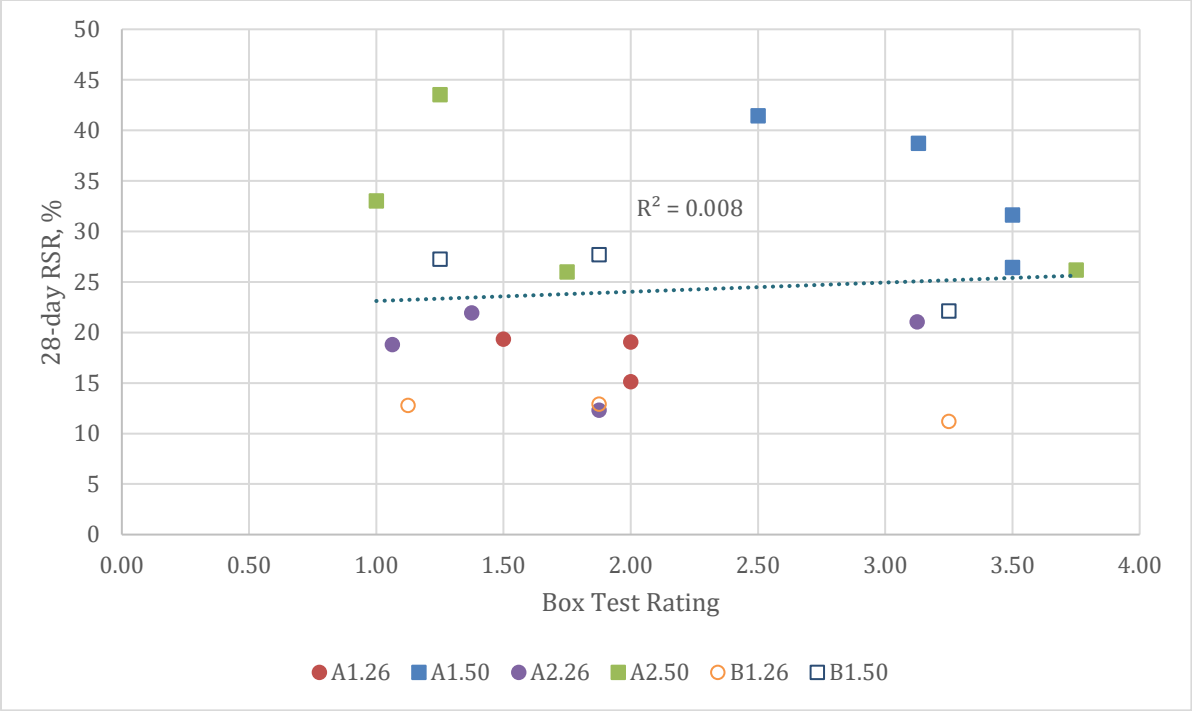

Figure 5-52. RSR vs Box test rating

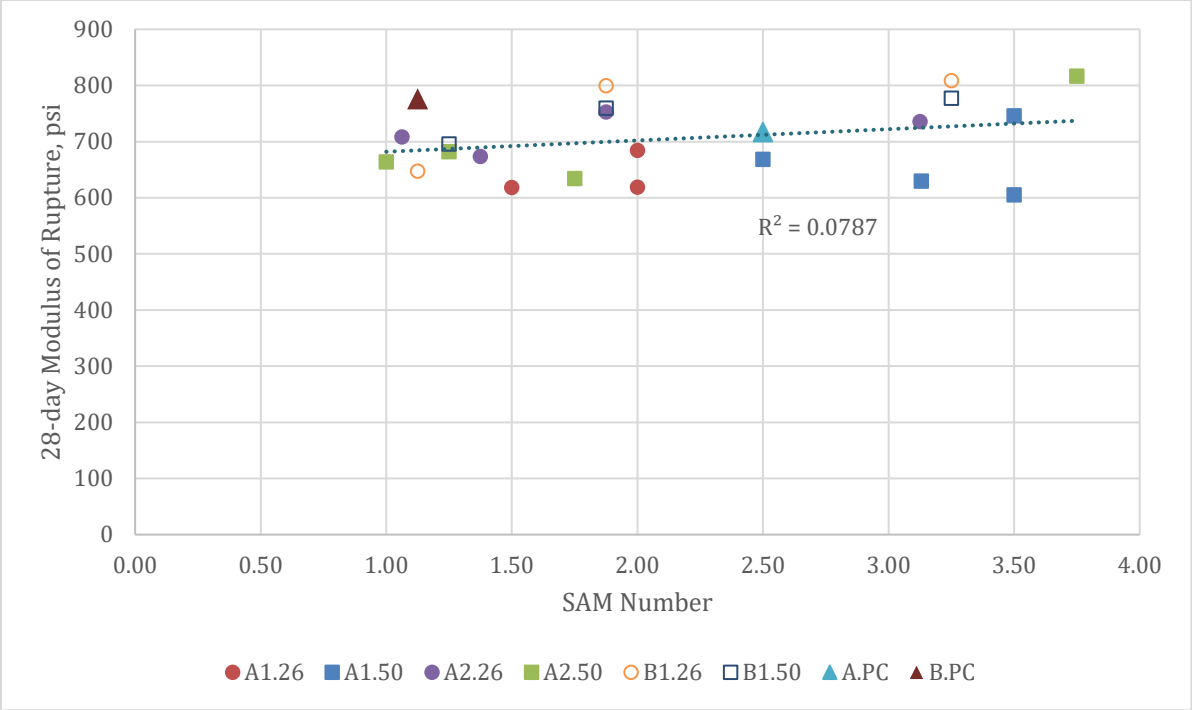

Figure 5-53. MOR vs Box test rating

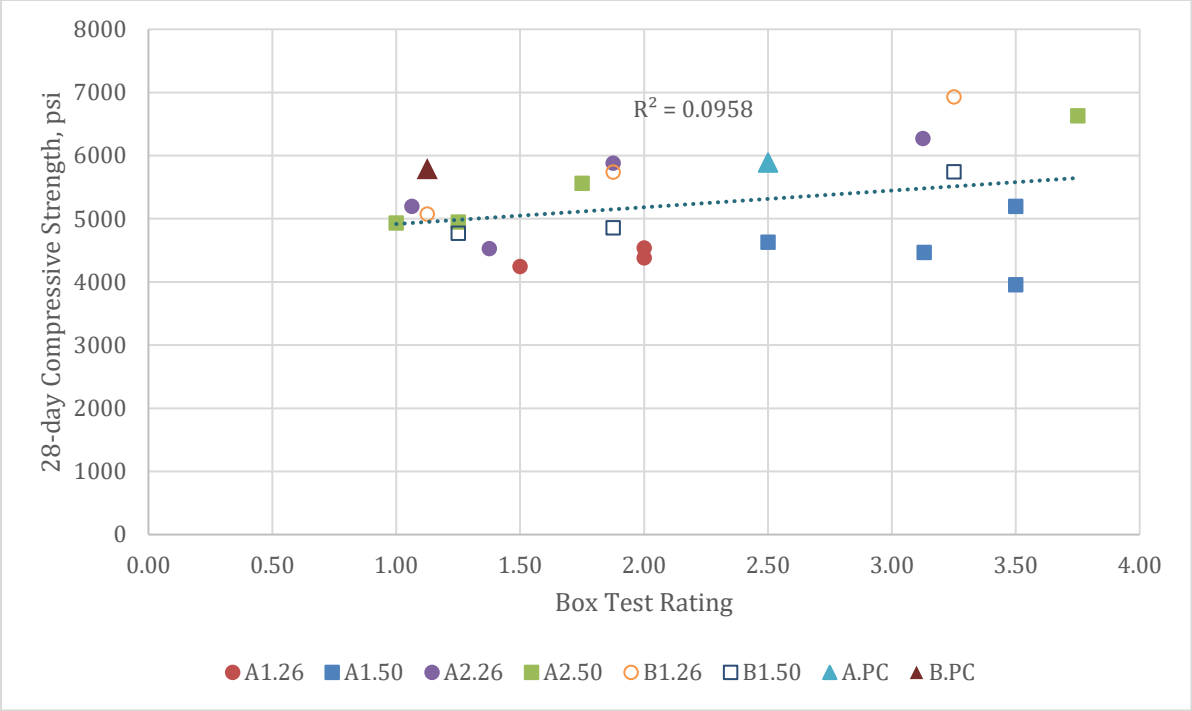

Figure 5-54. Compressive Strength vs Box test rating

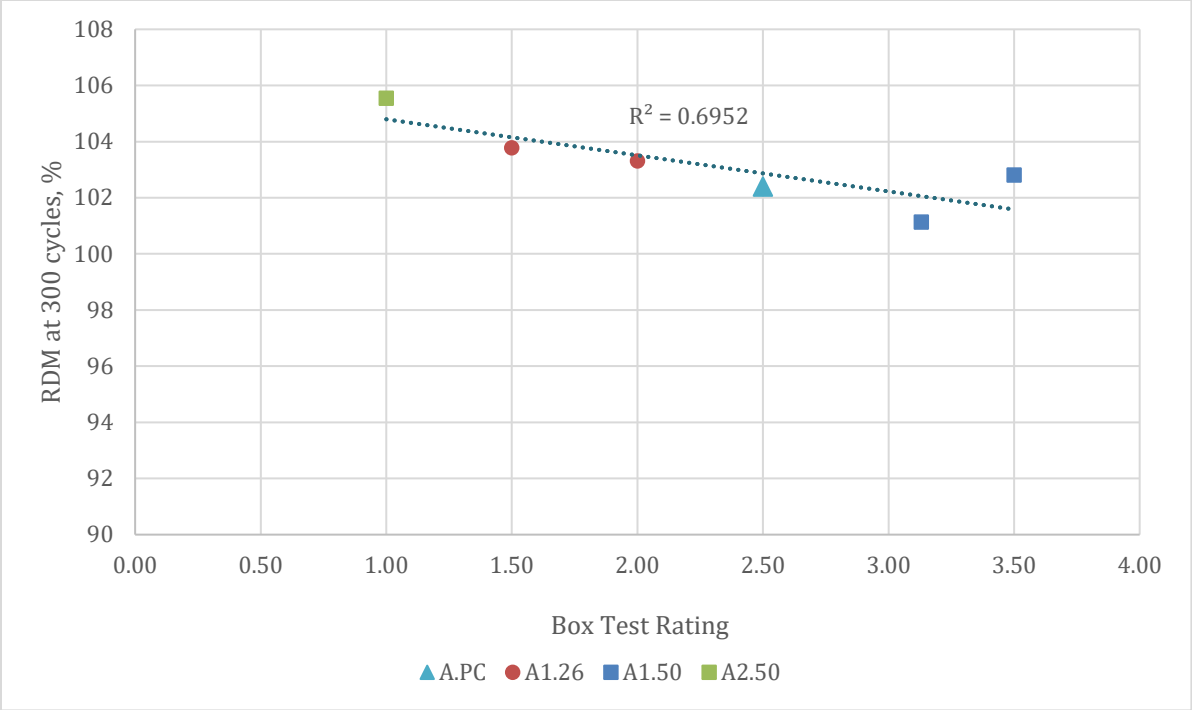

Figure 5-55. RDM vs Box test rating

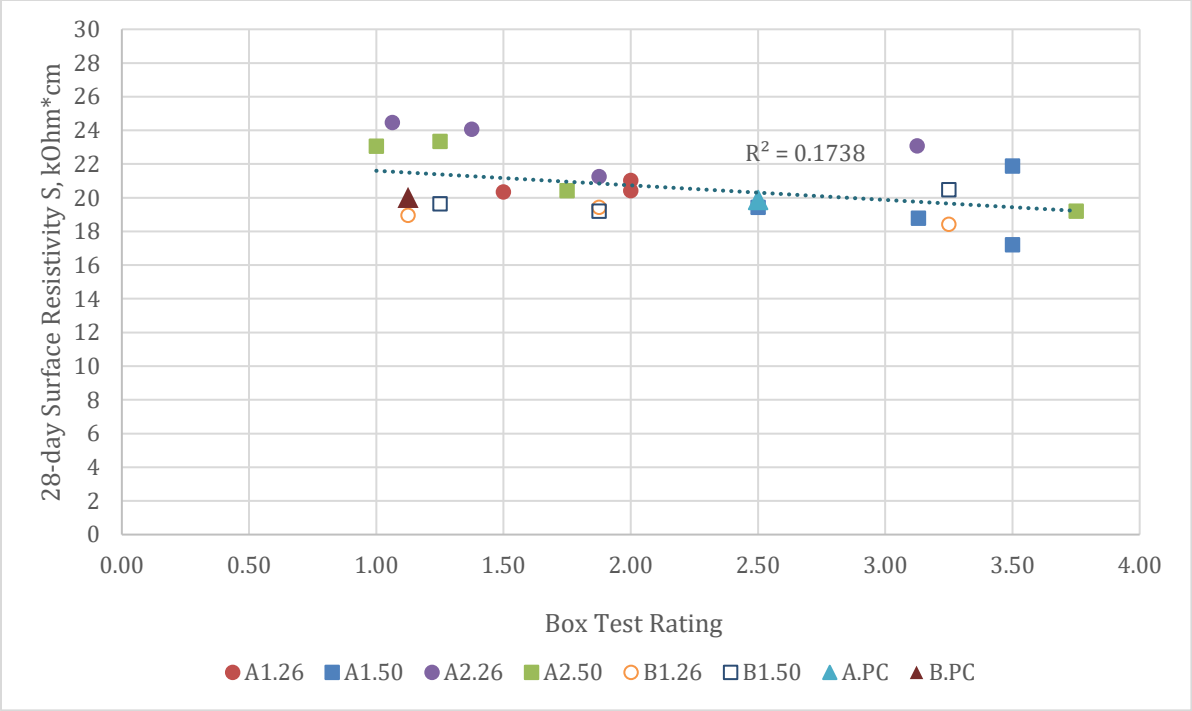

Figure 5-56. Surface resistivity vs box test rating

CHAPTER 6: CONCLUSIONS

Structural fibers are used in concrete mixtures to improve the long-term performance of concrete pavements and overlays. In addition to using structural fibers in concrete pavements, this study has implemented PEM procedure to assess the quality of concrete based on various factors affecting the performance of concrete in the field during pouring and throughout its service life. PEM mixture design produces concrete pavements that are resistant to weather- and material- related distresses by assessing key engineering parameters that determine the serviceability of concrete pavements. By studying the PEM design procedure with FRC through laboratory experiments, this research investigated the effect of fiber dosage, type, and geometry on SAM number, V-Kelly index, V-Kelly slump, Box test visual rating, electrical surface resistivity, compressive strength, modulus of elasticity, modulus of rupture, residual strength, residual strength ratio, post-crack toughness, and freeze-thaw durability. Based on the test results of the following conclusions are made:

- The limited fiber dosage variation adopted in this study did not significantly influence the SAM number. However, it seems that the fiber type may play a role. The twisted fibers used in this study can increase the SAM number compared to the plain concretes or concretes with embossed fibers. A large set of SAM number values were close to the 0.20, the recommended maximum value for plain concrete. An increase in entrained air content decreased the SAM number (R^2= 0.54). Mixes with air content less than 4% consistently showed a very high SAM number.
- The addition of fiber in the mixture has a very significant influence on the V-Kelly index. Mixtures with fiber dosage of 0.26% volume fraction had a V-Kelly Index slightly below 0.8 in/√s (the recommended minimum value for plain concrete) and mixtures with fiber dosage of 0.50% volume fraction were further below.
- In addition to the fiber dosage, fiber type had a significant influence on the V-Kelly index. However, no significant influence of the aggregate type on V-Kelly index was noticed.

- An increase in fiber dosage generally increased the Box test rating above the recommended rating of 2 (which corresponds to 10 to 30 percent surface voids). The influence of fiber dosage was more evident in mixes with a 0.50% volume fraction fiber.
- Structutal synthetic fibers have minimal effect on the compressive strength. Mixes containing Fiber 2 (embossed geometry) had slightly higher compressive strength than identical mixes containing Fiber 1 (twisted geometry) due to the embossed geometry and higher aspect ratio of Fiber 2.
- Aggregate types had some influence on the compressive strength. Mixtures with limestone class B aggregate had higher compressive strength than identical mixtures with granite class A aggregate due to the spherical shape with lower surface to volume ratio of Class B aggregate that provides better aggregate interlock.
- MOR remained minimally influenced by the volume fraction of synthetic fibers.
- The fiber dosage and type had significant influence on the post-crack behavior and flexural toughness of hardened concrete.
- The average RSR improved from 16 to 31% when the fiber dosage increased from 0.26% to 0.50% volume fraction. However, the types of aggregates used did not have a significant influence on concrete toughness.
- The resistivity results indicated that the addition of synthetic fibers into the mixture had no significant effect on the resistivity readings. Concrete mixture provided low chloride ion penetrability.
- The RDM values obtain from the rapid freeze-thaw test indicated that the addition of fiber did not influence the resistance of concrete to freeze-thaw durability issues.
- The target values for the fresh properties for the FRC needs to be further investigated as fibers have varying influence on those properties.

6.1 RECOMMENDATION FOR FUTURE STUDIES

Even though this study has given insight on the influence of fibers on various test results that are required under PEM design procedure, fiber dosage difference of 0.24% v_f is probably not enough to cause a noticeable difference in results. Below are some recommendations for future research:

- Further study with additional fiber dosages and types is recommended for a more reliable conclusions.
- Further study with additional aggregate types is recommended.
- Field validation of results obtained in lab is recommended.

REFERENCES

1. ACI (2018). *Guide to Design with Fiber-Reinforced Concrete.* American Concrete Institute Committee 544, Farmington Hills, MI.
2. Acikgenc, M., Alyamac, K. E., & Ulucan, Z. C. (2013). *Fresh and Hardened Properties of Steel Fiber Reinforced Concrete Produced with Fibers of Different Lengths and Diameters*. 2nd International Balkans Conference on Challenges of Civil Engineering, BCCCE, 23-25 May 2013, EPOKA University, Tirana, ALBANIA.
3. Al-Assadi, G.; Casati, M.J.; Gálvez, J.C.; Fernández, J.; Aparicio, S. (2015) The influence of the curing conditions of concrete on durability after freeze-thaw accelerated testing. Mater. Construcc. 65 [320], e067 http://dx.doi.org/10.3989/mc.2015.06514.
4. Barman, M. (2014). *Joint Performance Characterization of Bonded Concrete Overlay*. Ph. D. Dissertation, Department of Civil and Environmental Engineering, University of Pittsburgh, Pittsburgh, PA.
5. Barman, M. & Hansen (2018). *Comparison of Performances of Structural Fibers and Development of a Specification for Using Them in Thin Concrete Overlays*. Minnesota Department of Transportation, St. Paul., MN.
6. Barman, M., Crick, C. & Burnham, T. (2019). *Performance Benefits of Fiber-reinforced Thin Concrete Pavement and Overlays*. Task-2: First Year Annual Cell Performance Report, Minnesota Department of Transportation, St. Paul, MN.
7. Barman M., Hansen B., Arepalli U., (2018). *Performance benefits of Fibers-reinforced Thin Concrete Pavement and Overlays*. NRRA Long-term Research Project. Minnesota Department of Transportation, St. Paul., MN.
8. Barman, M., Vandenbossche, J. M., & Li, Z (2017). *Influence of Interface Bond on the Performance of Bonded Concrete Overlays on Asphalt Pavements*. Journal of Journal of Transportation Engineering, Part B: Pavements, ASCE, 143(3).
9. Cackler, T., Harrington, D., & Taylor, P. C. (2017). *Performance Engineered Mixture (PEM) for Concrete Pavement*. CP Road Map, National Concrete Pavement Technology Center, Ames, IA.
10. Cook D., Ghaeezadeh A., Ley T., & Russell B. (2013). Investigation of optimized graded concrete for Oklahoma-Phase I. Oklahoma State University, Stillwater, OK.
11. Cook, D., Ghaeezadah, A., & Ley, T. 2014. A workability test for slip formed concrete pavements. Construction and Building Materials, 68, 376–383.
12. Delatte N. (2007). Concrete pavement design, construction, and performance. Taylor & Francis, USA.
13. Dhir, R. K., McCarthy, M. J., Zhou, S., & Tittle, P. A. J. (2006). *Discussion: Role of cement content in specifications for concrete durability: aggregate type influences.* Structures & Buildings, Vol. 159. 361-363

14. Issa, M., A. (2017). Effect of Early-Age Concrete Elastic Properties on Fatigue Damage in PCC Pavements Containing Fibers. Publication FHWA-ICT-17-019, Illinois Center for Transportation, IL.
15. Kosmatka, S. H., & Wilson, M. L. (2016). *Design and Control of Concrete Mixtures*. Portland Cement Association, Skokie, IL.
16. Ley, T. (2015). *Producing Freeze-Thaw Durable Concrete*. *Producing Freeze-Thaw Durable Concrete* (pp. 1–3). CP RoadMap. National Concrete Pavement Technology Center, Ames, IA.
17. Ley, T., & Cook, D. (2014). *Aggregate Gradations for Concrete Pavement Mixtures*. CP Road Map. National Concrete Pavement Technology Center, Ames, IA.
18. MnDOT, (2017). MnROAD concrete special provision. (Table 2301).
19. Superairmeter (2015). *Operating Instruction*. < https://myerstest.com/wp-content/uploads/2016/06/Super-Air-Meter-manual-vers-3-2_15-1.pdf>
20. Taylor, P. C. (2013). *Long-Life Concrete: How Long Will My Concrete Last?*. National Concrete Pavement Technology Center, Ames, IA.
21. Taylor, P. (2017). *Performance Engineering Mixtures Program*. National Concrete Pavement Technology Center, Ames, IA.
22. Taylor, P. C., Yurdakul, E., & Ceylan, H. (2014). *Performance Engineered Mixtures for Concrete Pavements in the US*. National Concrete Pavement Technology Center, Ames, IA.
23. Weiss, J. (2014). *Relating Transport Properties to Performance in Concrete Pavements*. CP RoadMap. National Concrete Pavement Technology Center, Ames, IA.
24. Jenkins, 2015
25. Erntroy, H. & Shacklock, B.W. (1954) *Design of High-Strength Concrete Mixes*, Proceeding of Symposium on Mix Design and Quality Control of Concrete, London, Cement and Concrete Association,
26. Neville, A. M. (1996). *Properties of concrete*. John Wiley & Sons

APPENDIX

LAB DATA

Table 0-1. Data collected from Bucket Test.

Mixture	Air	Resistivity values (kΩ*cm)	
		Initial	Final (after 7 days)
6A2.26	7	7	12
8A2.26-1	7.7	7	13
8A2.26-2	7.6	8	13
6A2.50	6.3	8	12
6B.PC	5.4	7	10
4B1.26	3.5	7	9
6B1.26	6.9	7	10
8B1.26	8.5	5	9
4B1.50	4	7	9
6B1.50	6.4	6	9
8B1.50	8.9	8	9

Table 0-2. Composition of Class-F fly-ash

Chemical Analysis	Results
Silicon Dioxide (SiO2)	52.75 %
Aluminum Oxide (Al2O3)	15.44 %
Iron Oxide (Fe2O3)	4.95 %
Sum (SiO2+Al2O3+Fe2O3)	73.14 %
Sulfur Trioxide (SO3)	0.66 %
Calcium Oxide (CaO)	13.02 %
Magnesium Oxide (MgO)	4.41 %
Sodium Oxide (Na2O)	2.92 %
Potassium Oxide (K2O)	2.30 %
Sodium Oxide Equivalent (Na2O+0.658K2O)	4.43 %
Moisture	0.04 %
Loss on Ignition	0.09 %
Available Alkalies, as Na2Oe	1.52 %
Physical Analysis	
Fineness, % retained on 45-µm sieve	25.07 %
Fineness Uniformity	3.18 %
Strength Activity Index - 7 or 28 day requirement	
7 day, % of control	85 %
28 day, % of control	82 %
Water Requirement, % control	93 %
Autoclave Soundness	0.01 %
Density	2.56
Density Uniformity	1.85 %

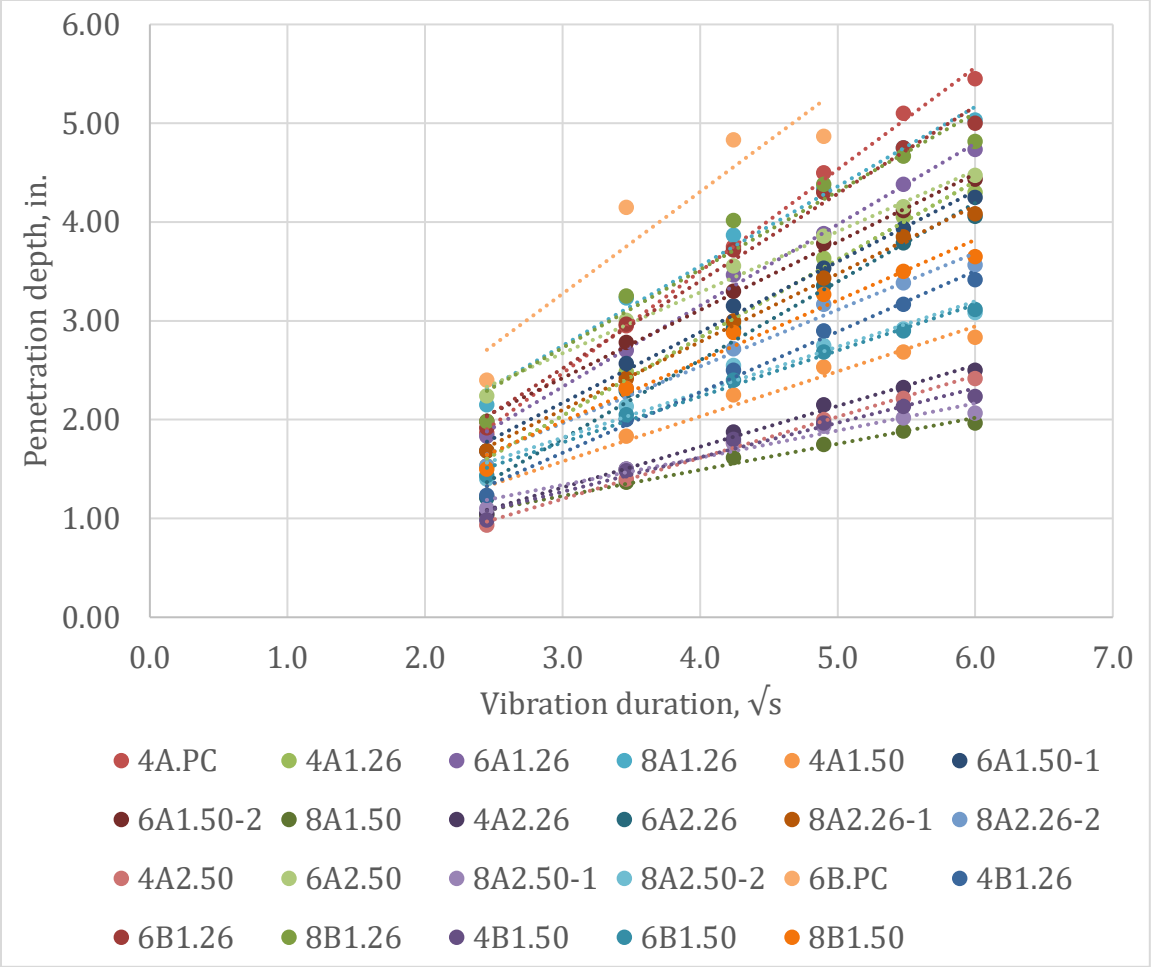

Figure 0-1. V-Kelly test results

LOAD VS DISPLACEMENT PLOTS

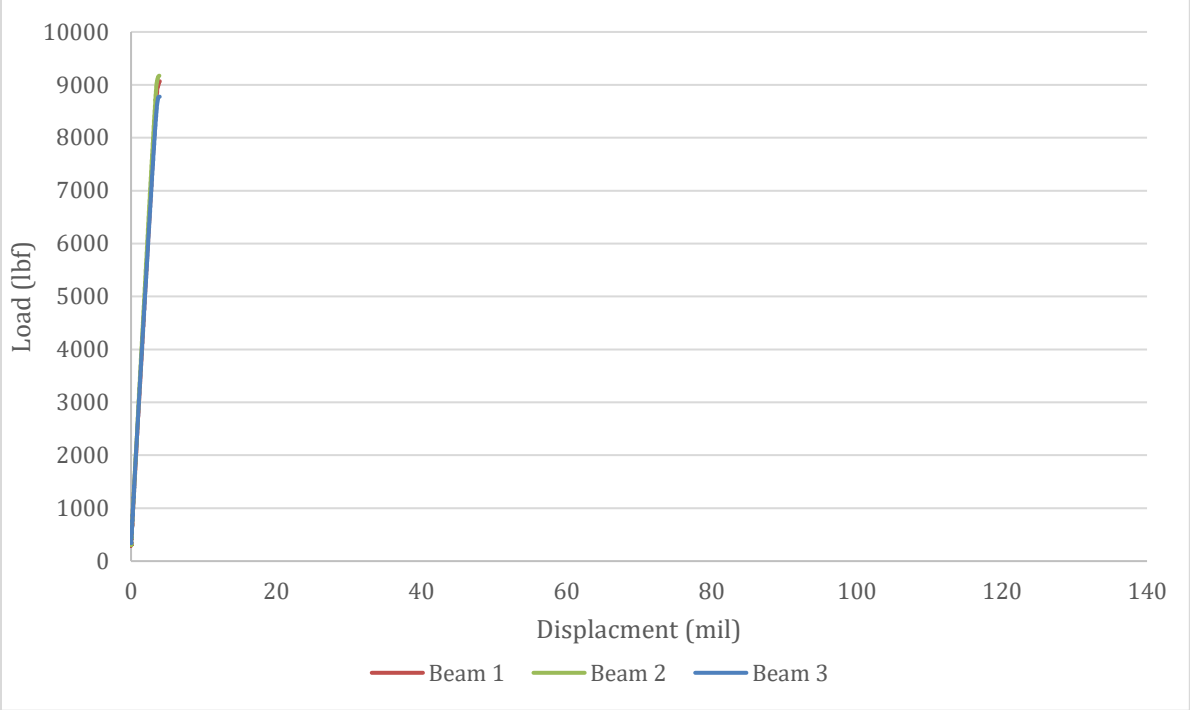

Figure 0-2. Load vs Displacement for A. PC

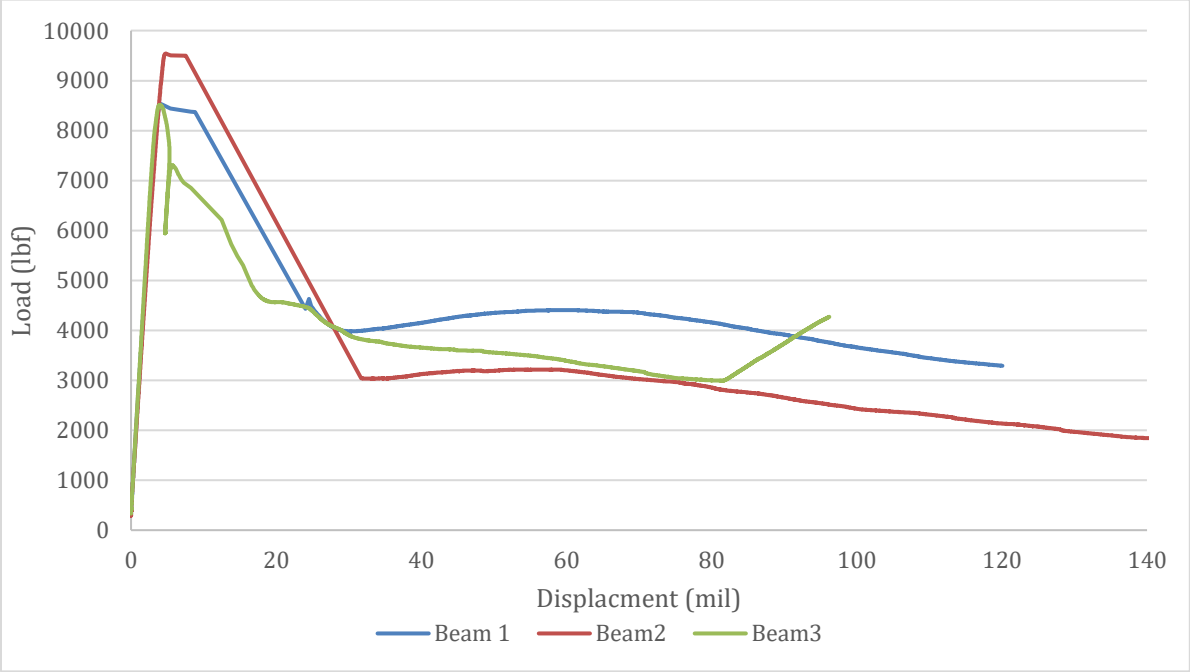

Figure 0-3. Load vs Displacement for 4A1.50

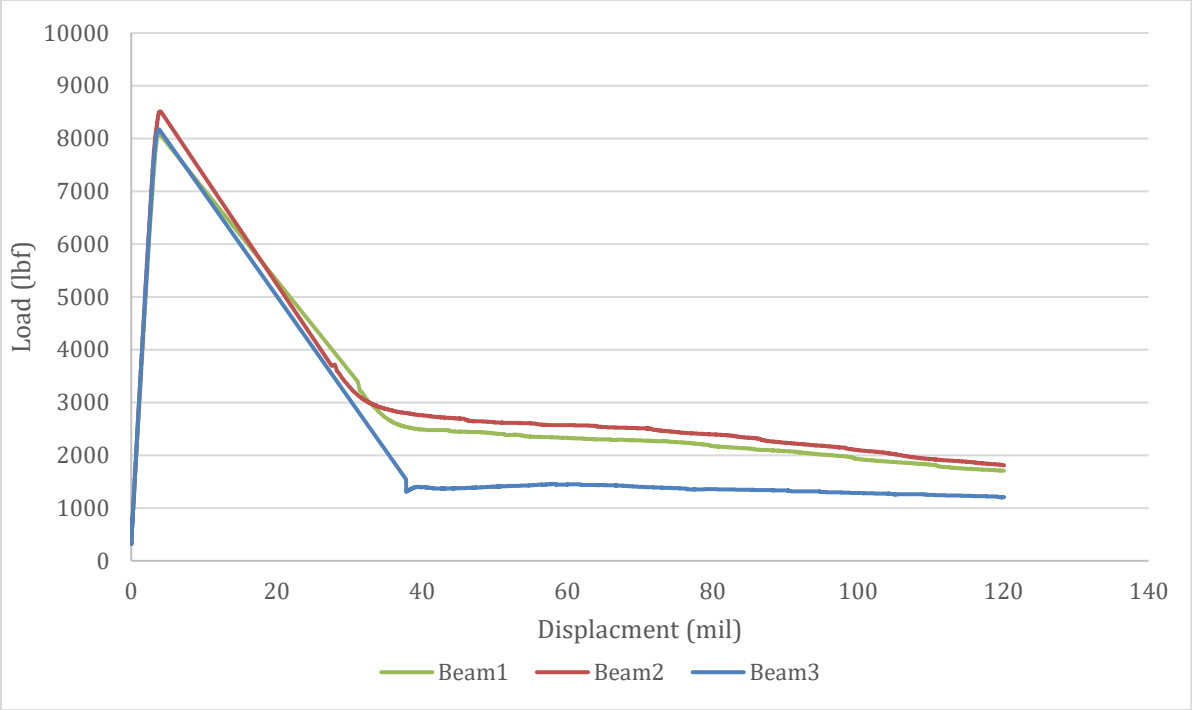

Figure 0-4. Load vs Displacement for 4A1.26

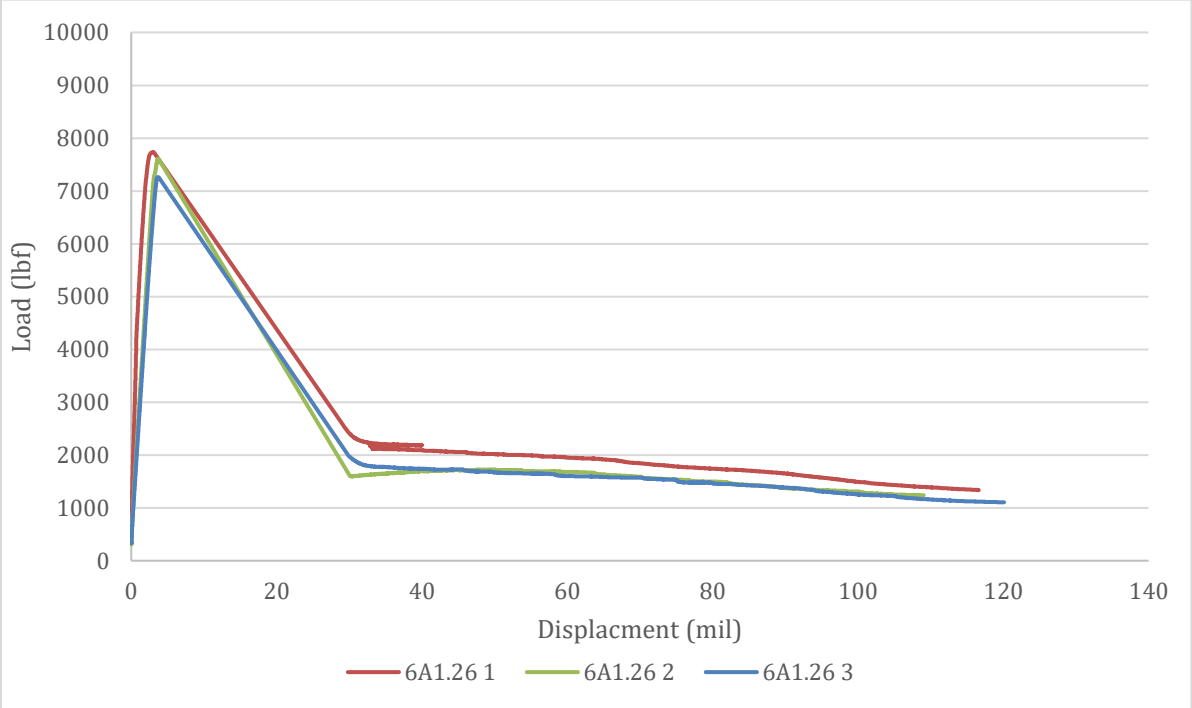

Figure 0-5. Load vs Displacement for 6A1.26

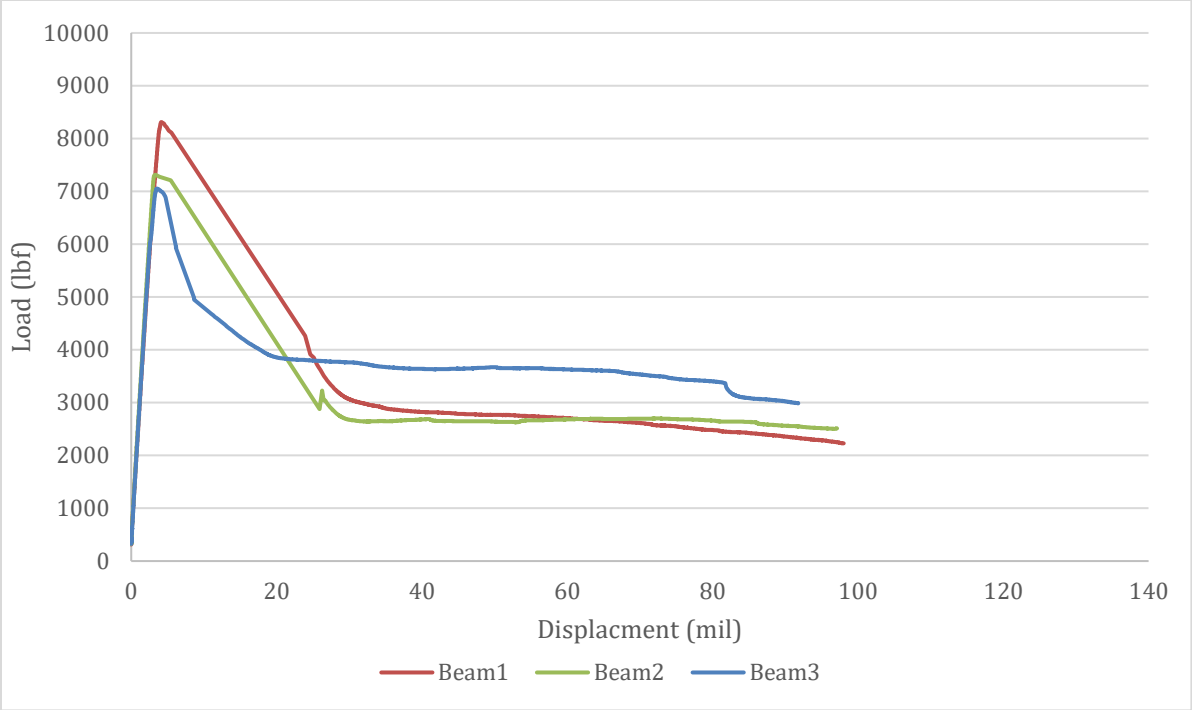

Figure 0-6. Load vs Displacement for 6A1.50-1

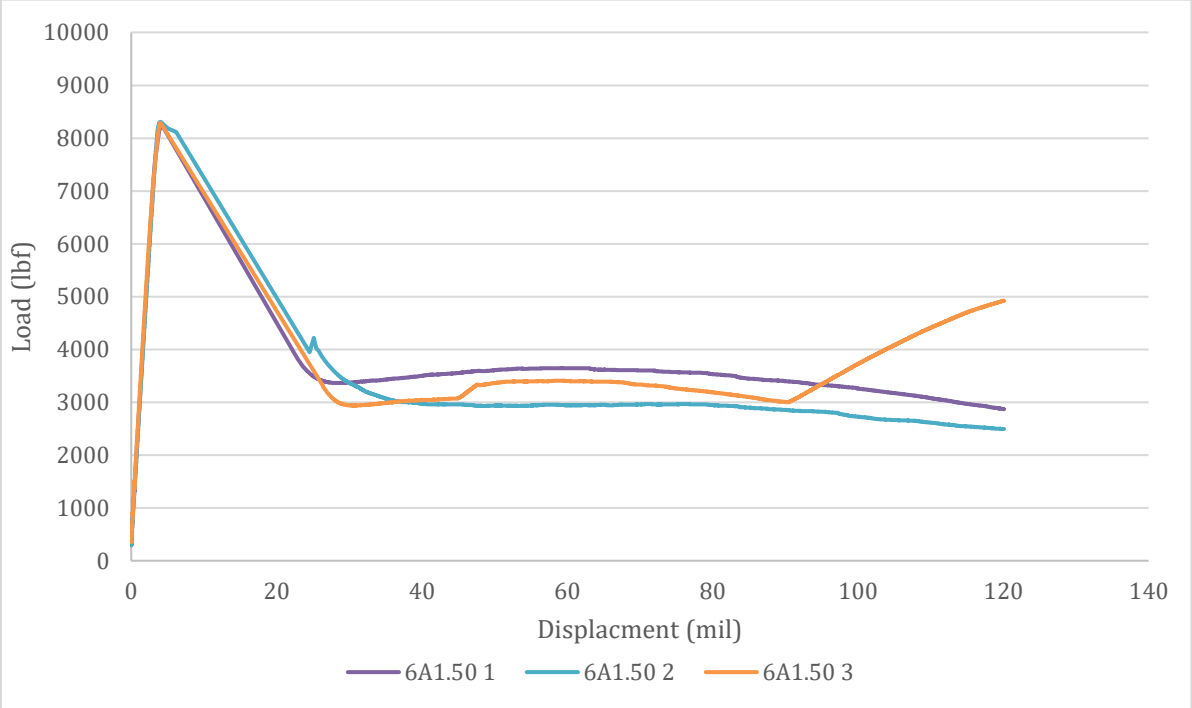

Figure 0-7. Load vs Displacement for 6A1.50-2

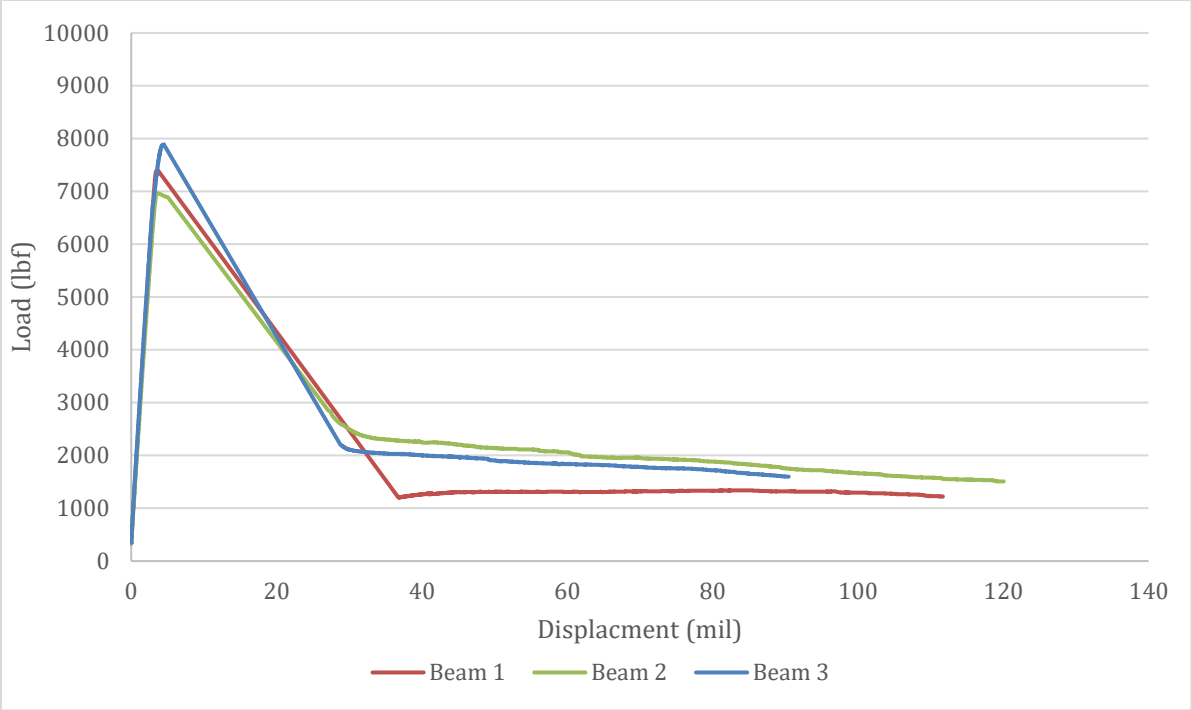

Figure 0-8. Load vs Displacement for 8A1.26

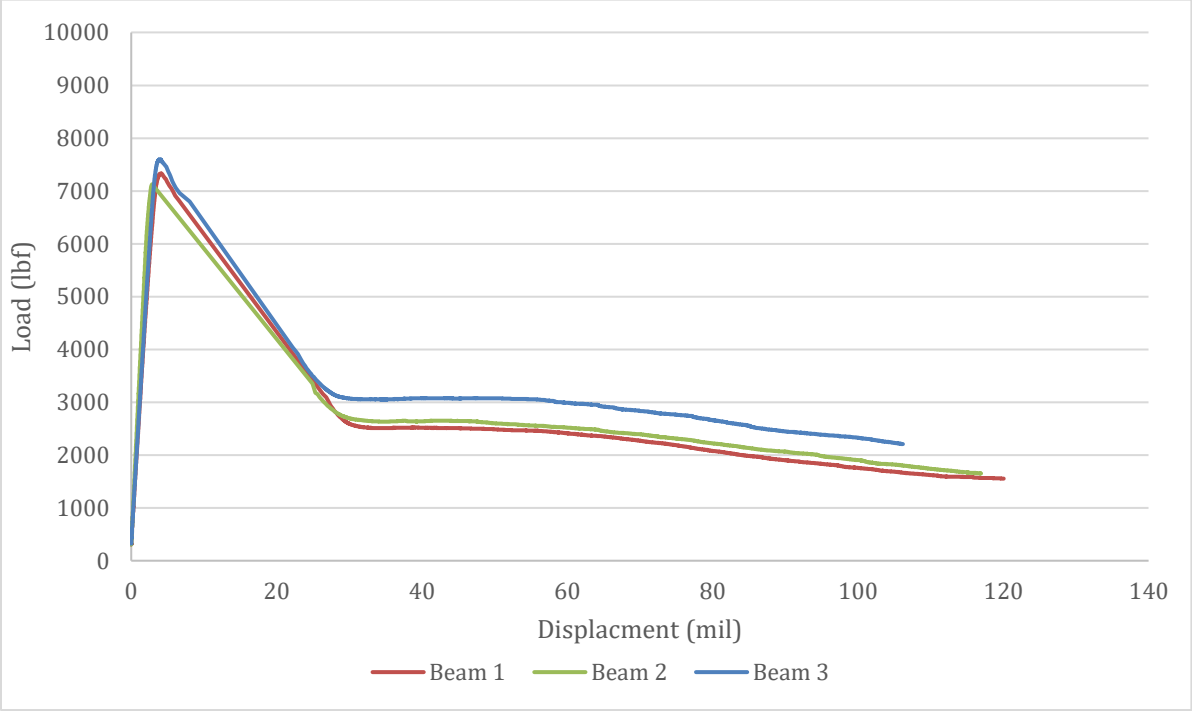

Figure 0-9. Load vs Displacement for 8A1.50

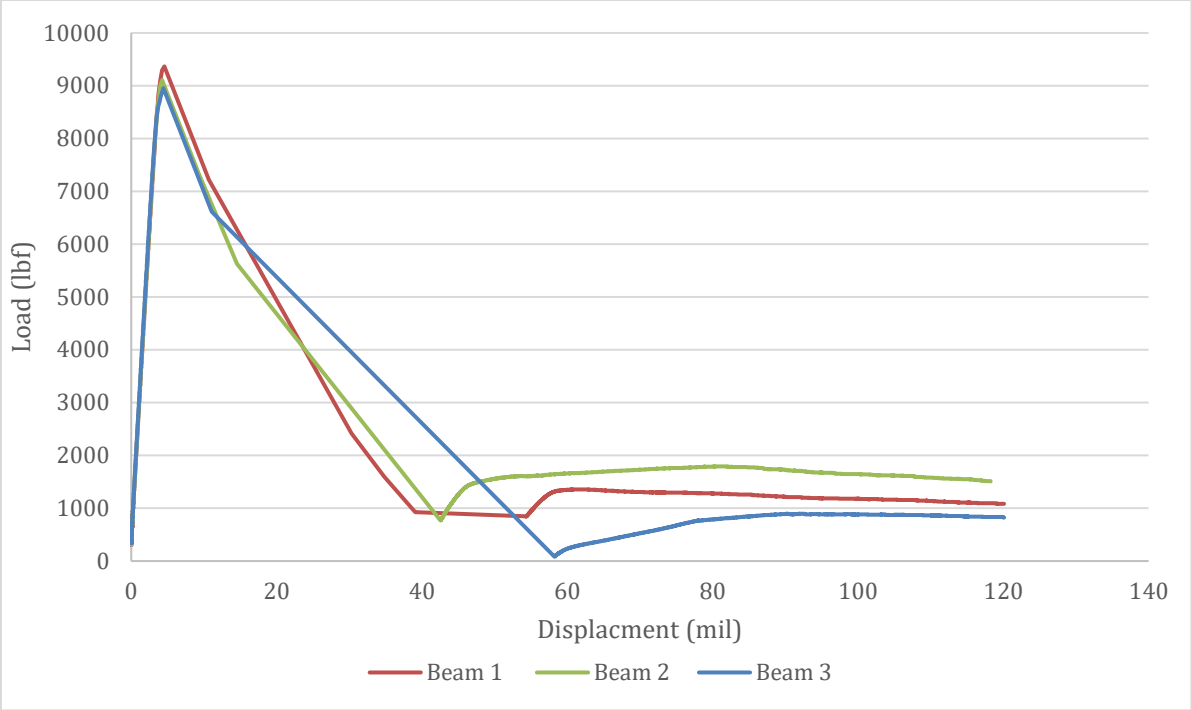

Figure 0-10. Load vs Displacement for 4A2.26

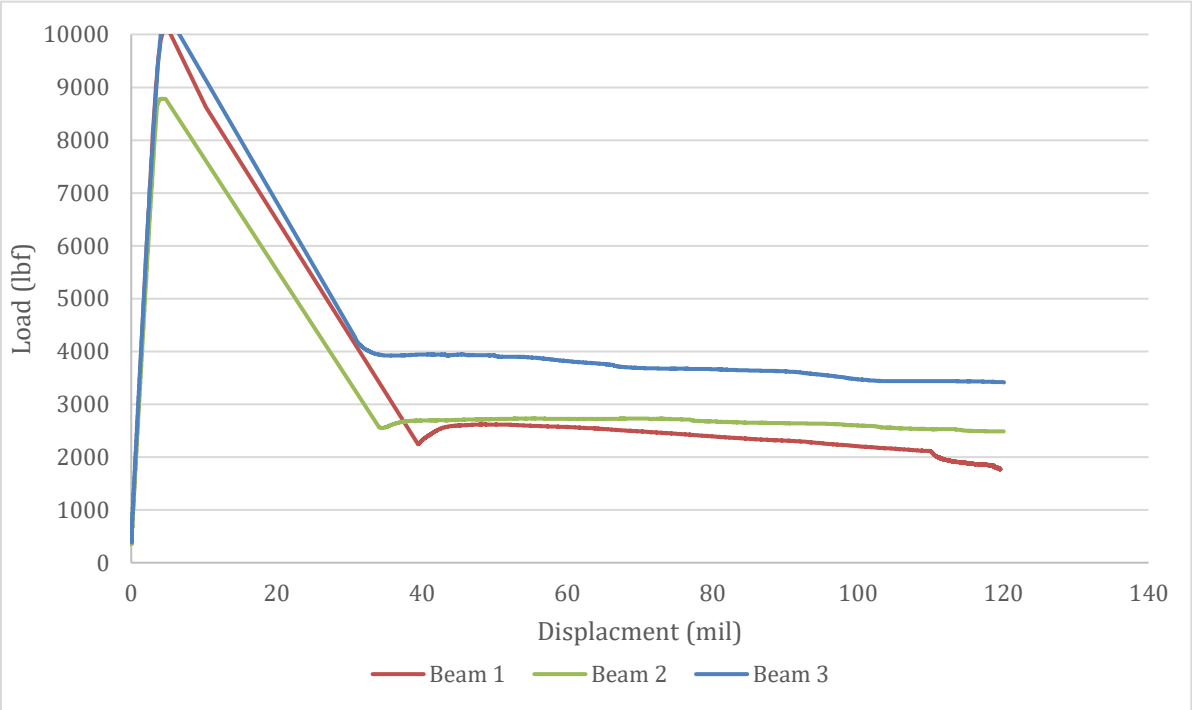

Figure 0-11. Load vs Displacement for 4A2.50

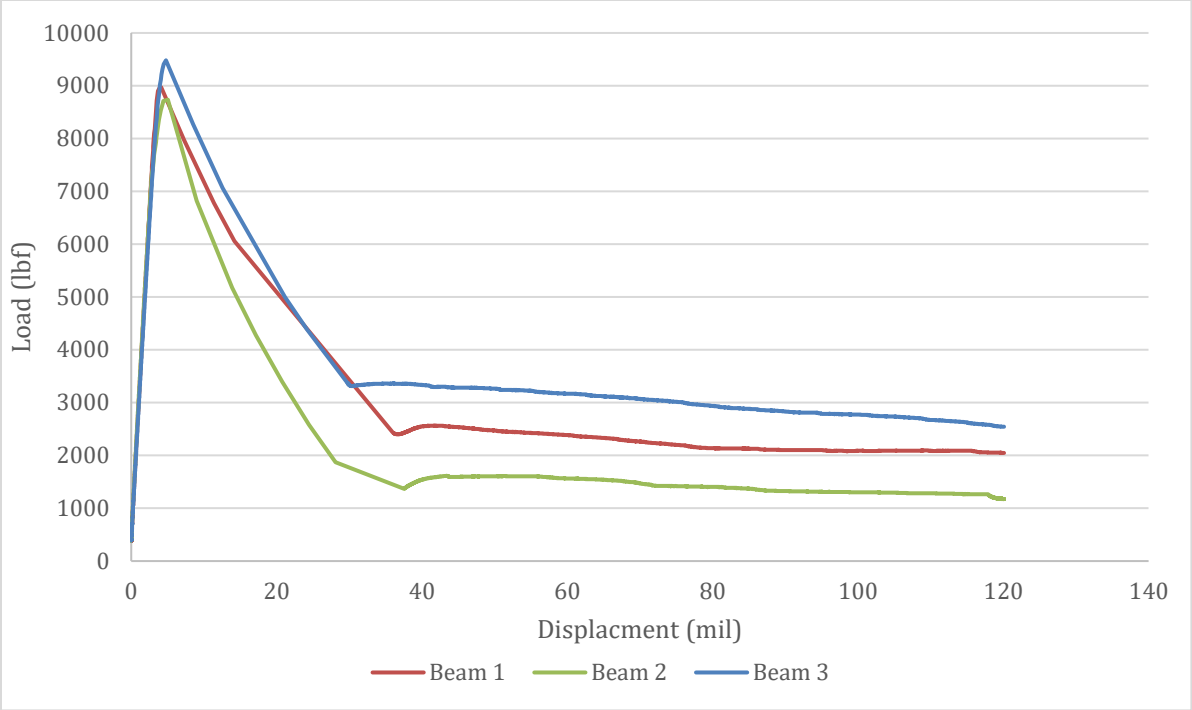

Figure 0-12. Load vs Displacement for 6A2.26

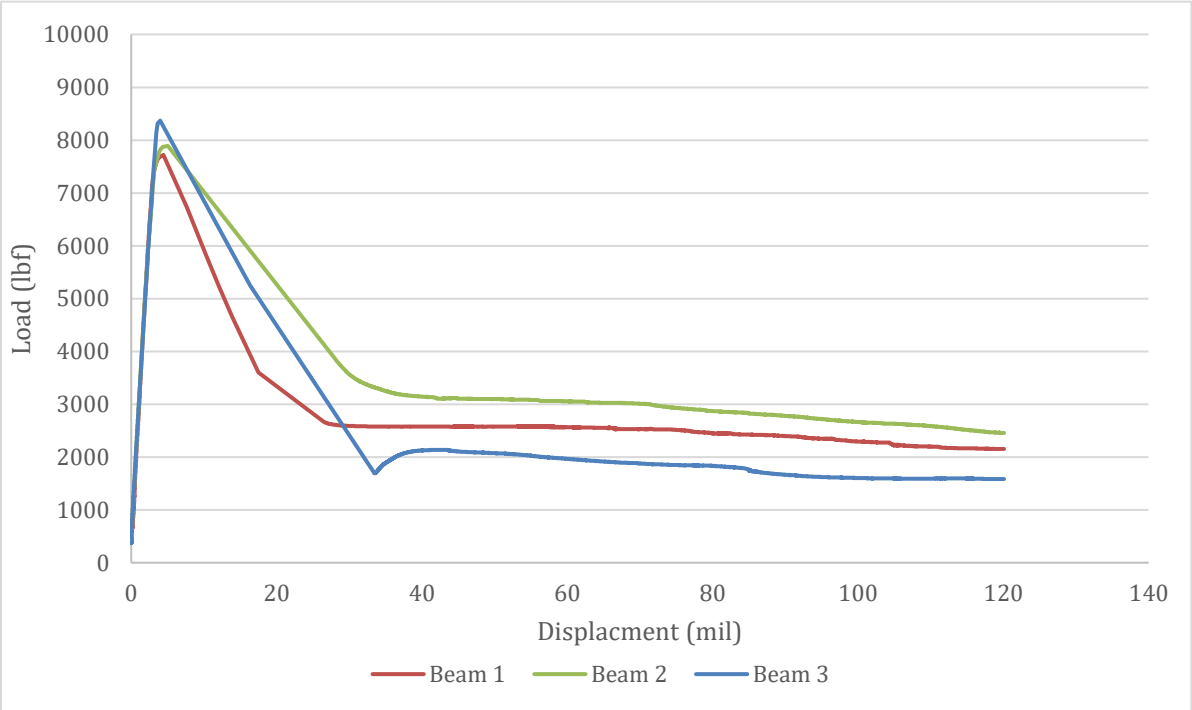

Figure 0-13. Load vs Displacement for 6A2.50

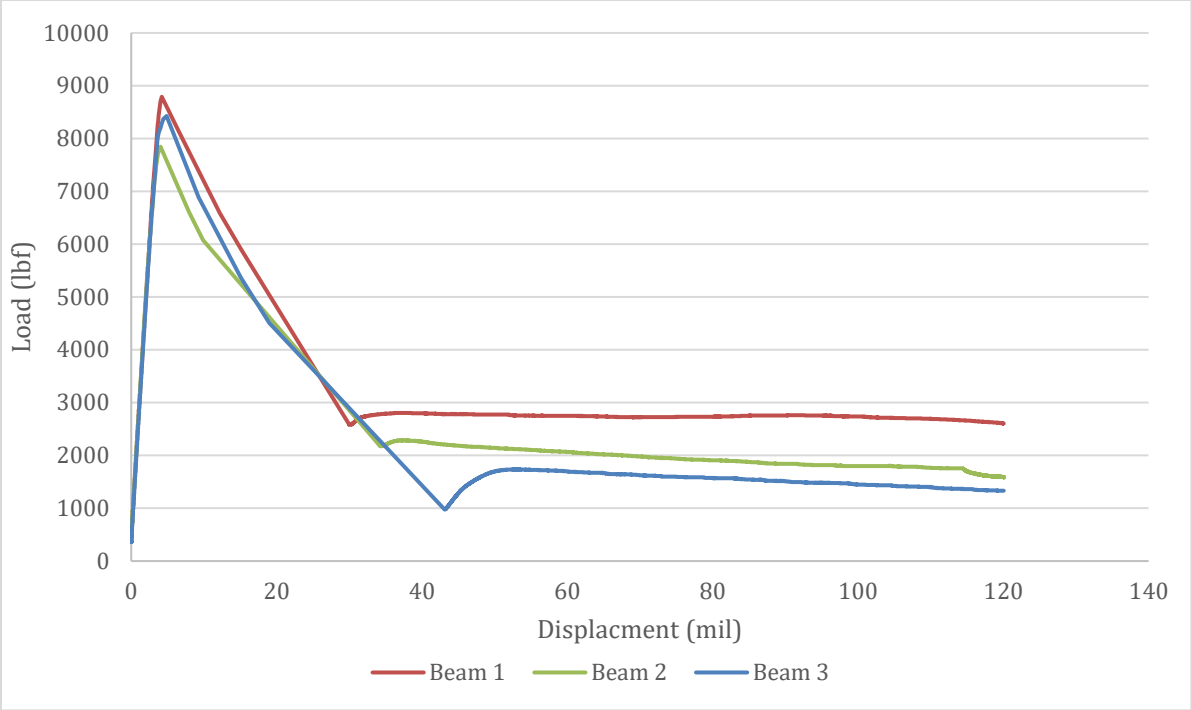

Figure 0-14. Load vs Displacement for 8A2.26-1

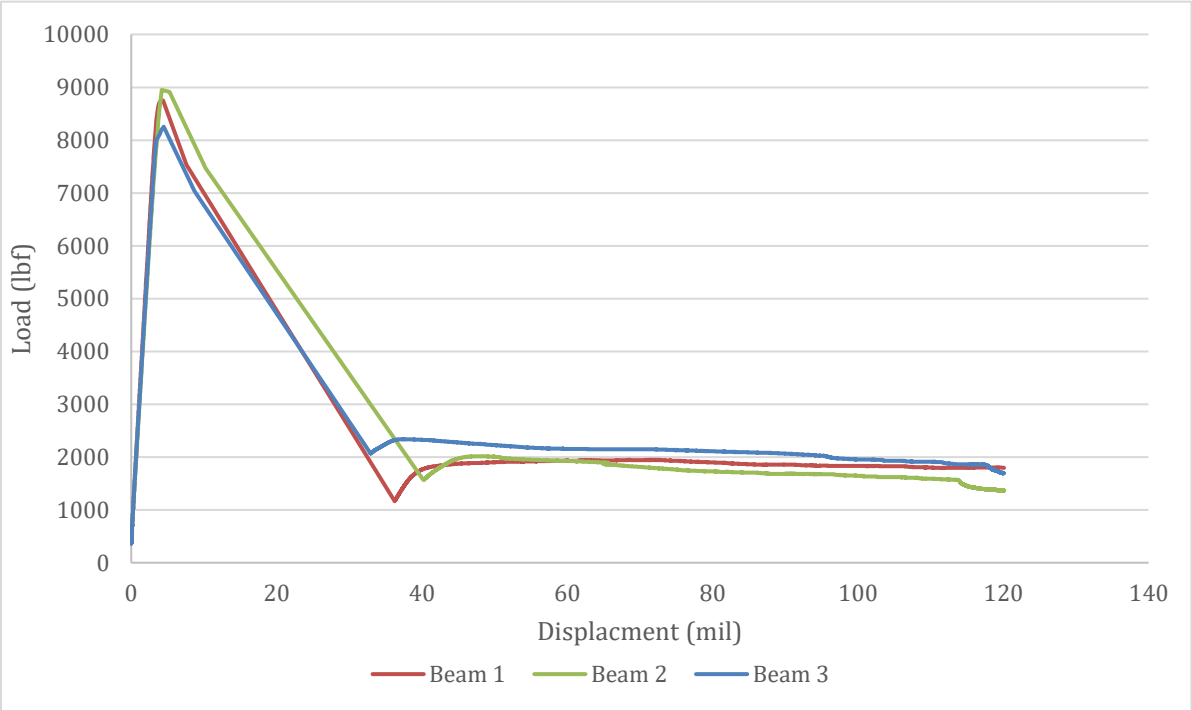

Figure 0-15. Load vs Displacement for 8A2.26-2

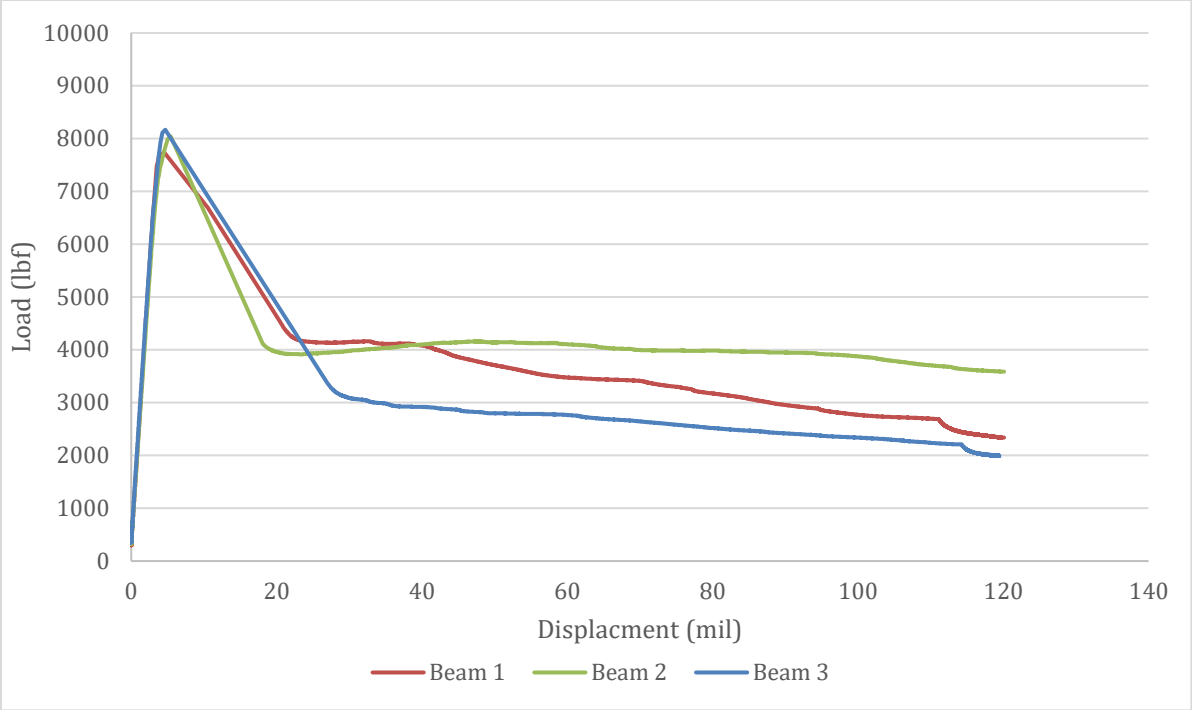

Figure 0-16. Load vs Displacement for 8A2.50-1

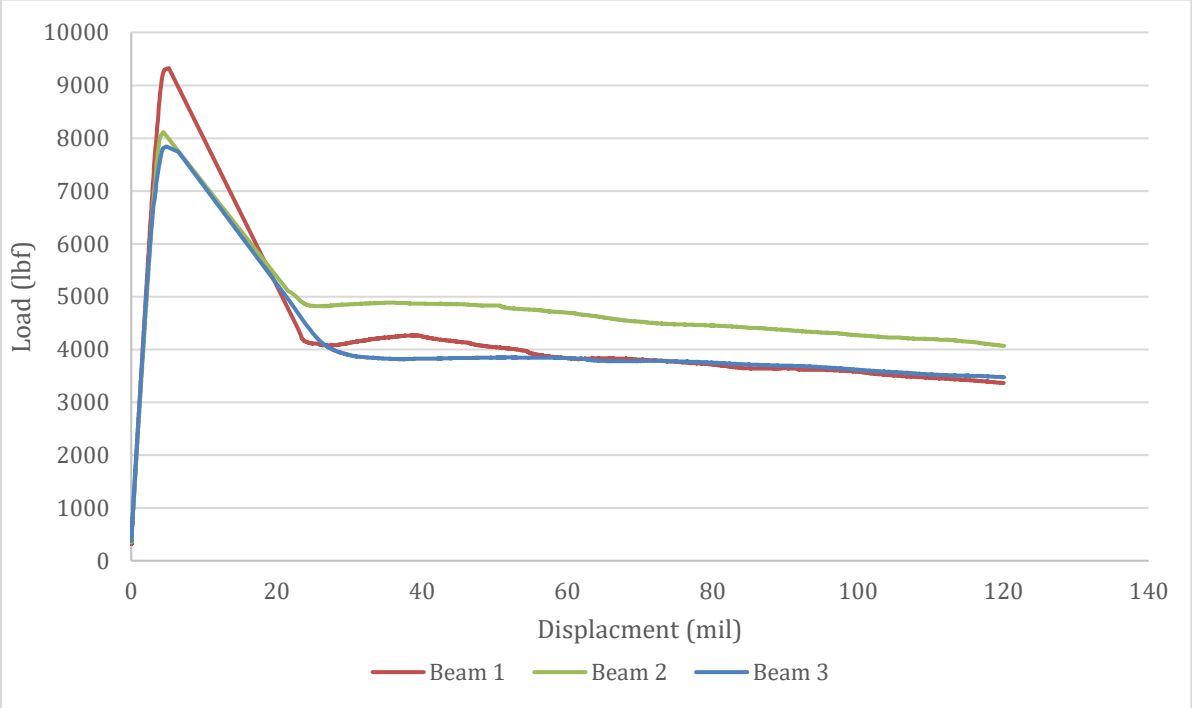

Figure 0-17. Load vs Displacement for 8A2.50-2

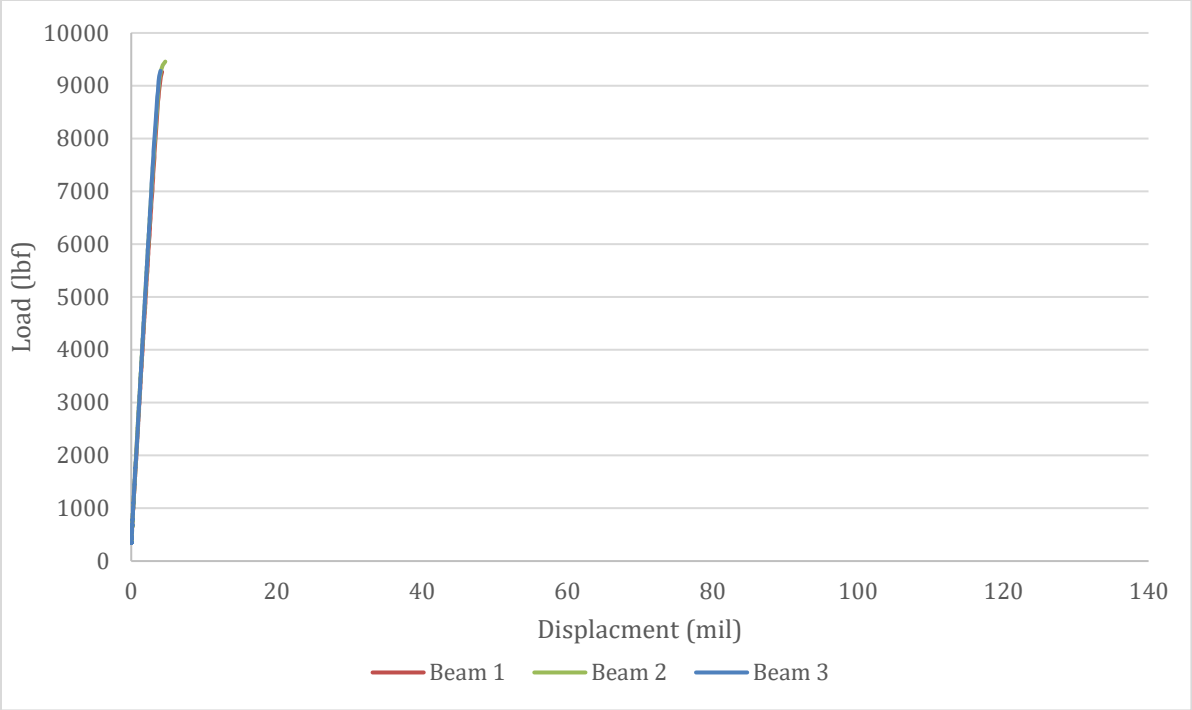

Figure 0-18. Load vs Displacement for B.PC

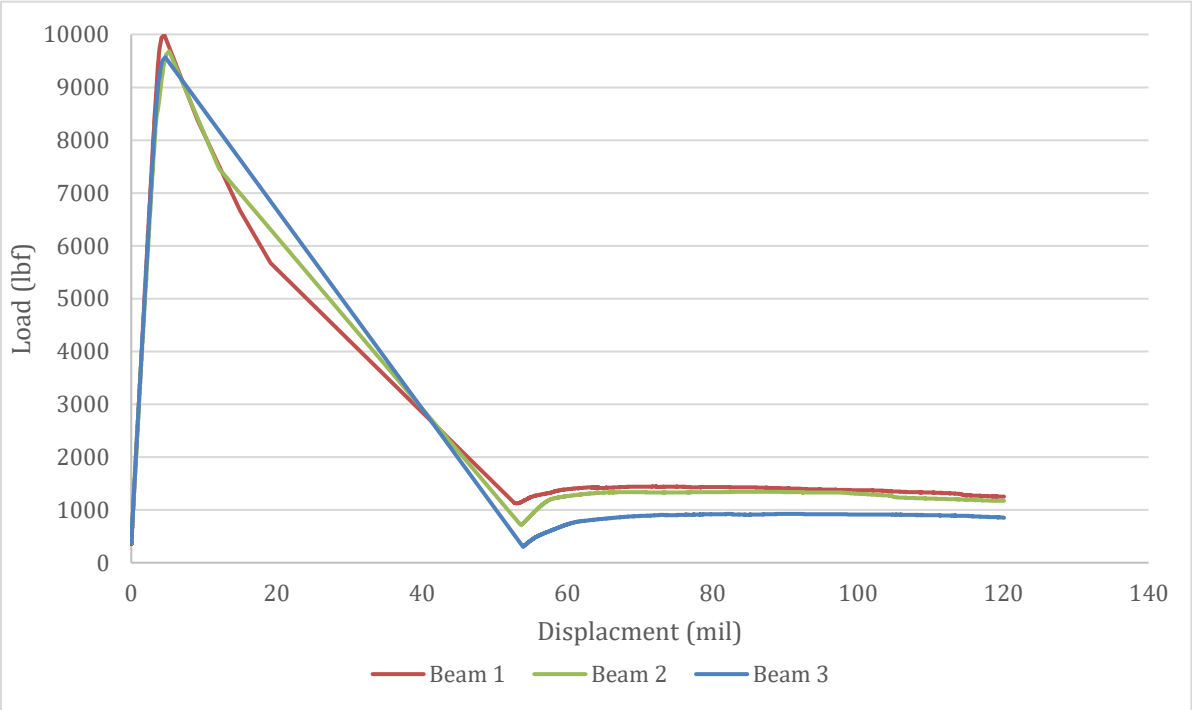

Figure 0-19. Load vs Displacement for 4B1.26

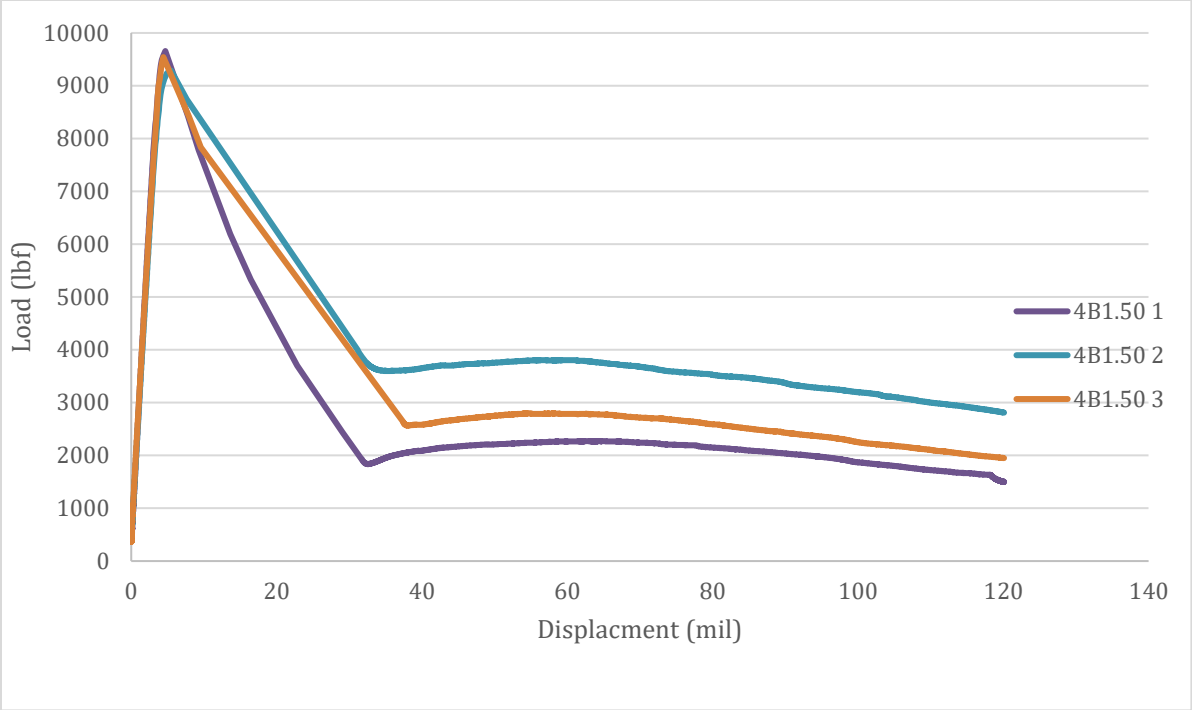

Figure 0-20. Load vs Displacement for 4B1.50

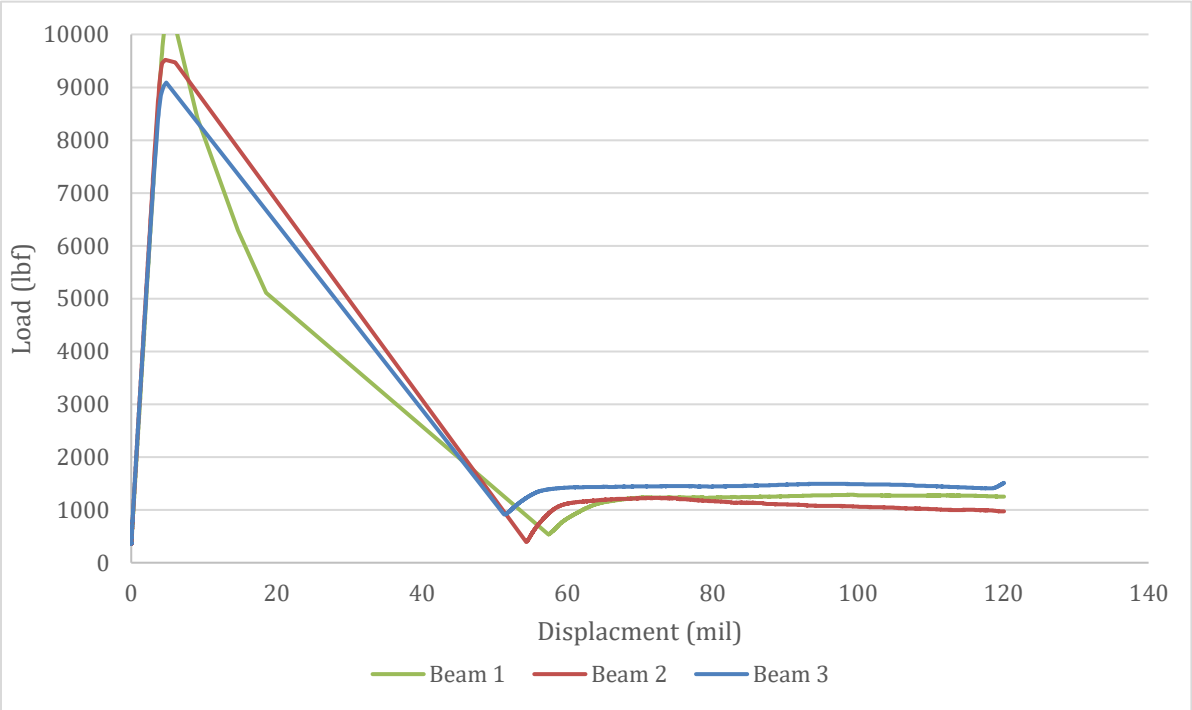

Figure 0-21. Load vs Displacement for 6B1.26

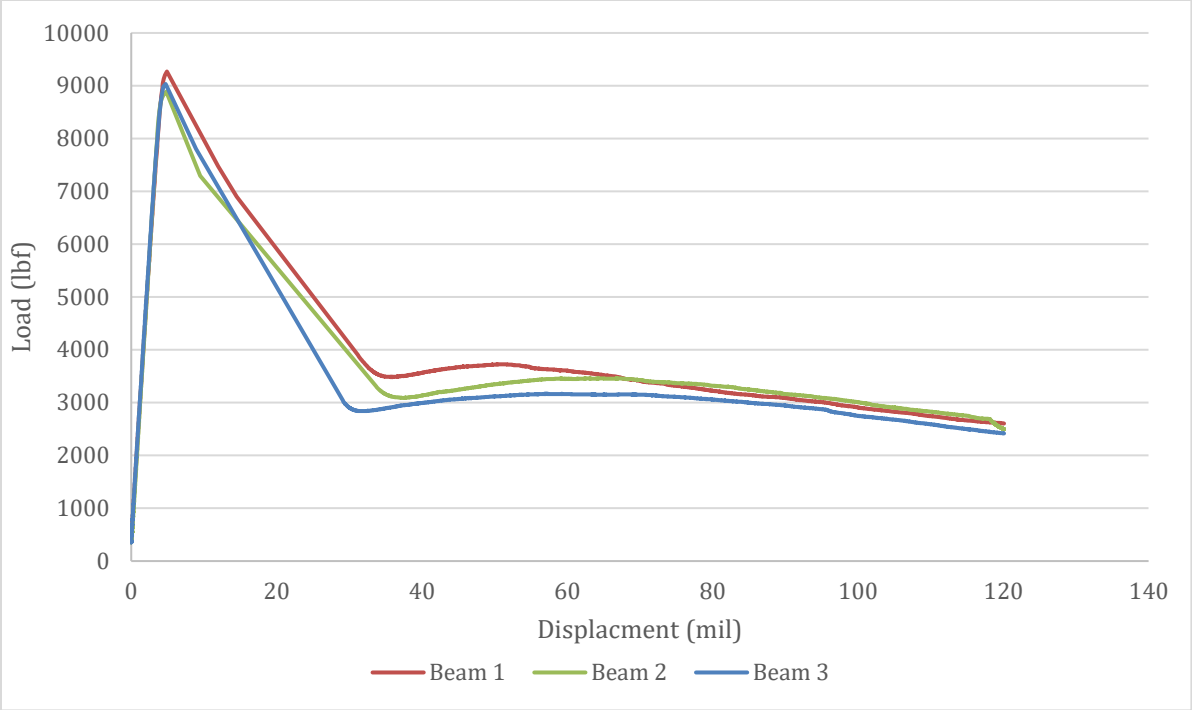

Figure 0-22. Load vs Displacement for 6B1.50

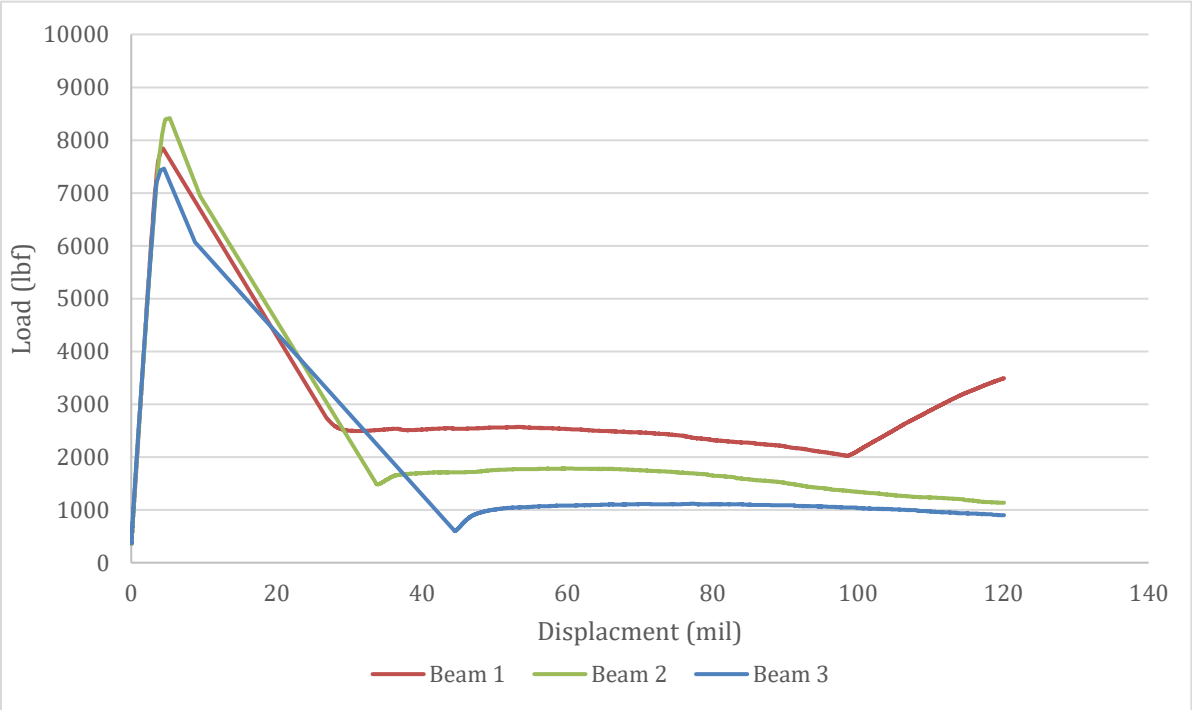

Figure 0-23. Load vs Displacement for 8B1.26

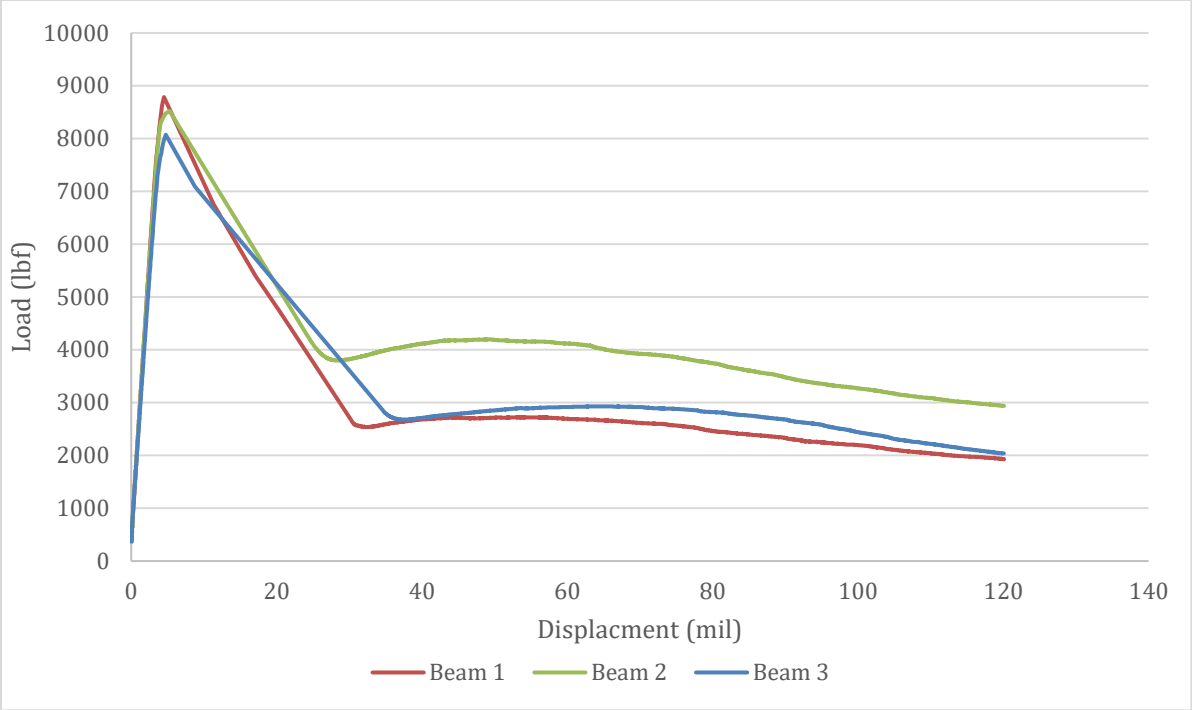

Figure 0-24. Load vs Displacement for 8B1.50

BOX TEST IMAGES

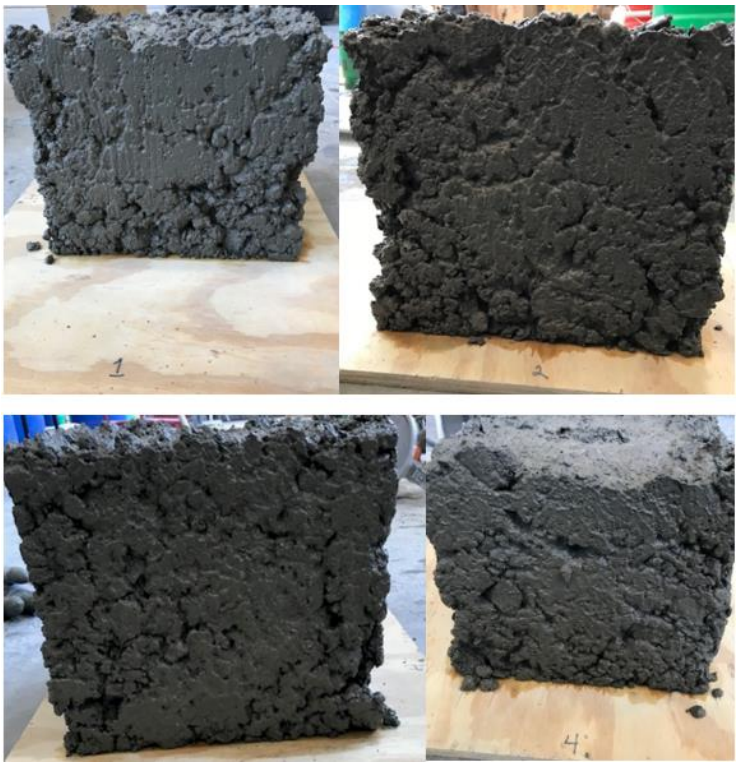

Figure 0-25. Box test images for mix A.PC

Figure 0-26.Box test images for mix 4A1.26

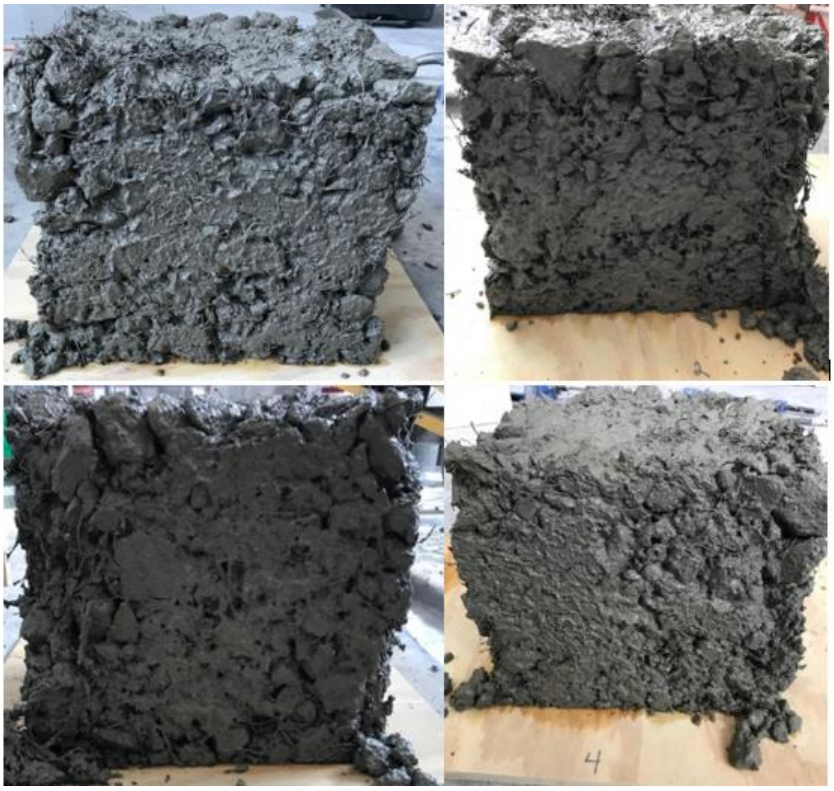

Figure 0-27.Box test images for mix 4A1.50

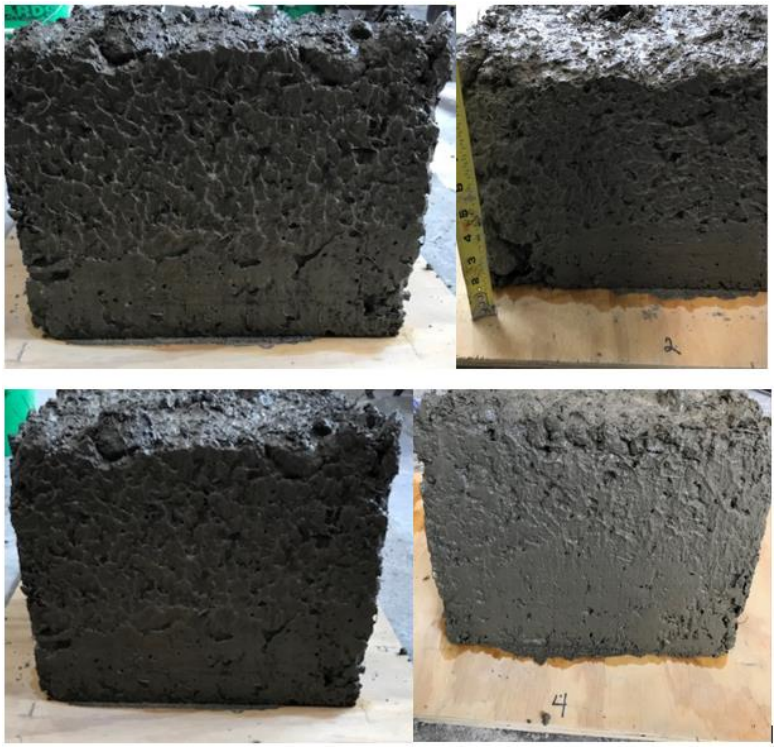

Figure 0-28. Box test images for mix 6A1.26

Figure 0-29. Box test images for mix 6A1.50

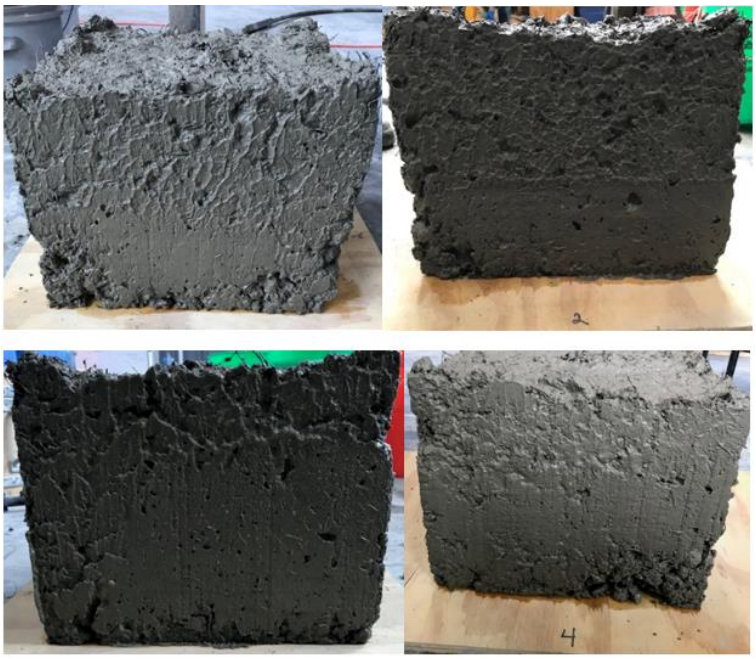

Figure 0-30. Box test images for mix 8A1.26

Figure 0-31. Box test images for mix B.PC-1

FREEZE-THAW IMAGES

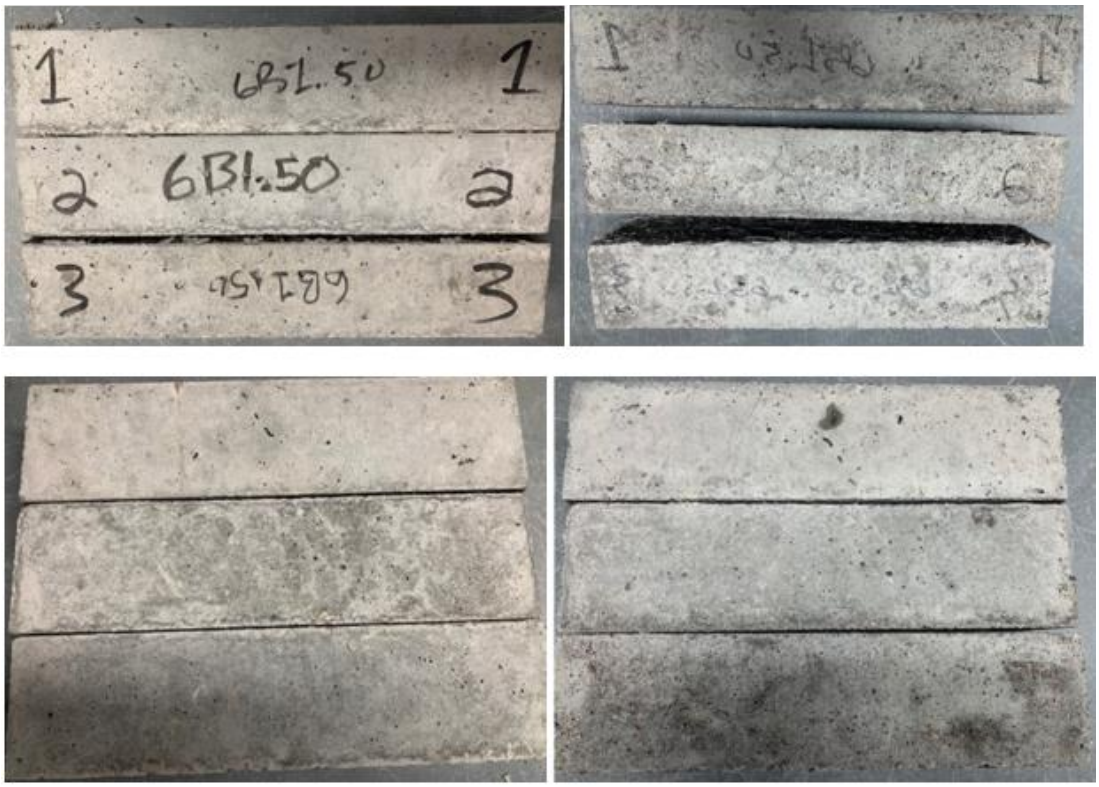

Figure 0-32. Before (Left) and After (Right) image of mix 6B1.50 beams subjected to 300 freeze-thaw cycles

Figure 0-33. Image of mix 6A1.50 beams after 300 freeze-thaw cycles

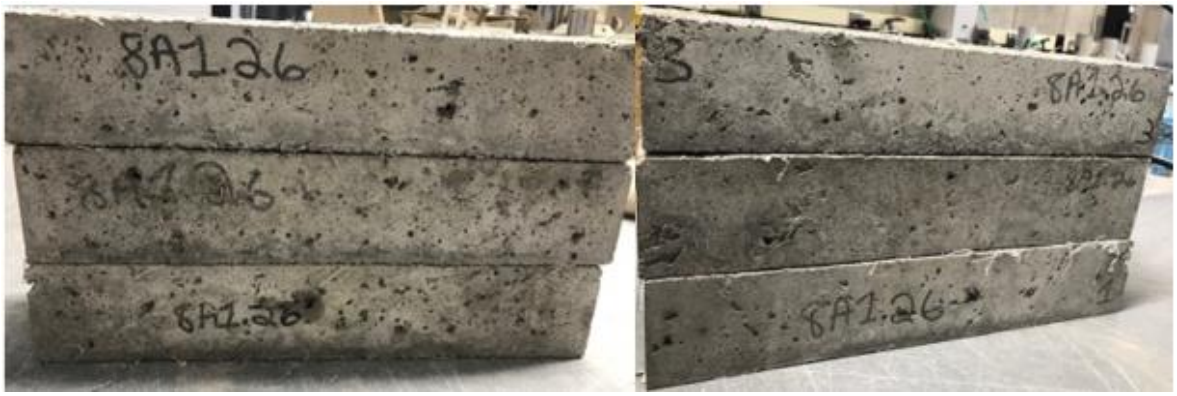

Figure 0-34. Image of mix 8A1.26 beams after 300 freeze-thaw cycles